Viewgraphs presented at International Symposium on Neutrino Astrophysics, Takayama, Japan (October 1992)—sent to us by Seiji Kawamura.

Distributed by R. Vogt 11/12/92

PLEASE PASS ALONG PROMPTLY

~~A. Abramovici~~ 11/18/92
~~J. Camp~~
~~A. Kuhnert~~ 11/20/92
F. Raab
~~M. Regehr~~ 12/9/92
R. Savage 11/30/92
L. Sievers 12/6/92
~~R. Spero~~ 20 Nov 92
M. Zucker

11/20/92

Science Library -last

cc: W. Althouse
R. Vogt
S. Whitcomb
MIT Science Group
Project File
Science Library

European Projects

- VIRGO (cf Brillet) Pisa. 3 km. ≃ approved. Recycling Fabry-Perot design
- GEO. Germany-UK. Hannover. 8 km. Money frozen. Dual-recycling delay line design.

Delay-line: With Dual Recycling (Meers)

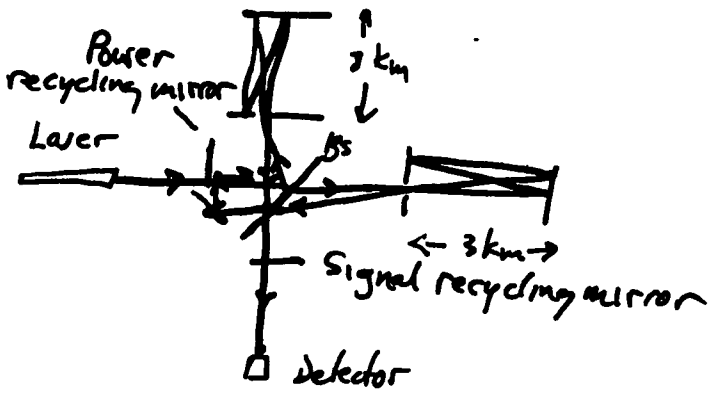

Groups presently operating prototypes of length 10 m and 30 m, sensitivity $\sim 10^{-16}$. Data run of 100 hrs set limit $\sim 10^{-17}$ on bursts. Further analysis going on. More runs possible.

Groups will collaborate with VIRGO.

Networks of GW detectors

- 2 detectors required for minimal confidence that an event is real
- 3 interferometers (5 bars) needed to reconstruct wave: direction, polarization, amplitude.
- 2 (nearby) detectors can search for cosmic background
- 1 interferometer can perform all-sky search for pulsars, with massive computing

Working with other instruments

- γ-ray burst detectors. 2 interferometers and BATSE (or equivalent) can reconstruct wave.
- ν burst detector. 2 interferometers and Superkam can reconstruct wave.

Such coincidences allow one to lower the threshold of gw detectors, increasing their range

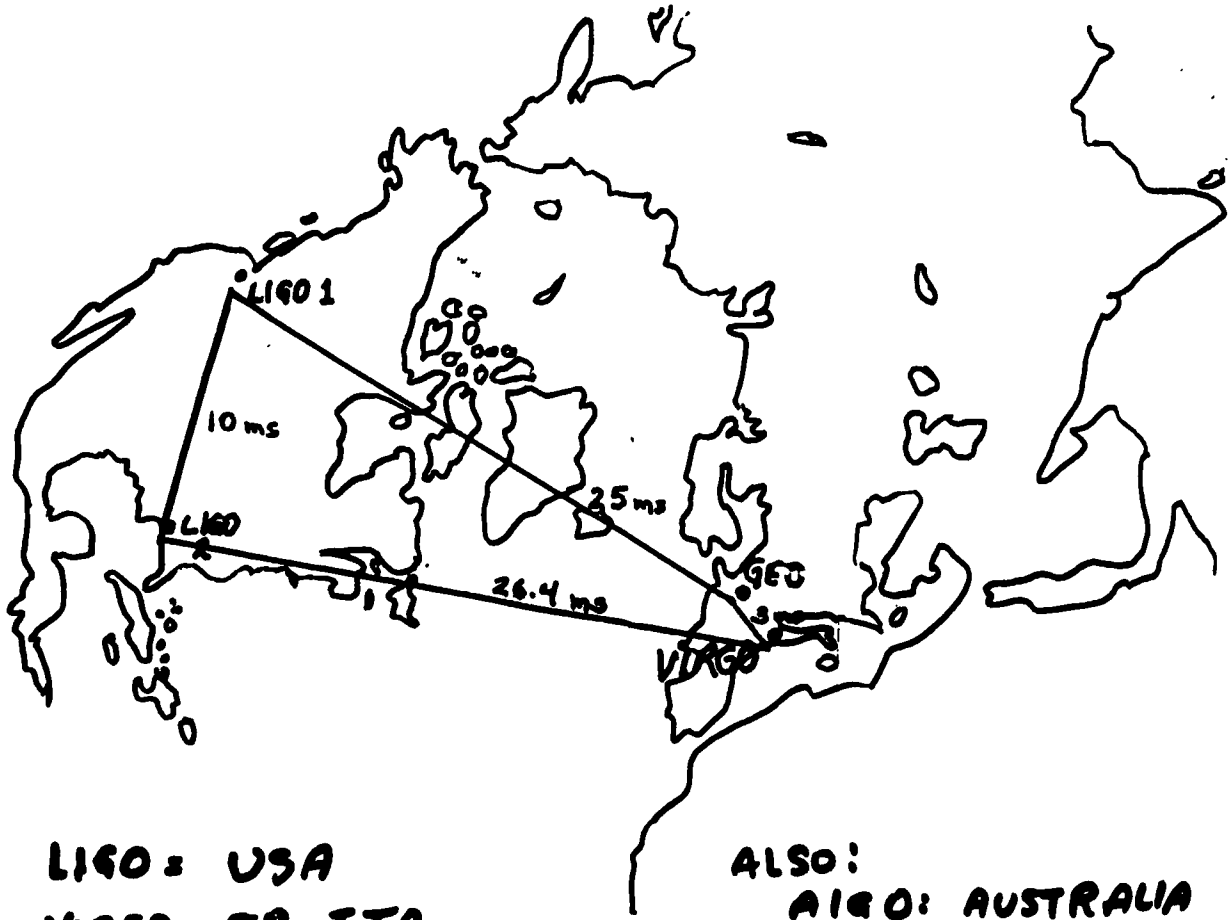

LIGO : USA
VIRGO: FR-ITA
GEO : GER-UK

ALSO:
AIGO: AUSTRALIA
TENKO: JAPAN

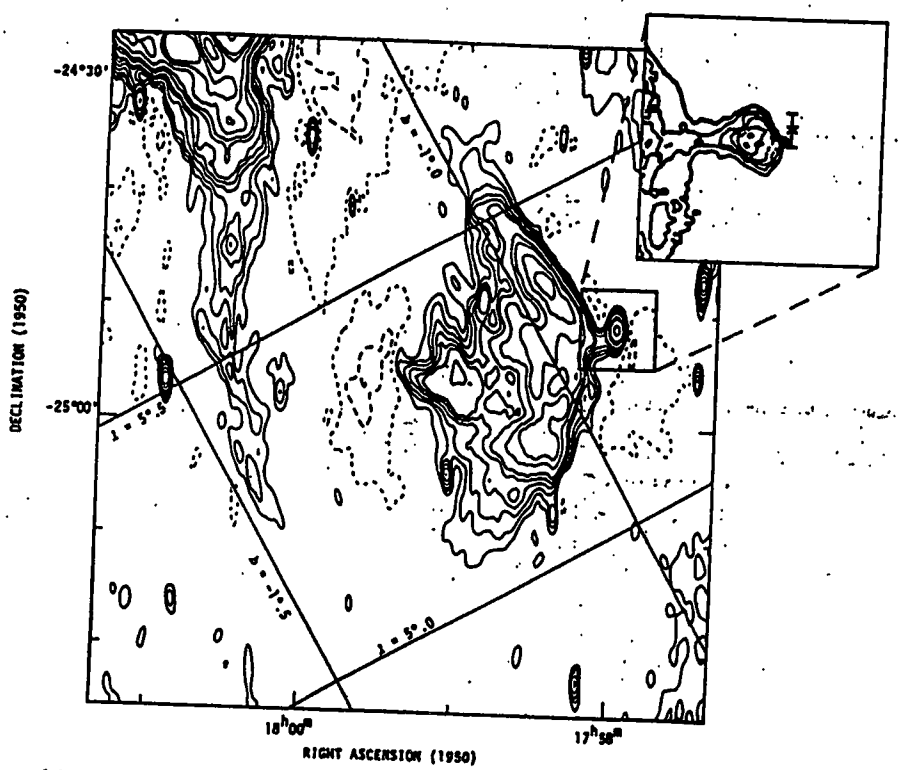

Figure 1. Radio image of the supernova remnant G5.4 − 1.2 (Caswell *et al.* 1987) with a VLA image of the compact component G5.27 − 0.90 (Becker & Helfand 1985) (inset). The timing position of the pulsar PSR 1758 − 24 is marked on the inset with a cross. Error bars in the declination direction are shown; in the right ascension direction the positional uncertainty is less than the width of the line.

the remnant as illustrated in Fig. 1 (inset). The position error in right ascension is smaller than the width of the line; the error in declination is larger because this pulsar lies close to the ecliptic plane. The pulsar is located at the extreme western edge of the compact nebula G5.27 − 0.90; the derived position is consistent with location within the small 'bump' on the Becker & Helfand (1985) image. Independent observations using the Very Large Array by Frail & Kulkarni (1991) confirm this location for the pulsar.

3 DISCUSSION

The location of the pulsar relative to G5.27 − 0.90 and G5.4 − 1.2 confirms the association with the supernova remnant and suggests that both the pulsar and the compact nebula are moving in a westerly direction at such a high velocity that they have overtaken the shell. Further evidence for the association is obtained from the agreement of the pulsar characteristic age with the estimated age for G5.4 − 1.2, about 14 000 yr (Caswell *et al.* 1987). Distance estimates for the pulsar and remnant are also in good agreement. Using the surface-brightness/diameter relationship of Caswell & Lerche (1979), Caswell *et al.* (1987) estimated the distance to G5.4 − 1.2 to be ~5 kpc which compares well with a distance to the pulsar of 4.4 kpc based on the dispersion measure (Table 1) and a new model for the galactic electron density distribution (Taylor, Lyne & Manchester, in preparation). Caswell *et al.* also suggested that G5.27 − 0.90 lies beyond ~5.9 kpc, based on the radial velocities of H_2CO absorption features. Given the small galactic longitude and the consequent uncertainties in the radial velocity–distance relation, this result is not inconsistent with associating G5.27 − 0.90 with the pulsar and with G5.4 − 1.2.

Table 1. Parameters for PSR 1758 − 24.

Right Ascension (J2000)	$18^h00^m59.^s87 \pm 0.^s03$
Declination (J2000)	$-24°50'57'' \pm 32''$
Right Ascension (B1950)	$17^h57^m55.^s14$
Declination (B1950)	$-24°50'55''$
Period	0.12487445209 ± 8 s
Period Derivative	$(127.898 \pm 0.010) \times 10^{-15}$
Second Period Derivative	$(-4.7 \pm 0.5) \times 10^{-24}$ s^{-1}
Period Epoch (Modified Julian Day)	47916.000
R.M.S. residual	930 μs
Dispersion Measure	289 ± 1 cm^{-3} pc
Mean Flux Density at 1520 MHz	0.7 mJy
Characteristic Age	15 500 years
Surface Magnetic Field Strength	4.0×10^{12} G

We conclude, therefore, that PSR 1758 − 24 is associated with both G5.4 − 1.2 and G5.27 − 0.90 and that, together, they form the eighth reasonably well-established pulsar–supernova remnant association after Vela (Large, Vaughan & Mills 1968), the Crab (Staelin & Reifenstein 1968),

ASTROPHYSICS FROM COALESCING BINARIES

- **Measure the masses of hundreds of neutron stars and dozens of black holes.** These masses are parameters that will be automatically measured as part of the detection of the binary.

- **Hubble's constant.** Easy if the event rate is a few per year from within 200 Mpc.

- **Cosmological mass distribution.** Length scales of 100–200 Mpc.

- **Observe black holes coalescing.** This provides a test of strong-field general relativity.

STOCHASTIC BACKGROUND

This could be left over from a number of processes inthe early universe, notably decaying cosmic strings. Two detectors situated within $\lambda/2\pi$ of each other (λ = gravitational wavelength) have optimum sensitivity:

$$\left(\frac{S}{N}\right)_{\text{stochastic}} = 3\left[\frac{f}{100\,\text{Hz}}\right]^{-5/2}\left[\frac{\sigma_{\text{bb}}}{10^{-22}}\right]^{-1} \times$$

$$\times\left[\frac{\Omega_{\text{gw}}}{10^{-8}}\right]^{1/2}\left[\frac{H_0}{100\,\text{km s}^{-1}\,\text{Mpc}^{-1}}\right],$$

where σ_{bb} is the broadband burst sensitivity of the detectors.

An experiment conducted at the lowest frequency gives the largest possible separation between detectors. Even at 100 Hz, however, the detectors need to be within 500 km of each other for optimum sensitivity.

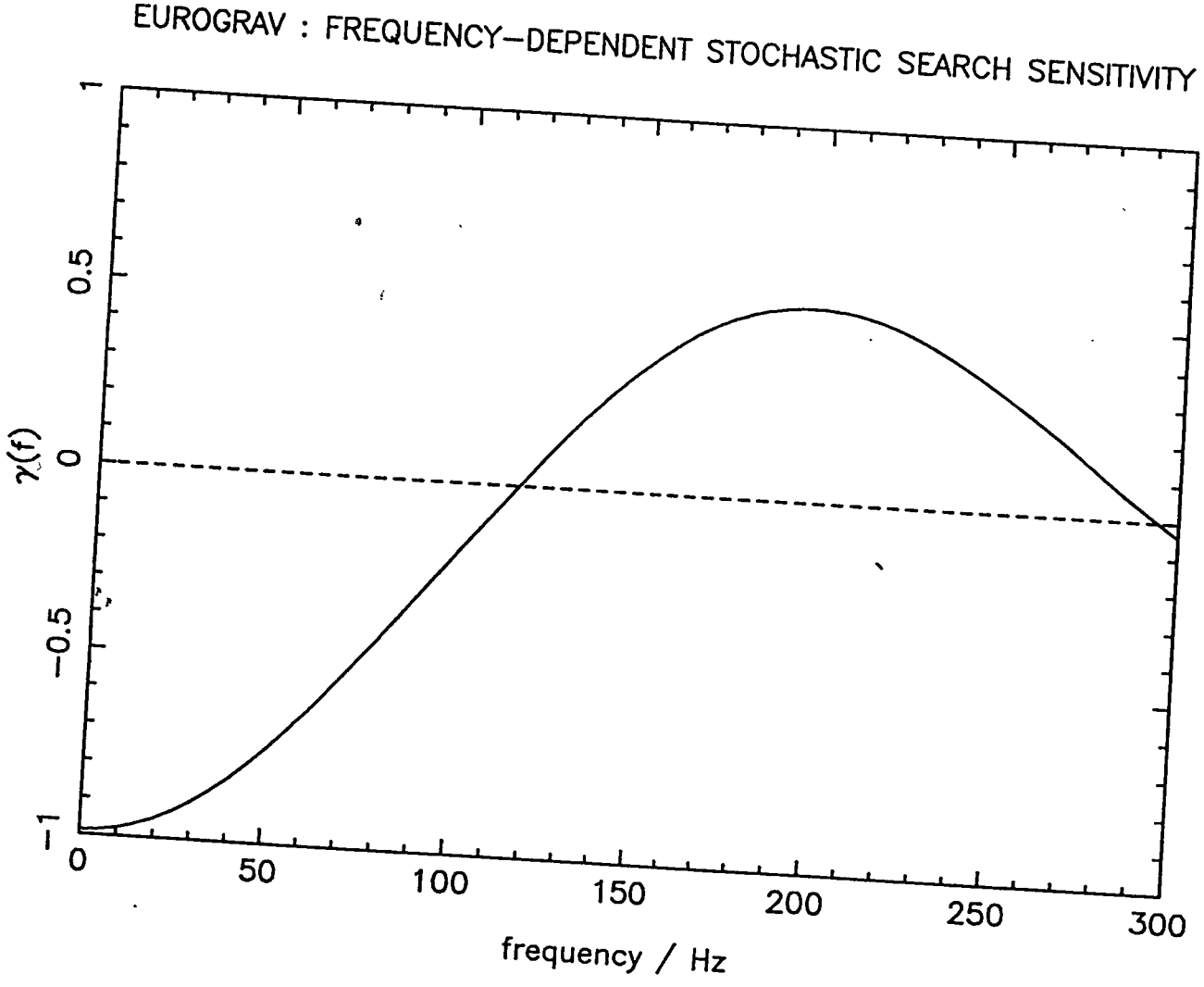

DXN 12–Jun–1992 20:50

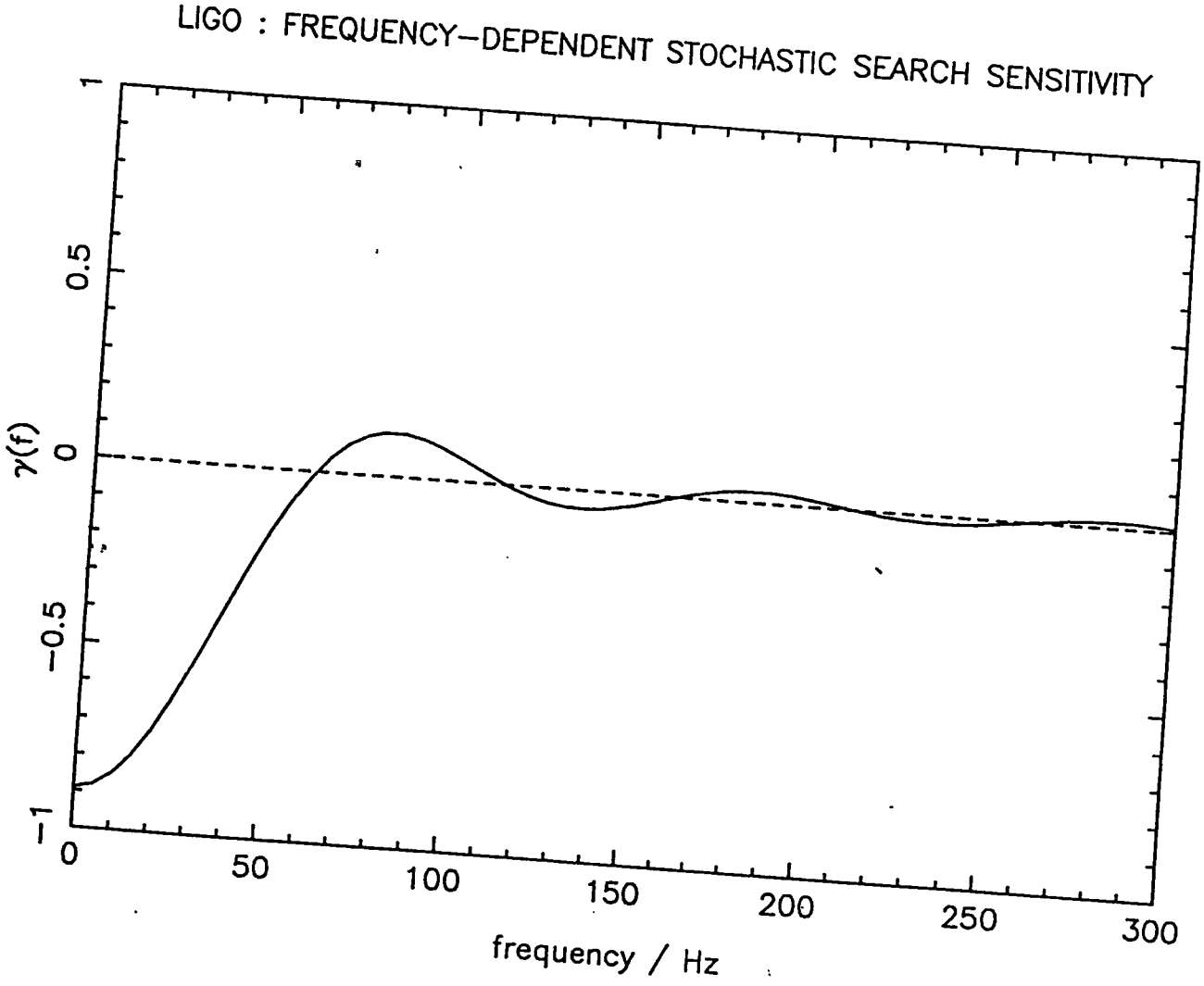
LIGO : FREQUENCY–DEPENDENT STOCHASTIC SEARCH SENSITIVITY
γ(f)
1
0.5
0
−0.5
−1
0
50
100
150
200
250
300
frequency / Hz

Projects of the laser interferometric gravitational wave detectors in Japan

K. Tsubono
Department of Physics, University of Tokyo
Bunkyo, Tokyo 113, Japan

I. Progress report in Japan

II. 3km×3km laser interferometer

III. 300m×300m laser interferometer

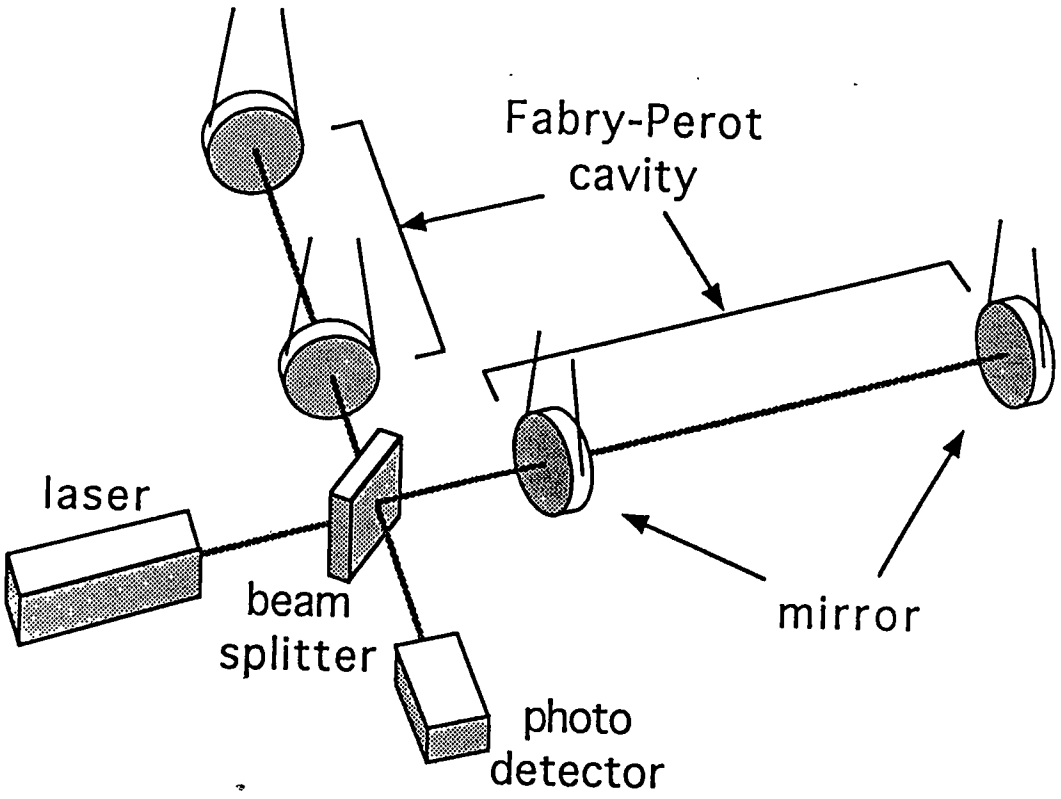

• Schematic view of the Fabry-Perot type laser interferometric gravitational wave detector

(3)

Progress report in Japan

R&D program (1991-1994, ~ $6M)

Institute of Space and Astronautical Science(ISAS)

100-m DL

National Astronomical Observatory(NAO)

20-m FP

The University of Electro-Communication

laser

Tokyo University

control & isolation

Kyoto University

GW theory

Insittute for Cosmic Ray Research(ICRR)

National Laboratory for High Energy Physics(KEK)

Tokyo Institute of Technology

ISAS 100-m DL

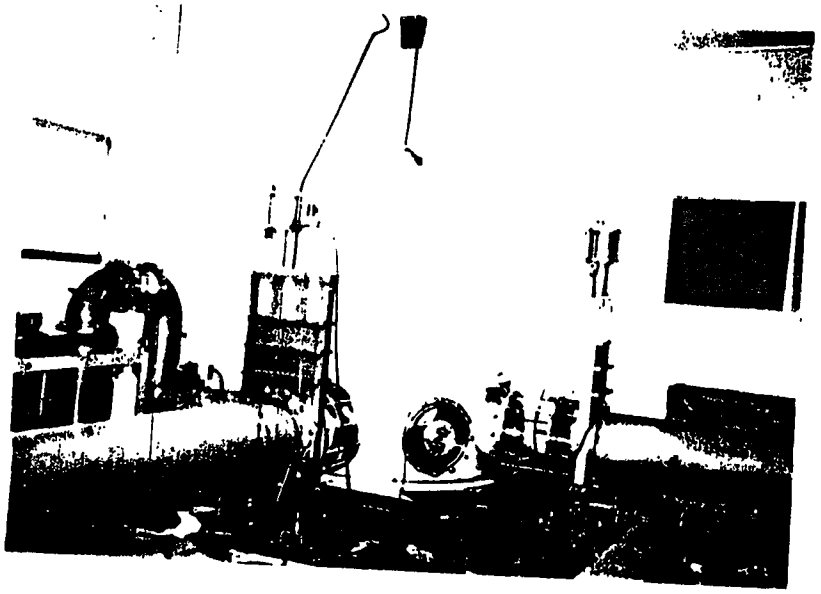

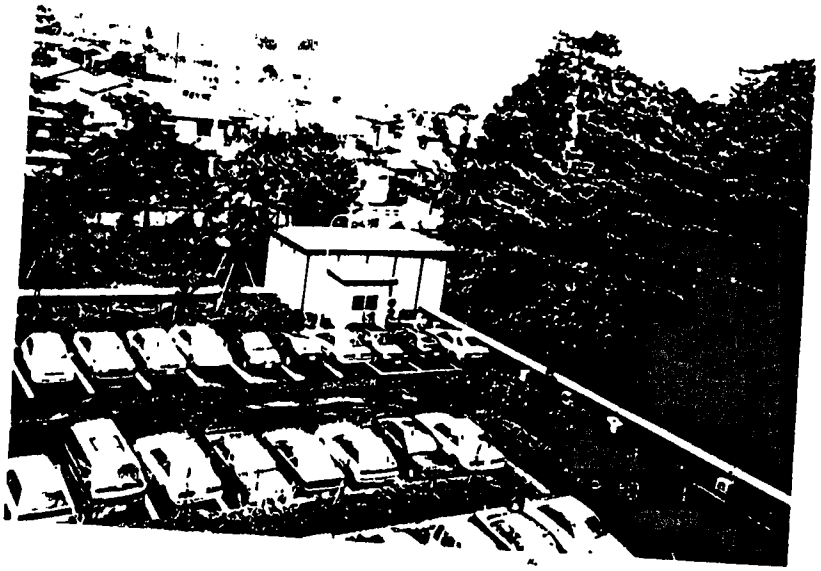

(5) NAO 20-m FP

国立天文台　レーザー干渉計センタータンク
Fabry-Perot 型、基線長20m、アルミ合金製、内径1.4m、高さ2.1m

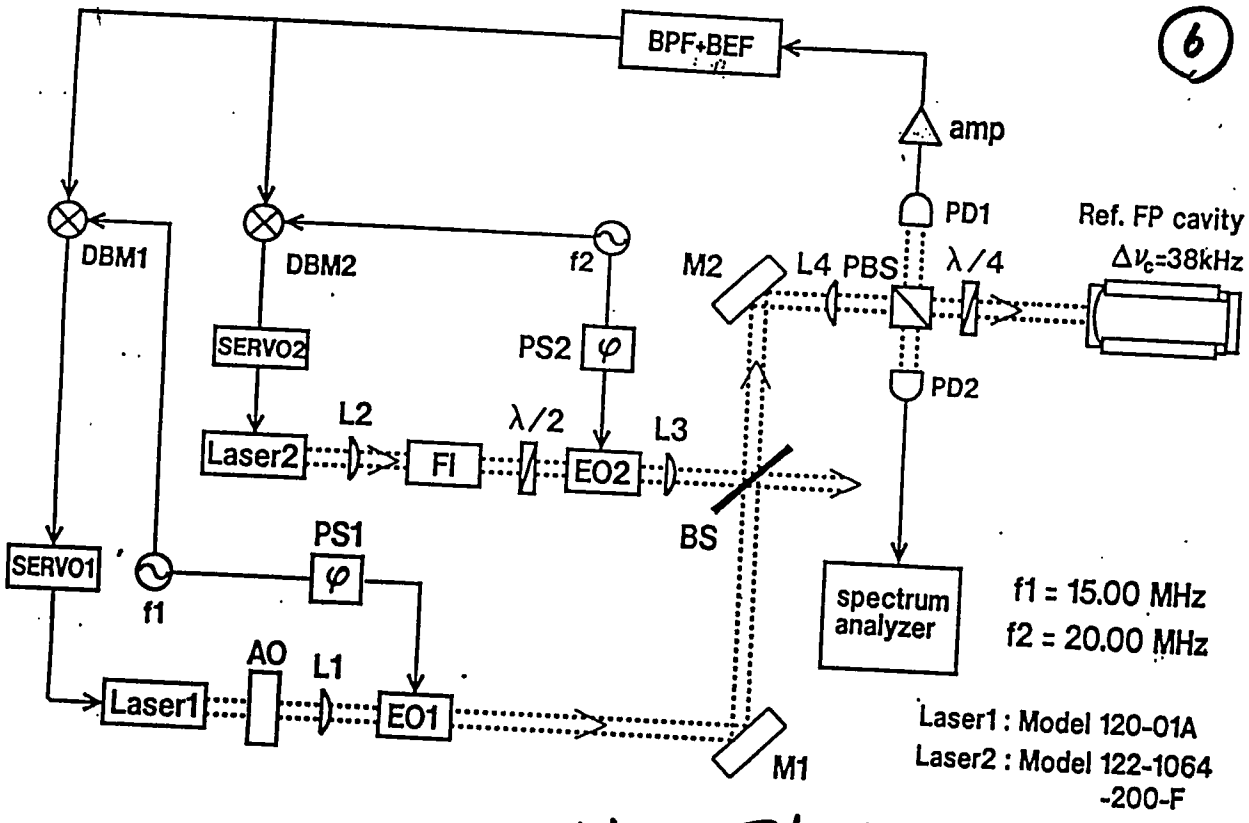

Univ. Electro-Communication

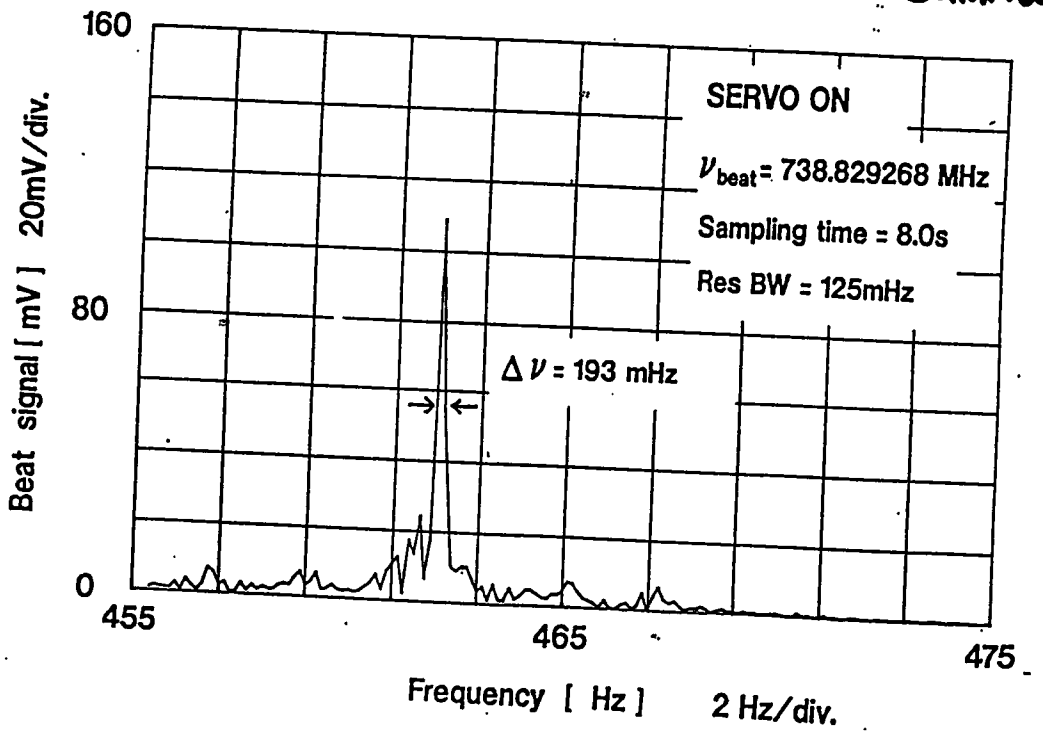

- Frequency satbilization of LD pumped Nd:YAG lasers

Univ. of Tokyo

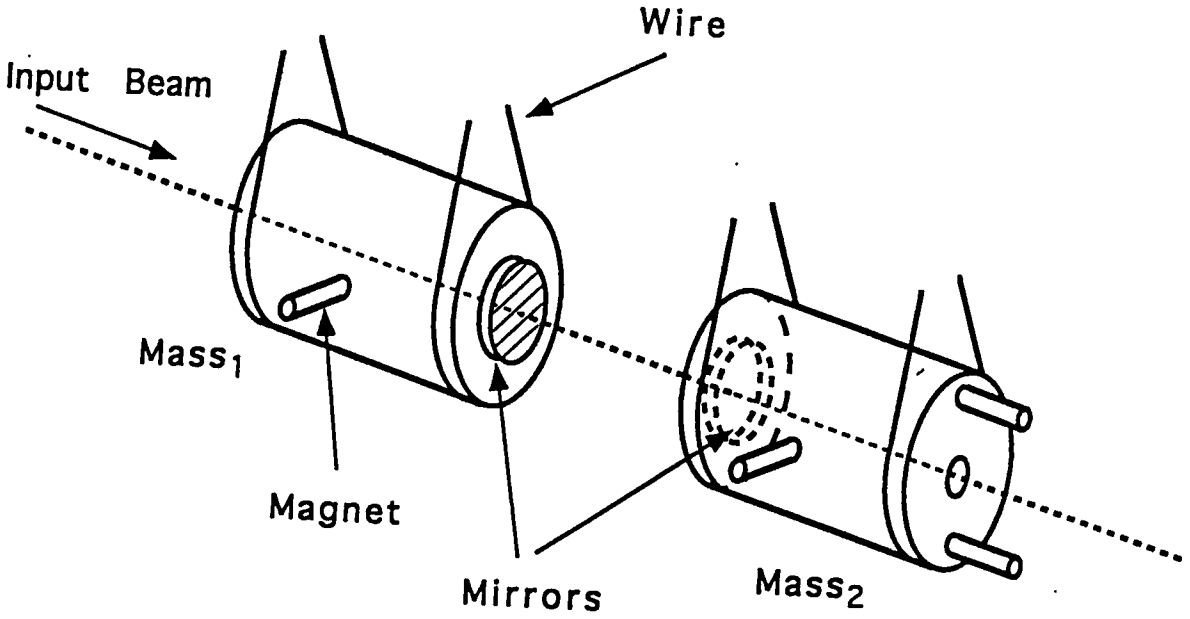

- Alignment control of the suspended Fabry-Perot cavity

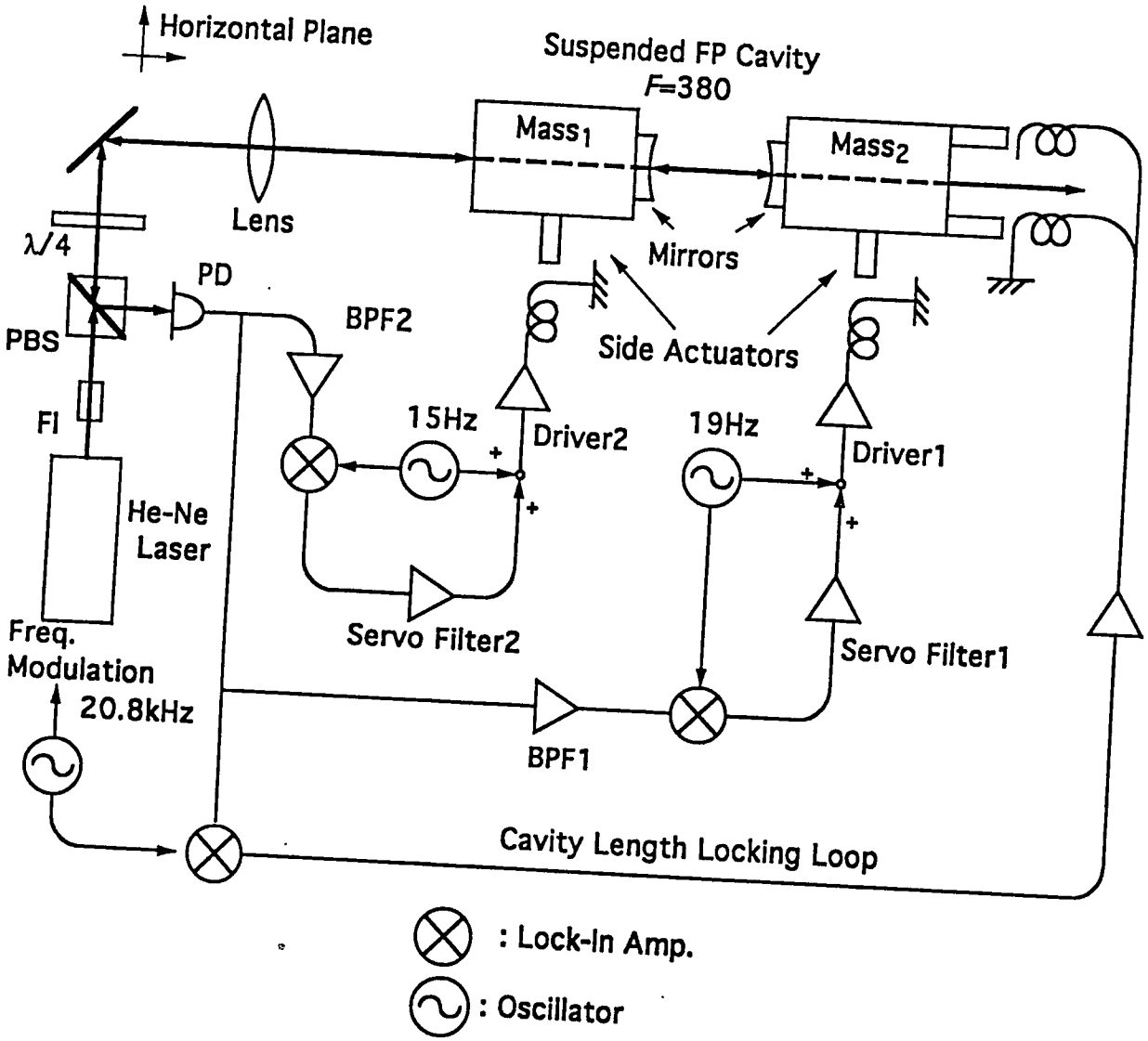

angle $< 4 \times 10^{-8}$ rad/$\sqrt{\text{Hz}}$

- Schematic diagram of the automatic alignment control of the suspended Fabry Perot cavity

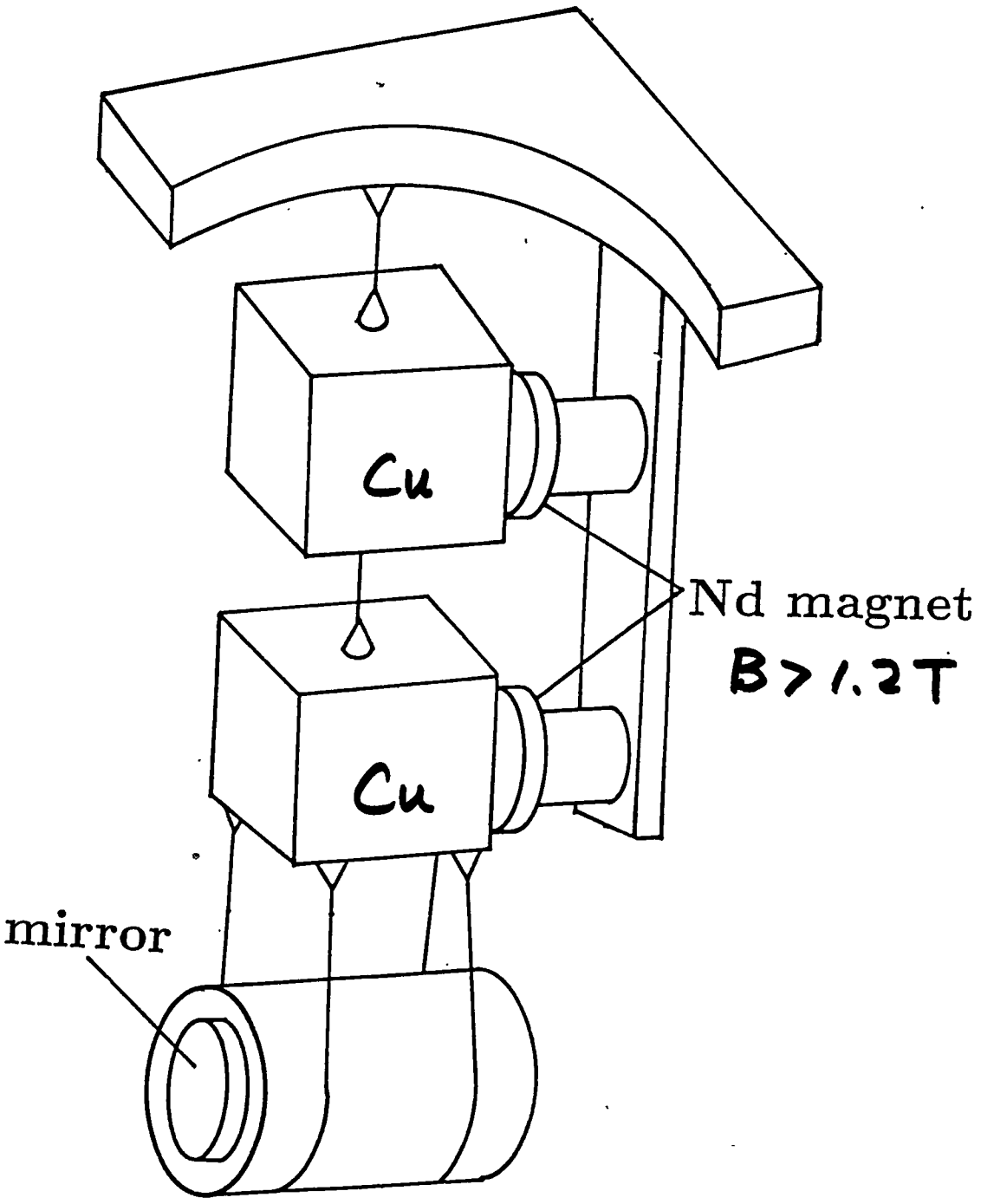

- Triple pendulum vibration isolation system for the suspended mirror

(10)

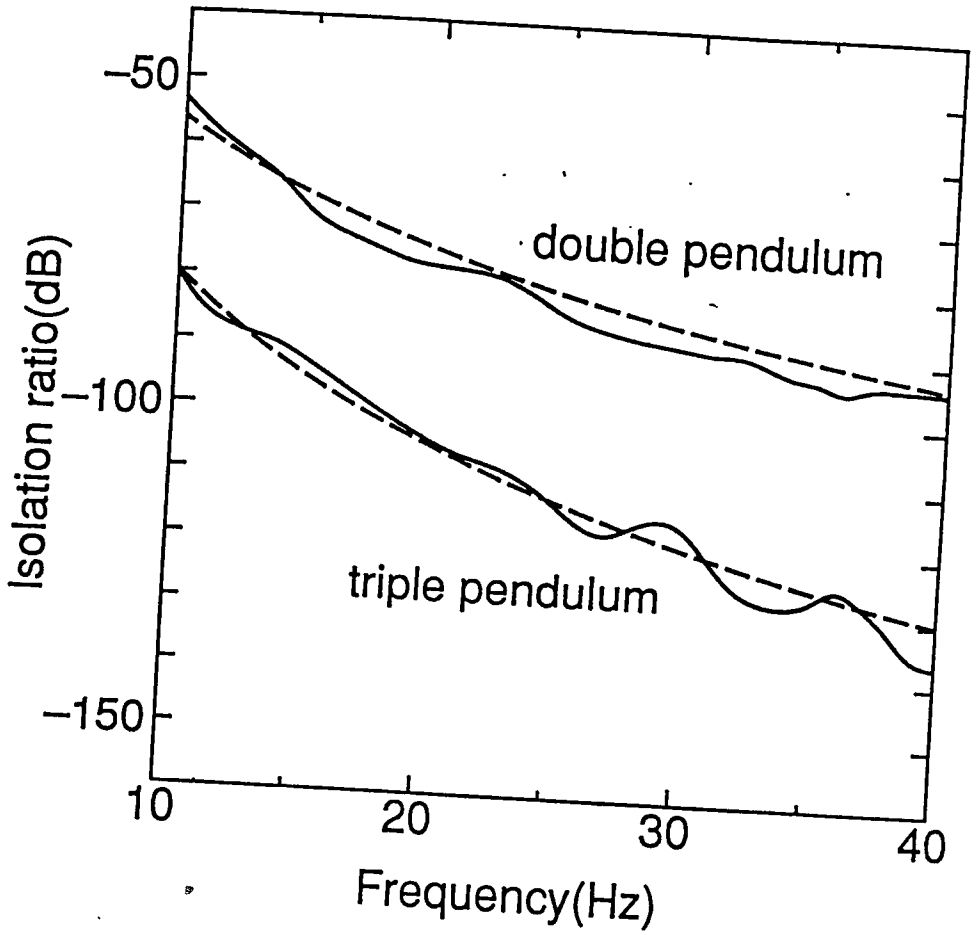

- **Measured and calculated vibration isolation ratio of the double and triple pendulums**

Univ. of Tokyo (12)

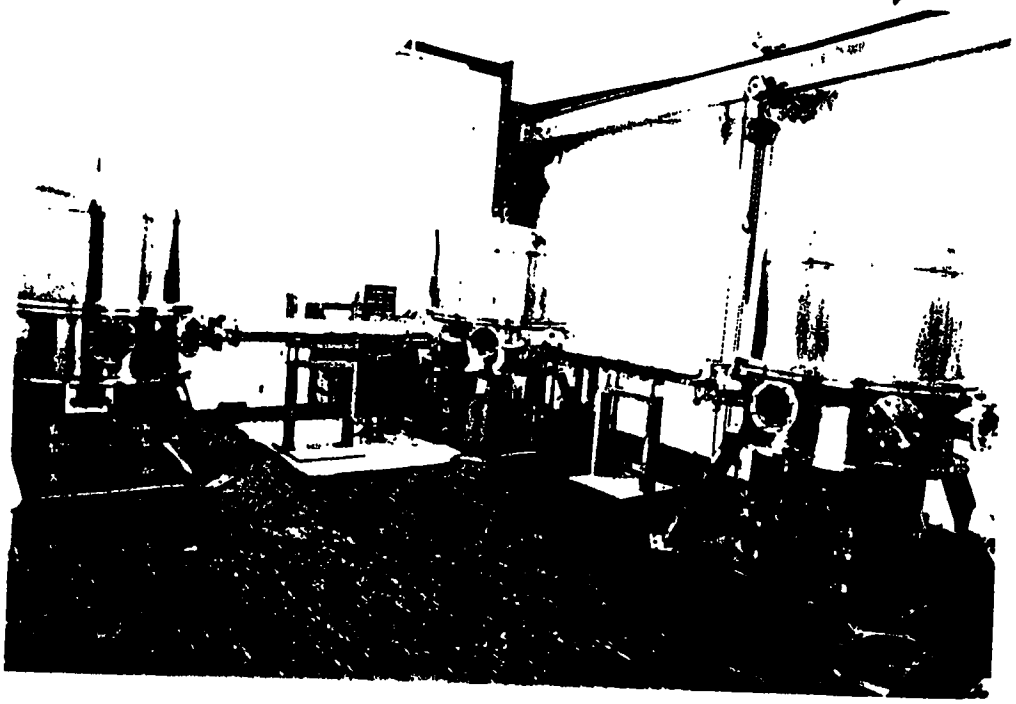

Operation of 3-m Fabry-Perot cavity with mirrors suspended by the double pendulum

- Cavity length L=3m
- Mirror reflectivity r^2=99%
- Mirror curvature R=5m
- Cavity finesse F~300
- Cavity FWHM $\delta\nu$ ~170kHz

ICRR & Univ. of Tokyo

see Kuroda's poster

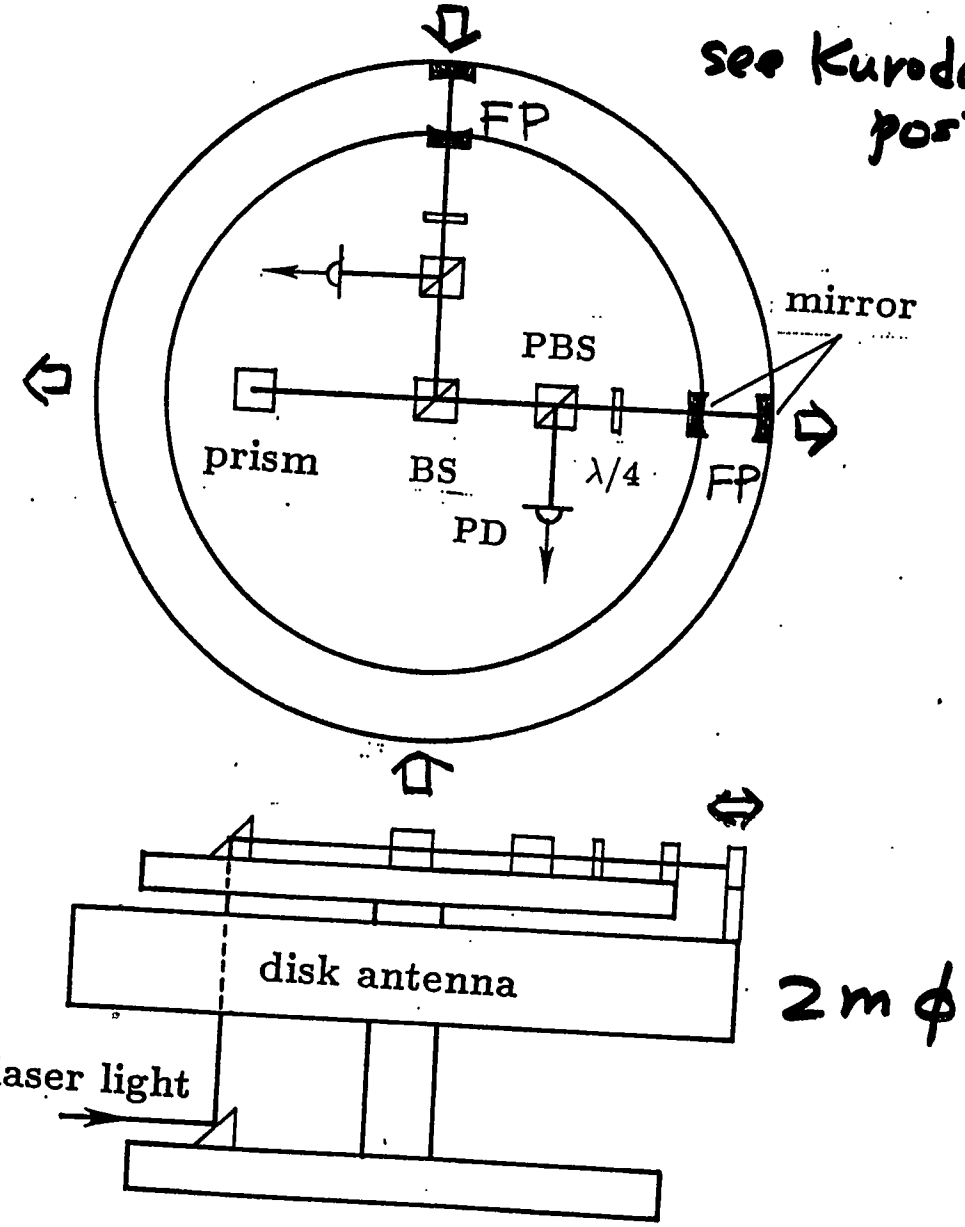

disk antenna

+ laser interferometer

(14)

Schematic View of Laser Transducer System

see Mio's poster

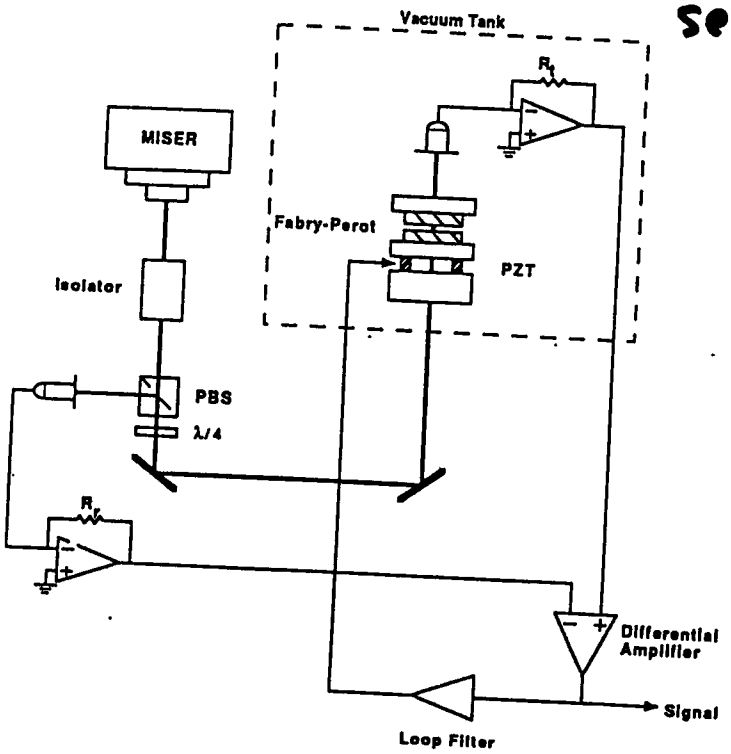

Noise Spectrum of Laser Transducer

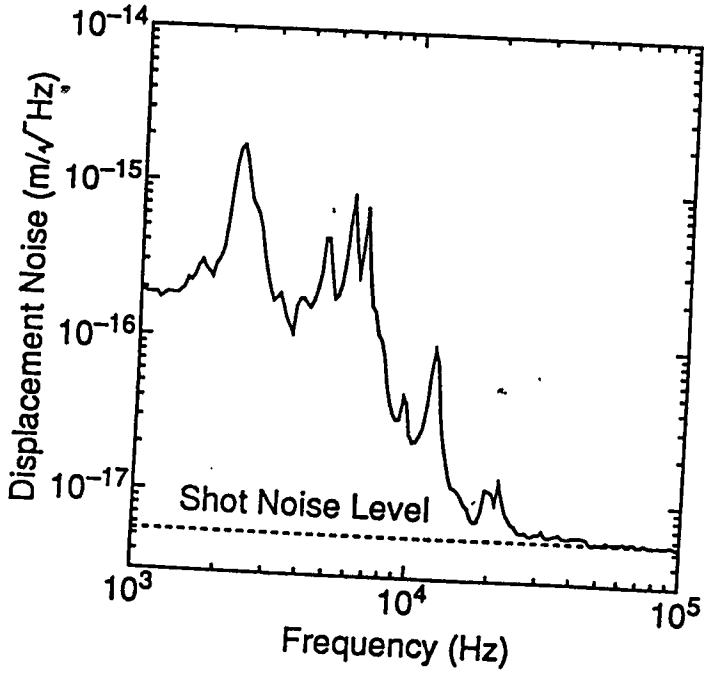

See Ogawa's poster

Seismic noise

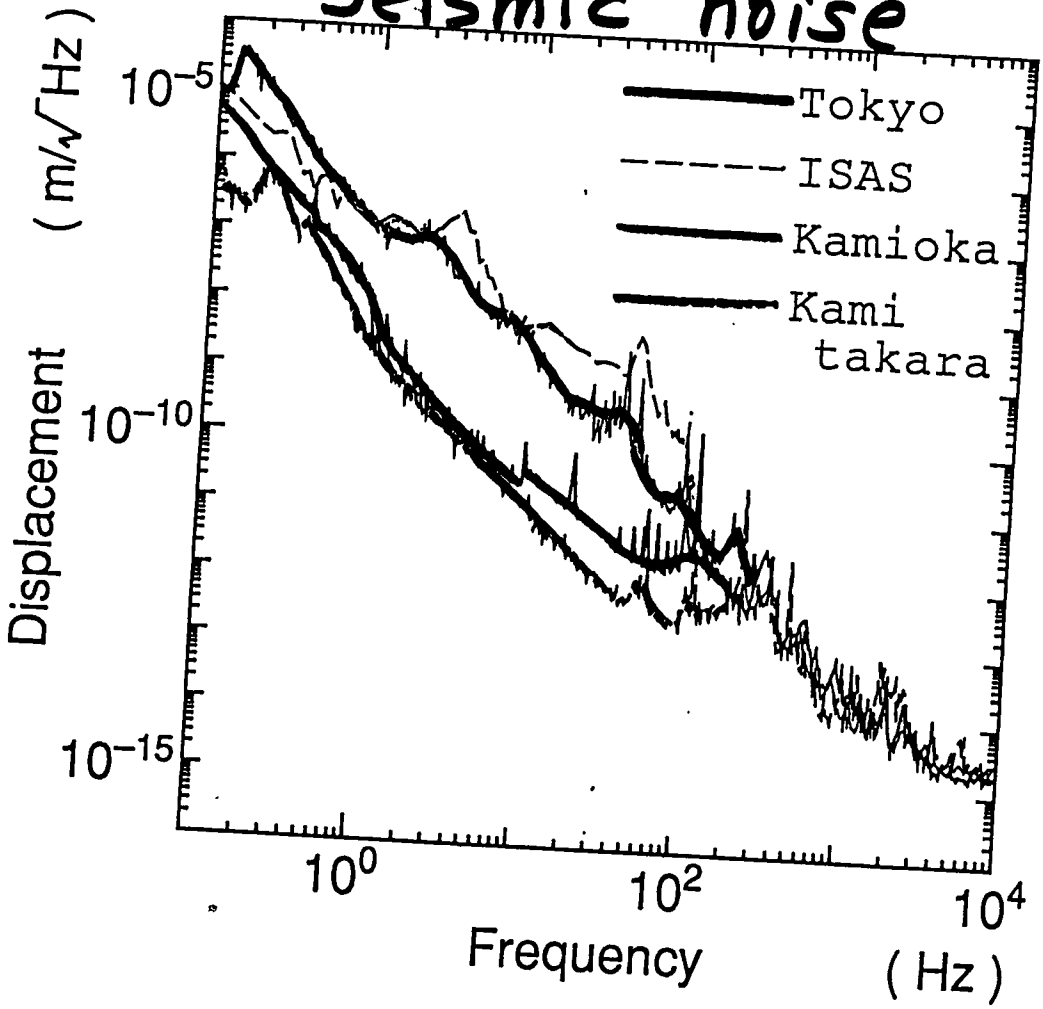

noisy $1 \times 10^{-7}\ m/\sqrt{Hz}$ @ 1 Hz

quiet $\sim 3 \times 10^{-9}\ m/\sqrt{Hz}$ @ 1 Hz

3km×3km Fabry-Perot cavity type laser interferometer

Conceptual design(1990)

- Sensitivity: $h_{\rm rms} = 10^{-21}$ at 1kHz
- Laser: Nd:YAG laser
  - P=1kW
  - Frequency noise $\delta\nu/\nu \sim 10^{-21}/\sqrt{\rm Hz}$
  - Intensity noise $\delta P/P \sim 10^{-9}/\sqrt{\rm Hz}$
- FP Cavity: finesse=80

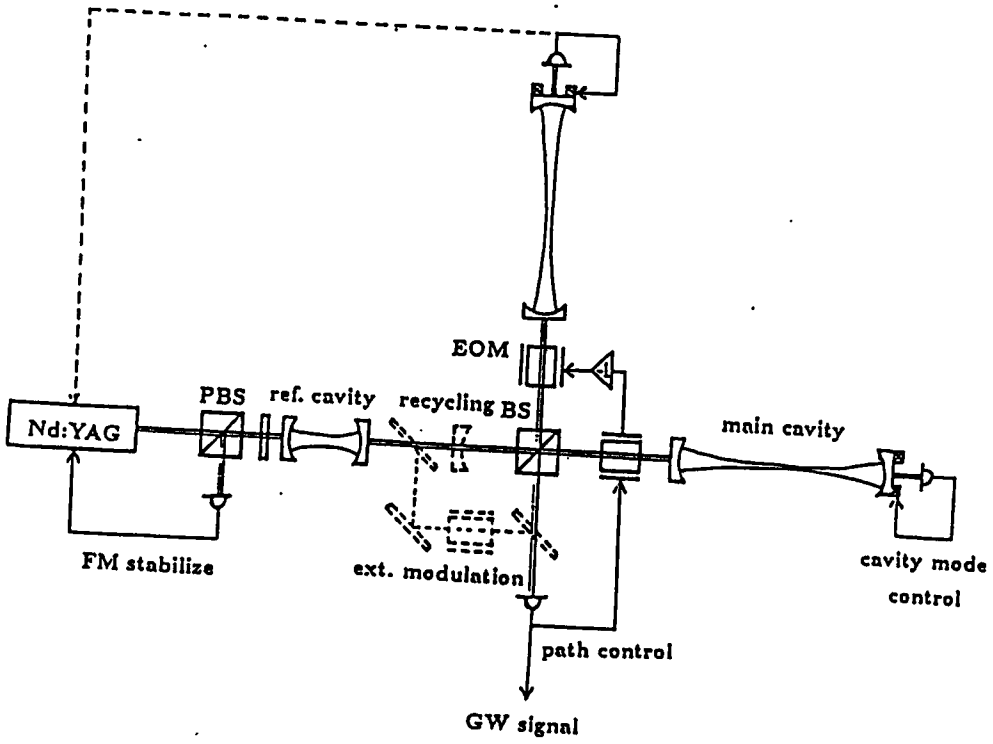

- Conceptual design of a 3km×3km Fabry-Perot type laser interferometer

300m×300m Fabry-Perot cavity type laser interferometer

- 300m×300m Fabry-Perot cavity type
  - quite feasible with the present technology
- $h_{\min} = 10^{-20}$
  - covers GW sources within the distance of Andromeda galaxy (700kpc)

Problems:

- GW sources?
  - two orders improvement over the present detector
- Too late?
  - three years construction
- Sufficient sensitivity?
  - main obstacles: thermal noise and seismic noise
    ⇒future technology will achieve $h_{\min} \sim 10^{-21}$

300m×300m Fabry-Perot cavity type laser interferometer

Design parameters

- Sensitivity: $h_{\rm rms} = 10^{-20}$ at 1kHz with 1kHz bandwidth
- Frequency range: 100Hz-5kHz
- Laser:
  - LD pumped Nd:YAG laser
  - Power=1W, Recycling gain=33
- FP cavity mirror:
  - 70mm(ϕ)× 100mm(ℓ), (m $\sim$ 1kg, Q $\sim 10^5$)
  - Near mirror R=97.5%, loss$\leq$ 100ppm
  - End mirror R=99.99%, loss$\leq$ 100ppm

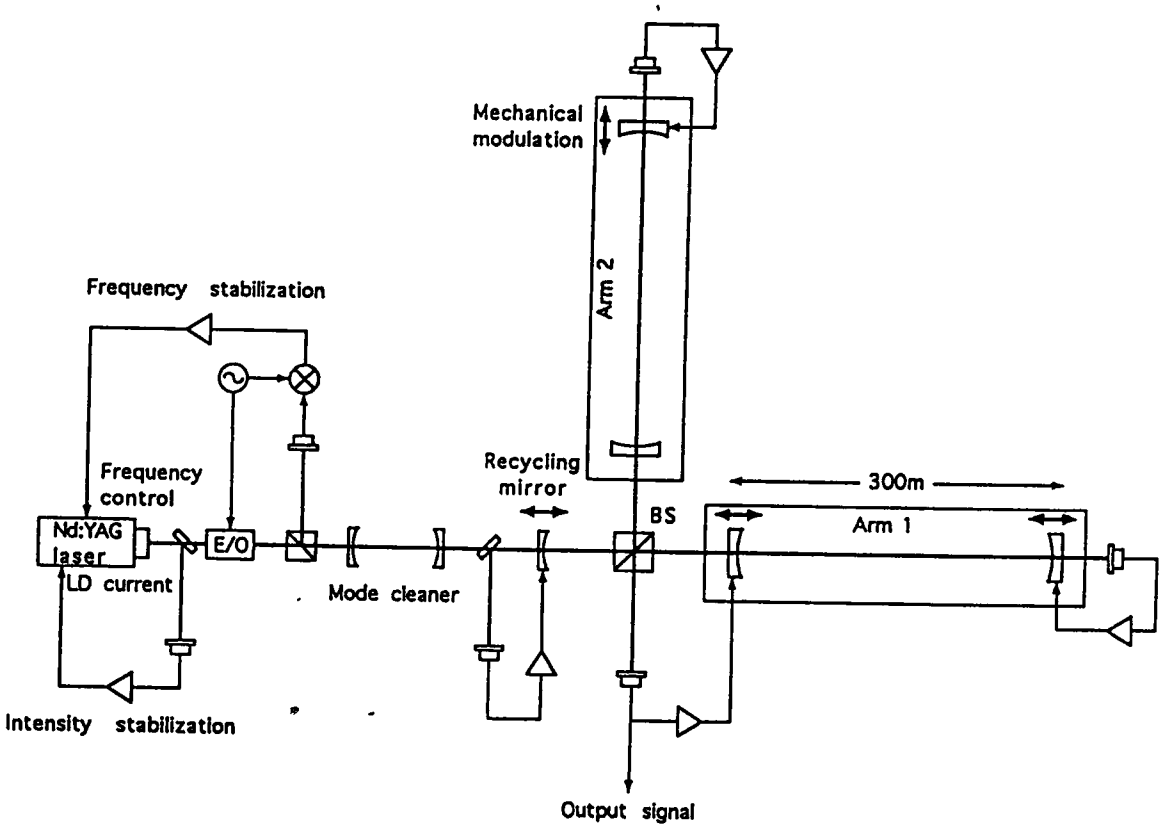

$h_{min} \sim 10^{-20}$

➡ $h_{min} \sim 10^{-21}$

- Conceptual design of a 300m×300m Fabry-Perot type laser interferometer

VIRGO

- PRESENTATION
- CRITICAL TECHNOLOGIES
- CONSTRUCTION DETAILS

ALAIN BRILLET
FOR
THE VIRGO COLLABORATION

VIRGO

FRENCH - ITALIAN INTERFEROMETER FOR G.W. DETECTION

1982 FIRST STUDIES

1986 COLLABORATION ORSAY - PISA

1989 PROPOSAL

1992 - "FINAL DESIGN"

- APPROVAL BY { CNRS in FRANCE / GOVT.
- APPROVAL BY INFN in ITALY

1993 - APPROVAL BY GOVT. in ITALY (?)

- START CONSTRUCTION

1997 - 1998

- END OF CONSTRUCTION
- DETECTIONS (?)

Scientific objectives

First detection of gravitational radiation
coïncidence detection with more than two antennas
or observation of a periodic source (Virgo)

Tests of the polarization properties
coïncidences between antennas with different orientations

Propagation velocity of gravitational waves
timing of events, with more than 3 antennas

Tests of gravity theories in strong field
coalescence of a binary black hole

Morphology of a supernova core
mass, angular momentum, ...

Neutron star equation of state
comparison with numerical models for supernovae or coalescences

Hubble's constant
observation of a coalescing binary associated with a visible galaxy (expected precision @ 1%)

Homogeneity and isotropy of the Universe
through statistics on coalescences up to 500 Mpc

The early universe
stochastic background : cosmic strings, phase transitions, generation of supermassive objects

RECYCLING INTERFEROMETER

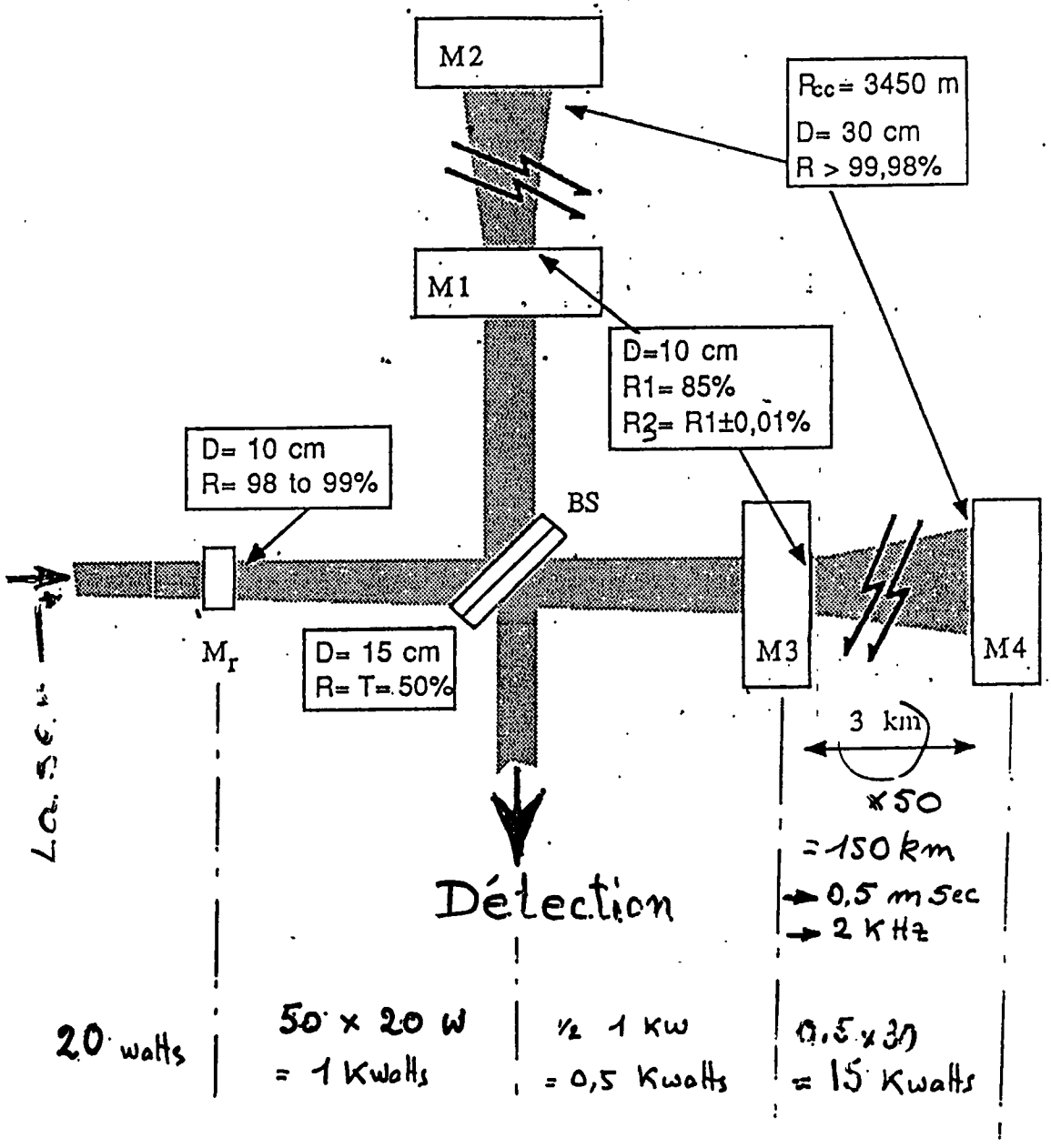

Ref. "Optimisation of long-baseline optical interferometers for Gravitational wave detection" Phys. Rev. D (1988) J.Y. Vinet, B. Meers, C.N. Man et A. Brillet.

Ground-based optical interferometers (VIRGO, LIGO, ... projects)

The main limitations

1) Low frequencies (below 10 Hz) --> Seismic noise

Typical ground motion : $\Delta x = \frac{4\,10^{-6}}{\omega^2}\,m.Hz^{-1/2}$, or $\Delta h = \frac{\Delta x}{L} = \frac{3\,10^{-11}}{f^2}\,Hz^{-1/2}$

An attenuation of 10^{10} is then needed @ 10 Hz

2) Intermediate frequencies (10 to 200 Hz) --> Thermal noise

$$\Delta h = \frac{1}{L}\sqrt{\frac{4\,kT\,\omega_o}{MQ\,\omega^4}}\ , \text{typically } \Delta h = 1\,0^{-22}\,Hz^{-1/2}\ @\ 100\,Hz$$

for M=100 kg, $Q = 10^6$, and L = 3 km

3) High frequency (above 200 Hz) --> Shot noise

$$\Delta h = \frac{\lambda}{2\pi L_{eq}}\sqrt{\frac{h\nu}{\eta P}} = 2\,10^{-23}\sqrt{\frac{1\,kW}{\eta P}}\,Hz^{-1/2}$$

for $\lambda = 1\mu m$, and Leq = 100 km

Solutions to the shot-noise problem :

- high power Nd:YAG lasers
- coherent addition of lasers
- recycling
- Squeezing ??

CRITICAL TECHNOLOGIES

VACUUM
- LOW H_2 OUTGASSING RATE
- PRESSURE STABILITY, CLEANLINESS

SEISMIC ISOLATION
$> 10^{10}$ @ $10 H_z$

MATERIALS
- HIGH MECHANICAL Q
  - WIRES
  - SILICA
  - DESIGN
- ULTRA LOW ABSORPTION } OPTICAL MATERIAL
- HIGH HOMOGENEITY }

MIRRORS
- VERY LOW LOSSES $< 10^{-5}$
- HIGH UNIFORMITY $< \lambda/100$
- LARGE SIZE > 30 cm

LASER
RELIABILITY, HIGH POWER ($\gg 10$W CW)

STABILITY
- FREQUENCY $< 10^{-20}/\sqrt{H_z}$
- AMPLITUDE $< 10^{-8}/\sqrt{H_z}$

OPTRONICS
SHOT NOISE LIMITED OPERATION

LASER STABILITY REQUIREMENTS

[DUE TO INTERFEROMETER ASYMETRIES(1) AND TO USE OF RESONANT CAVITIES (2)]

FREQUENCY (length asymetry and scattered light)

1 $$\frac{\delta\nu}{\nu} < h \left(\frac{\delta F}{F} + \frac{\delta L}{L} \right)^{-1}$$

$$< 10^{-23} \times 10^{+4} = 10^{-19} \, H_z^{-1/2}$$

$$\rightarrow \delta\nu < 10^{-5} \, H_z / \sqrt{H_z}$$

2 $\Delta\nu \ll \Delta\nu_c$ $\quad \Delta\nu \ll 50 H_z$ $\quad (\leq 0.005 H_z)$

POWER (mirors recoil, imperfect contrast)

$$\frac{\delta P}{P} < 10^{-8} / \sqrt{H_z}$$

GEOMETRY

- SINGLE TRANSVERSE MODE
- BEAM POINTING STABILITY $\delta\theta < 10^{-10}$ rad $/ \sqrt{H_z}$

$\Rightarrow$ ACTIVE STABILIZATION AND PASSIVE FILTERING of the LASER BEAM

Laser stabilizations

ORSAY + PISA

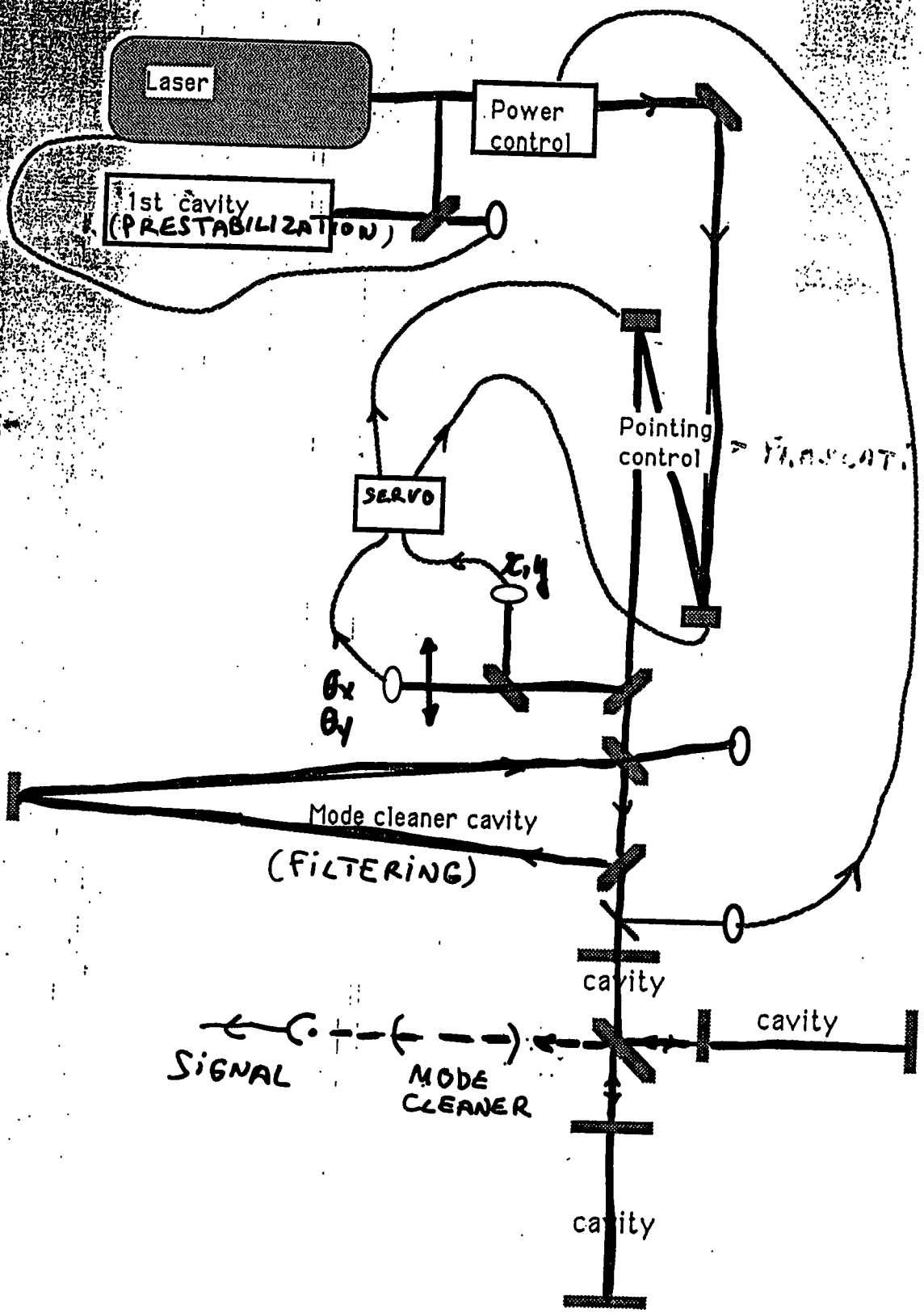

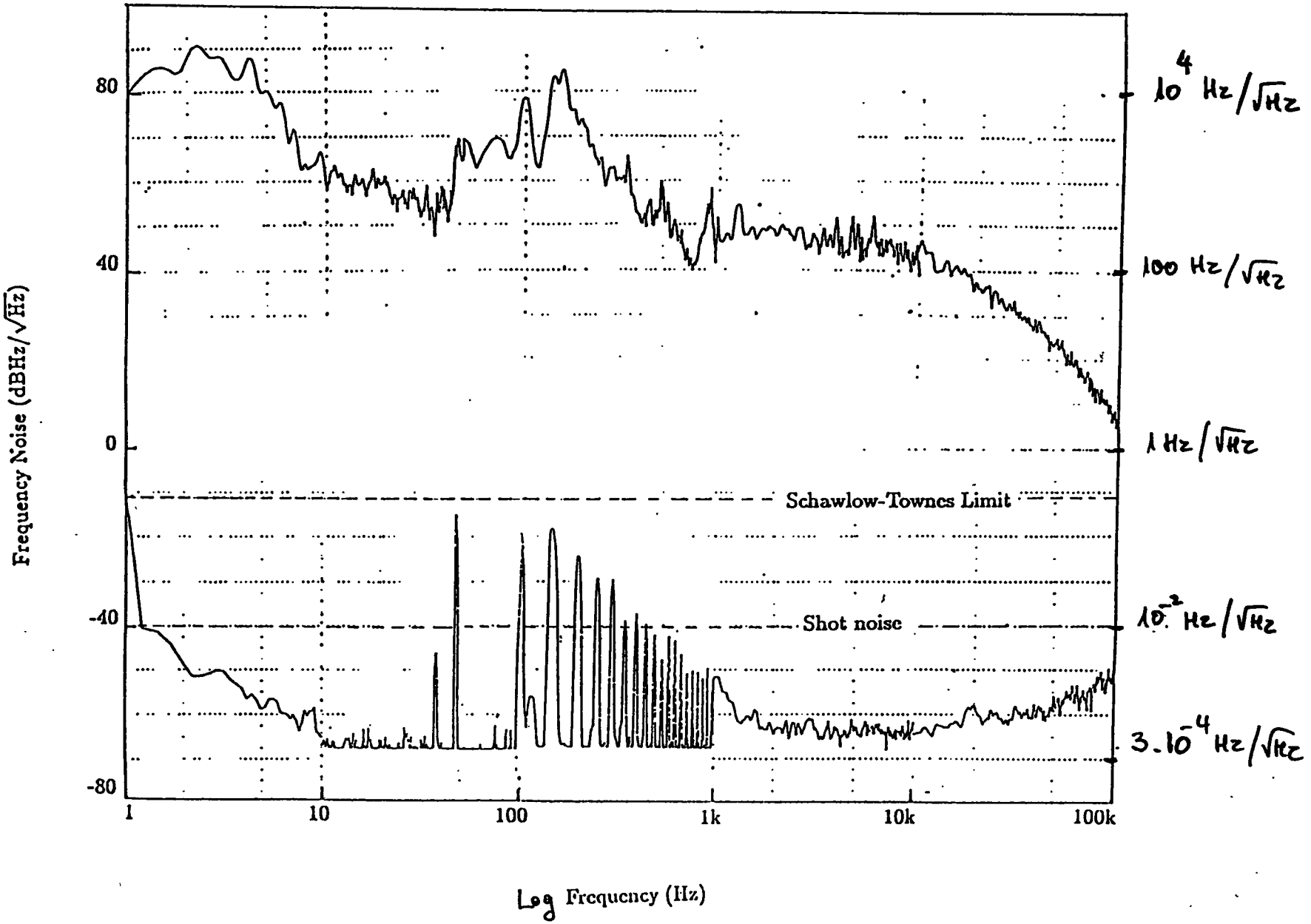
80
40
0
-40
-80
1
10
100
1k
10k
100k
Frequency Noise (dBHz/√Hz)
Log Frequency (Hz)
Schawlow-Townes Limit
Shot noise
10^4 Hz/√Hz
100 Hz/√Hz
1 Hz/√Hz
10^-2 Hz/√Hz
3.10^-4 Hz/√Hz

STABILISATION DE FREQUENCE

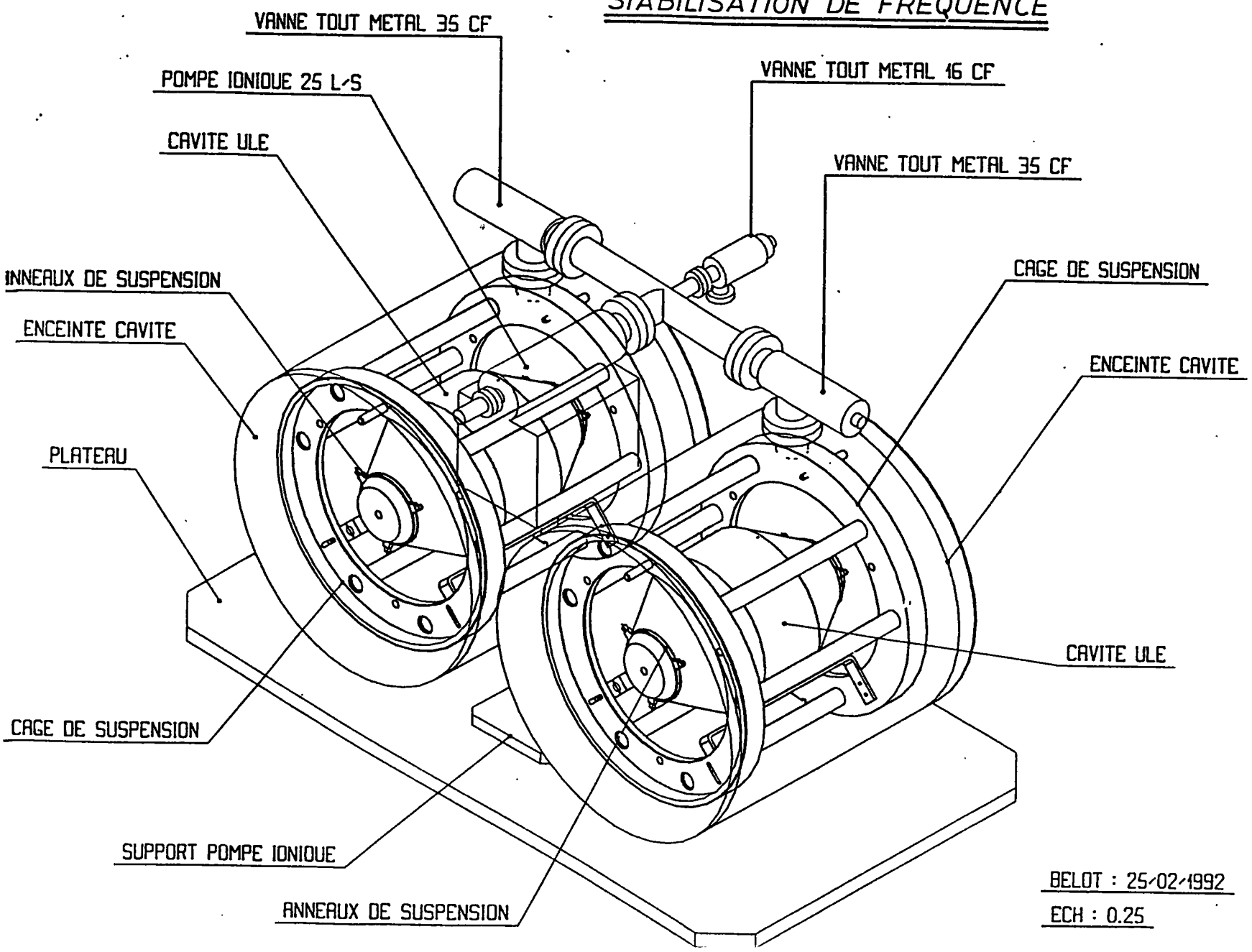

BELOT : 25/02/1992

ECH : 0.25

Suppression des oscillations de relaxation du laser YAG

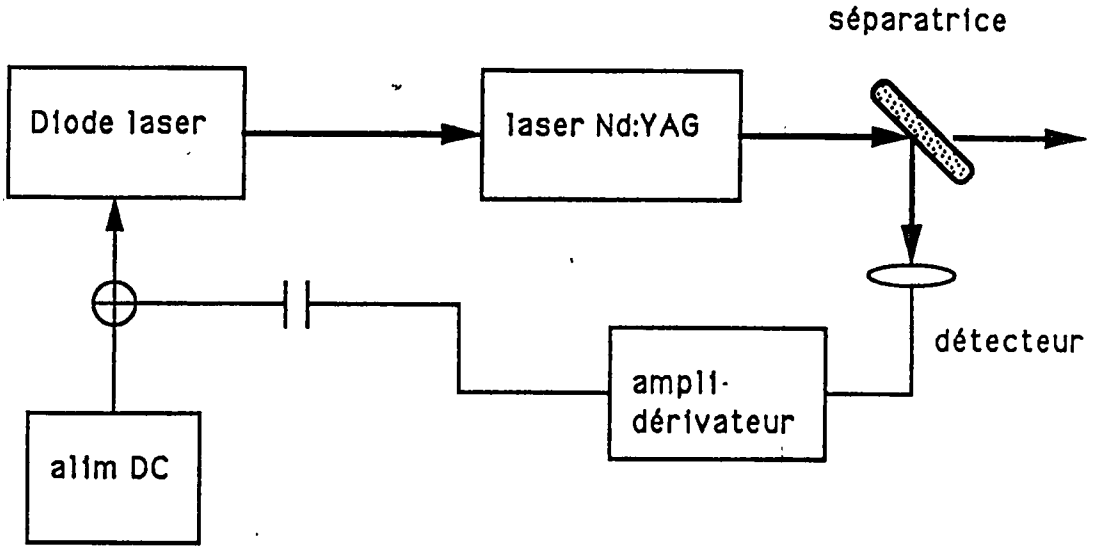

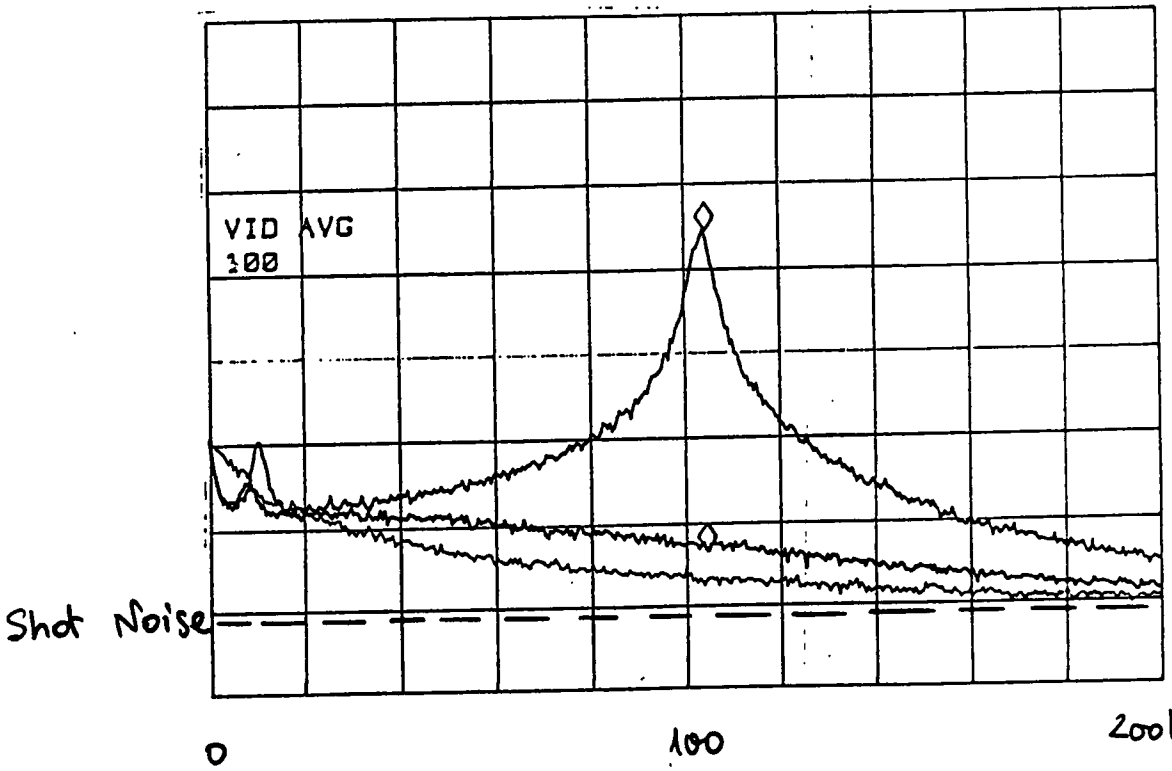

beam, and to use low thermal impedance submounts to extract the waste heat with minimum temperature rise. The pump array consist of an array of 10 diodes mounted on individual water cooled submounts, placed themselves on an insulating mounting, serving to hold the set of diodes.

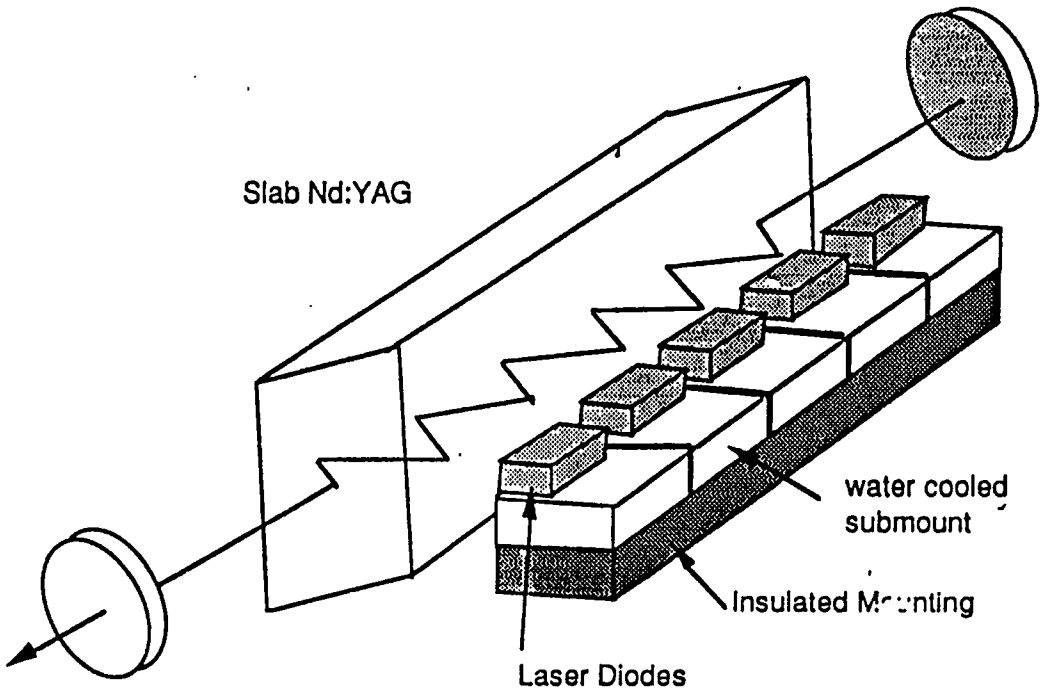

1.2 Performance of the Prototype

The output power will depend on many parameters: the pumping efficiency, the extraction efficiency, the cavity losses, the gain per pass in the medium, and the optimum output coupler. To choose the resonator parameters, one must consider two factors which play important roles: the filling factor and the aperture losses. A large beam radius fills well the volume of the slab but may be severely clipped by the slab edges and losses are the major obstacle to the laser performance. Therefore we choose a beam radius which is a good compromise between the two conditions. The other factor that counts in the design of the cavity is the ease of monomode operation. The first two conditions are quite contradictory with the third one, but we can find a way to fulfill all the conditions if we add a diaphragm into the cavity to select spatially only the TEM_{00} mode.

To avoid spatial hole burning in the laser and appearance of parasitic oscillations, we will use a ring cavity in a x configuration, formed by four mirrors. It is easy to find the equivalent linear cavity and to apply the usual stability conditions. If we take a cavity length of about 50 cm and a curved mirror of 1m radius of curvature, the TEM_{00} mode

le 8 Octobre 1992

R_c $R_{50} = 0{,}5$ mΩ

R $R_{50} = 2\,\Omega$

$L = 25$ µm

$L = 25$ µm.

2ω horizontal = 760 µm

2ω vertical = 970 µm

$P = 2{,}30$ W

16,0°C

105, 2-3

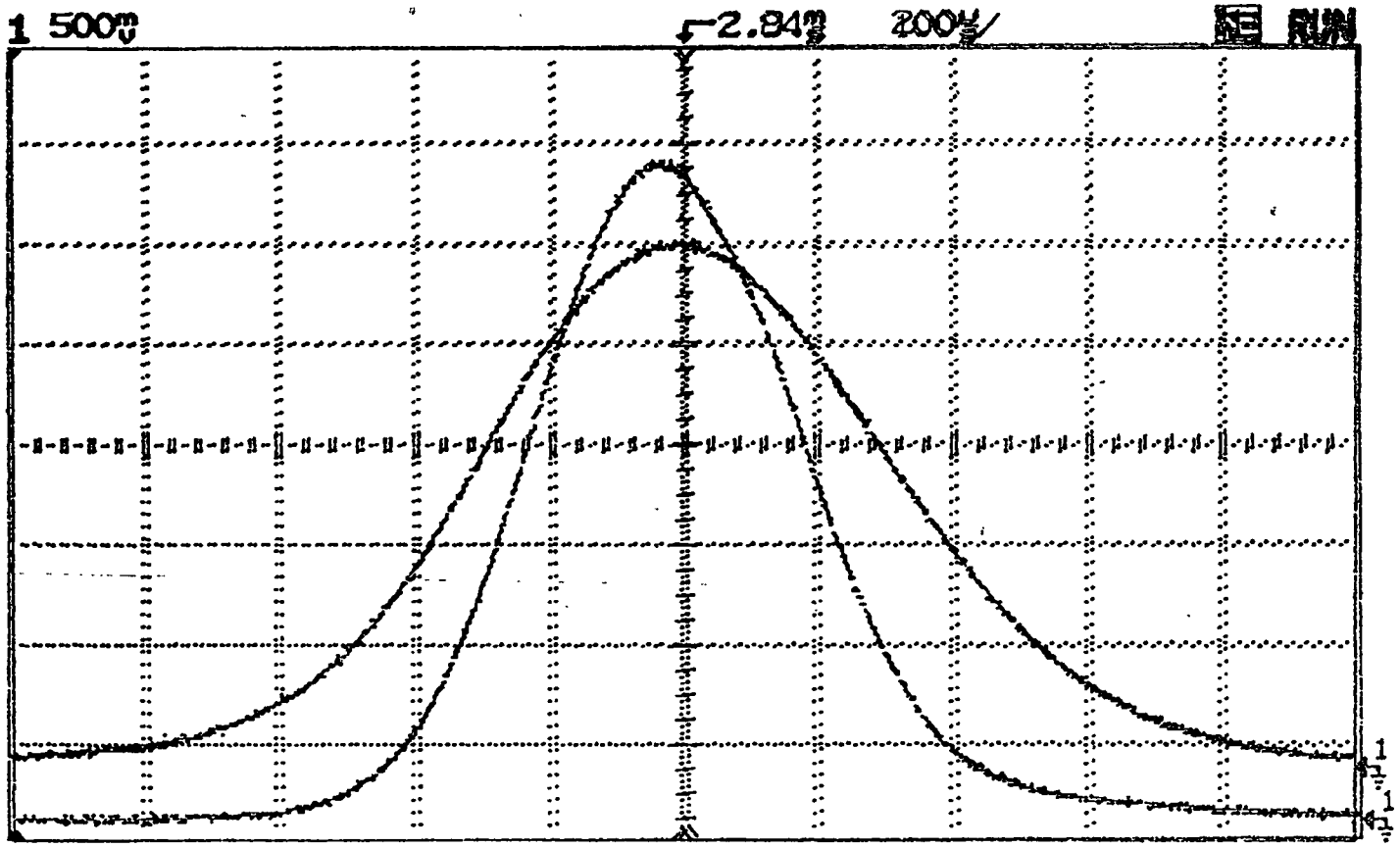

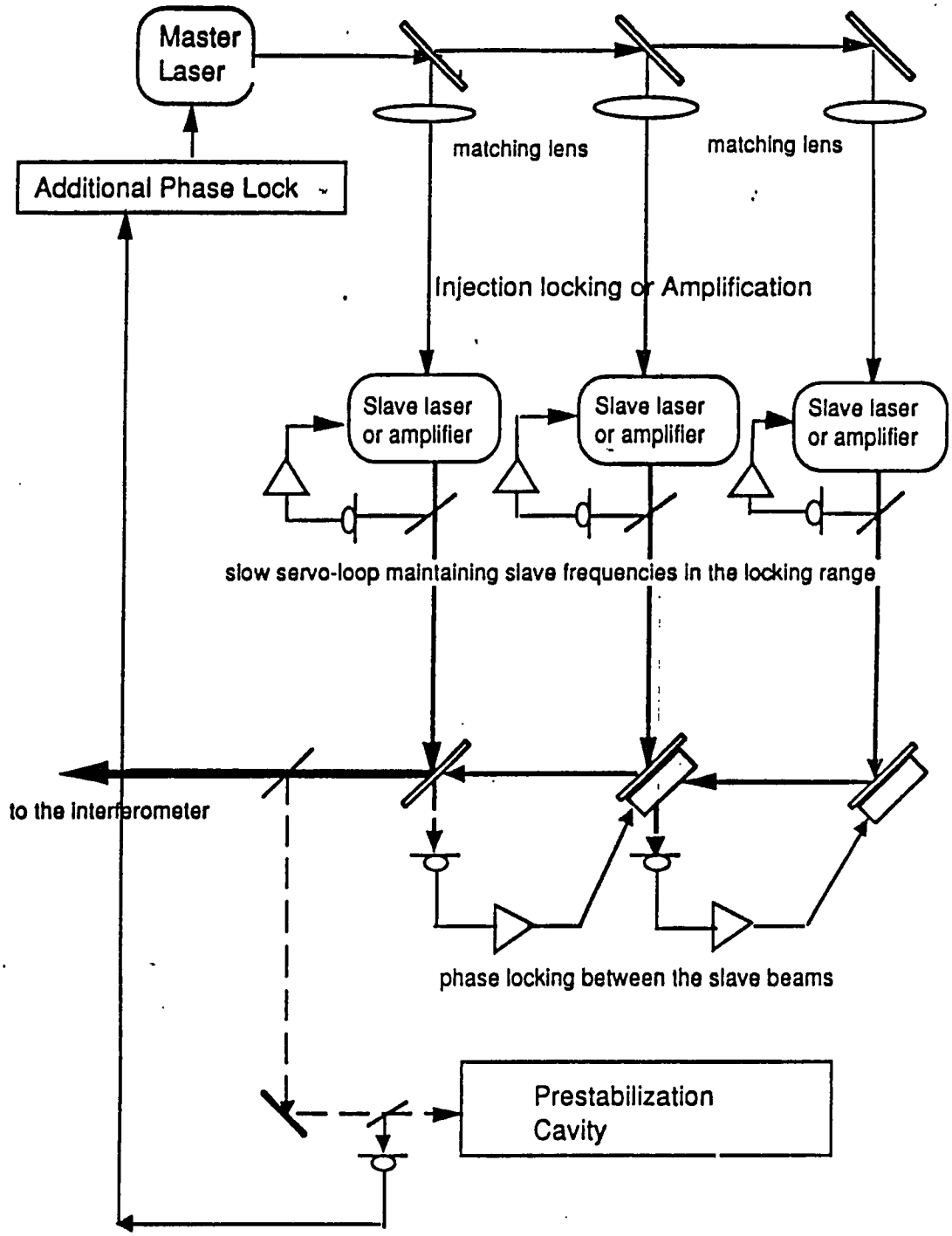

Figure 1 : Virgo Laser System and the Phase-Locking loops

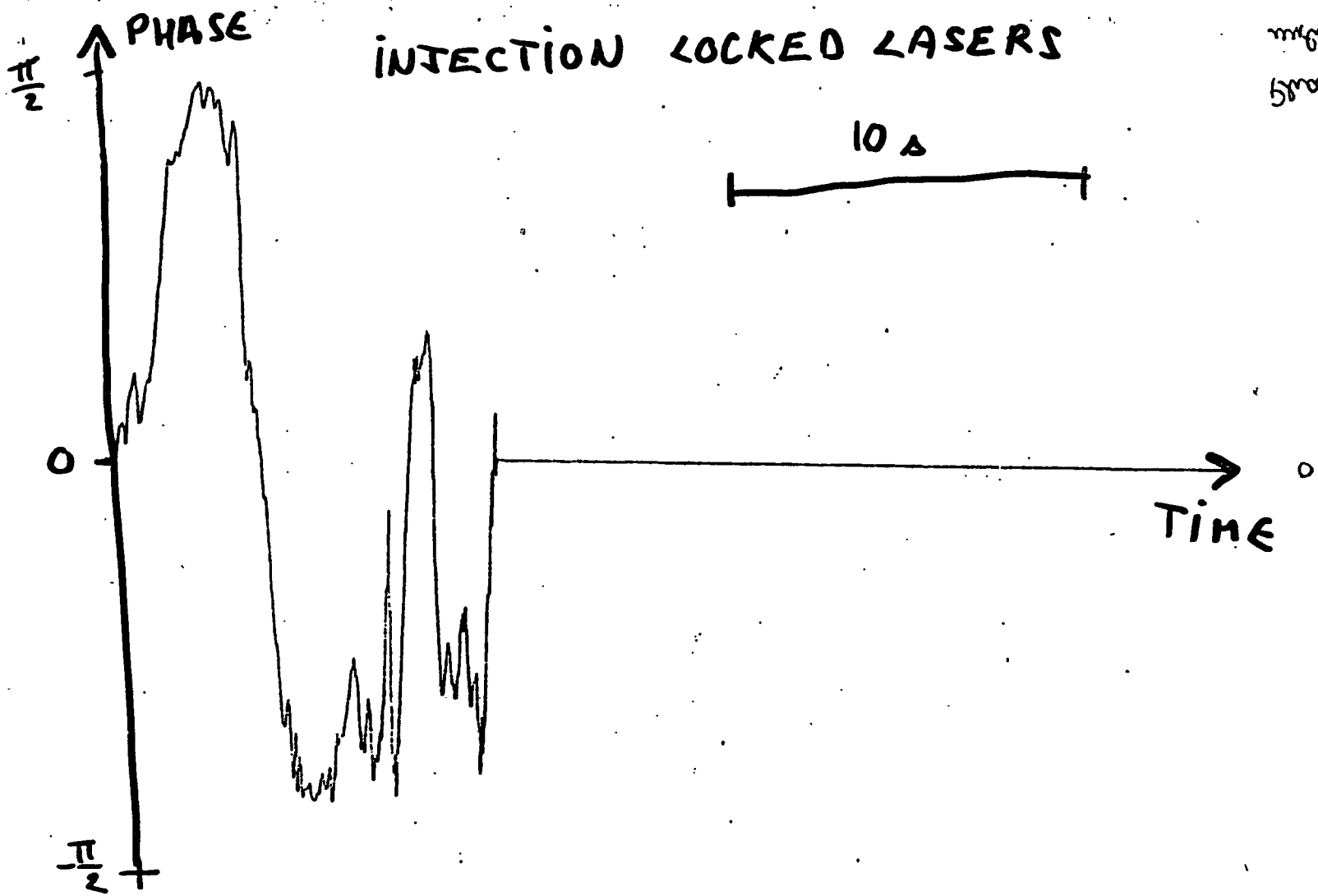
INJECTION LOCKED LASERS
PHASE
$\frac{\pi}{2}$
0
$-\frac{\pi}{2}$
10 s
TIME

Pour une direction transverse

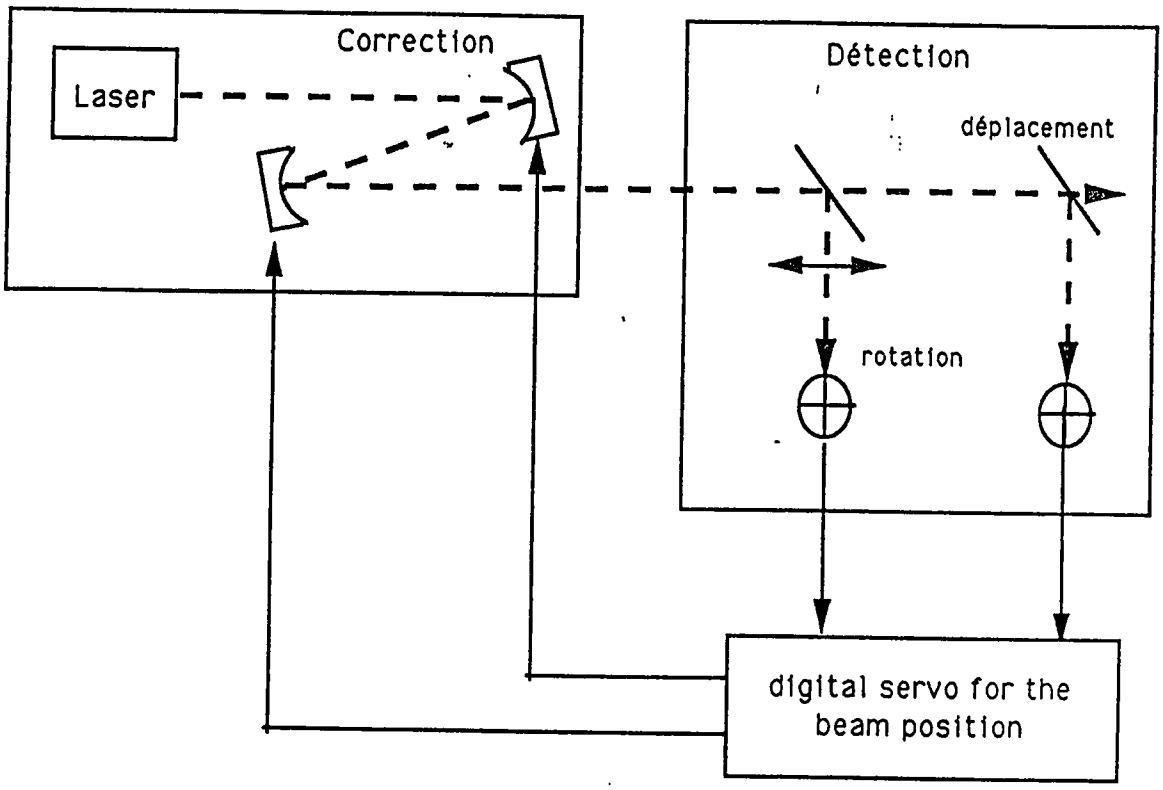

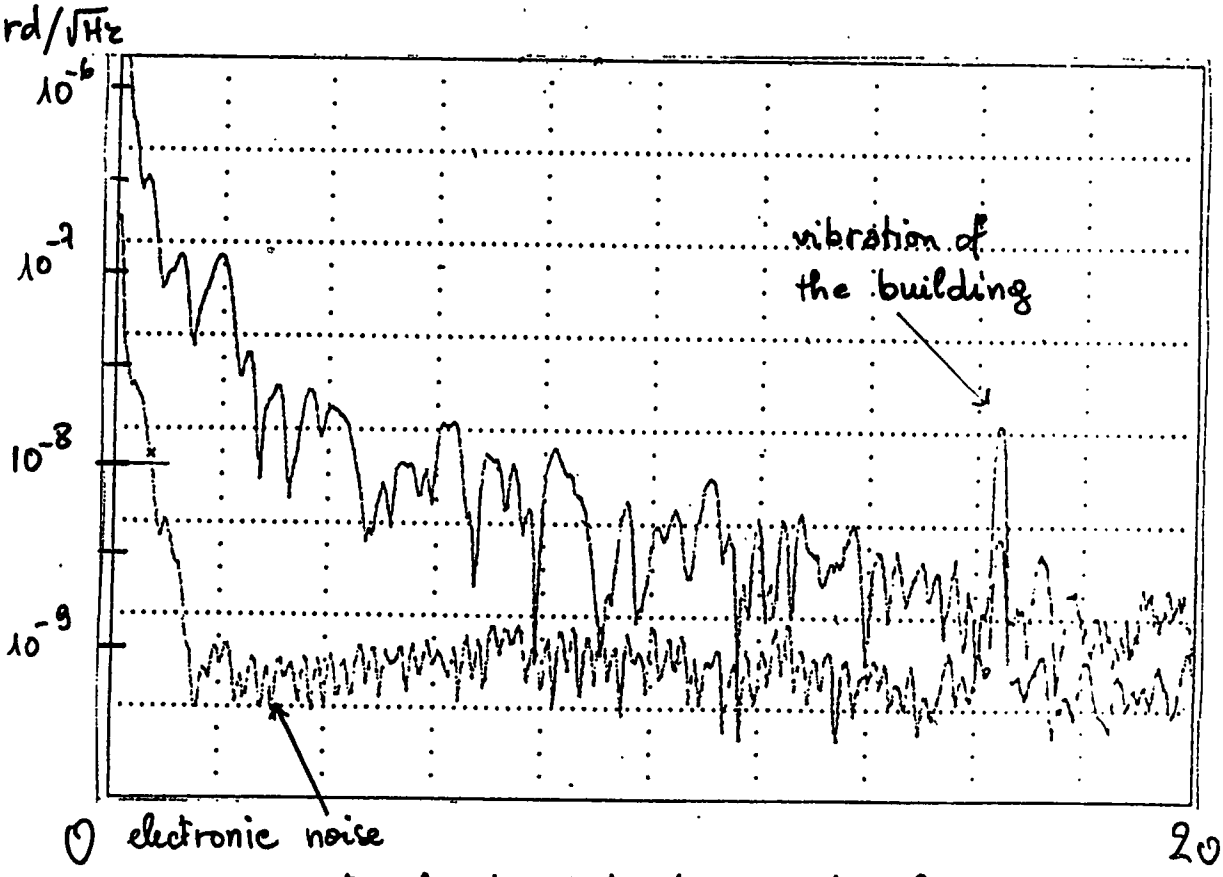

Measurement of absolute beam displacement

FIG. 3

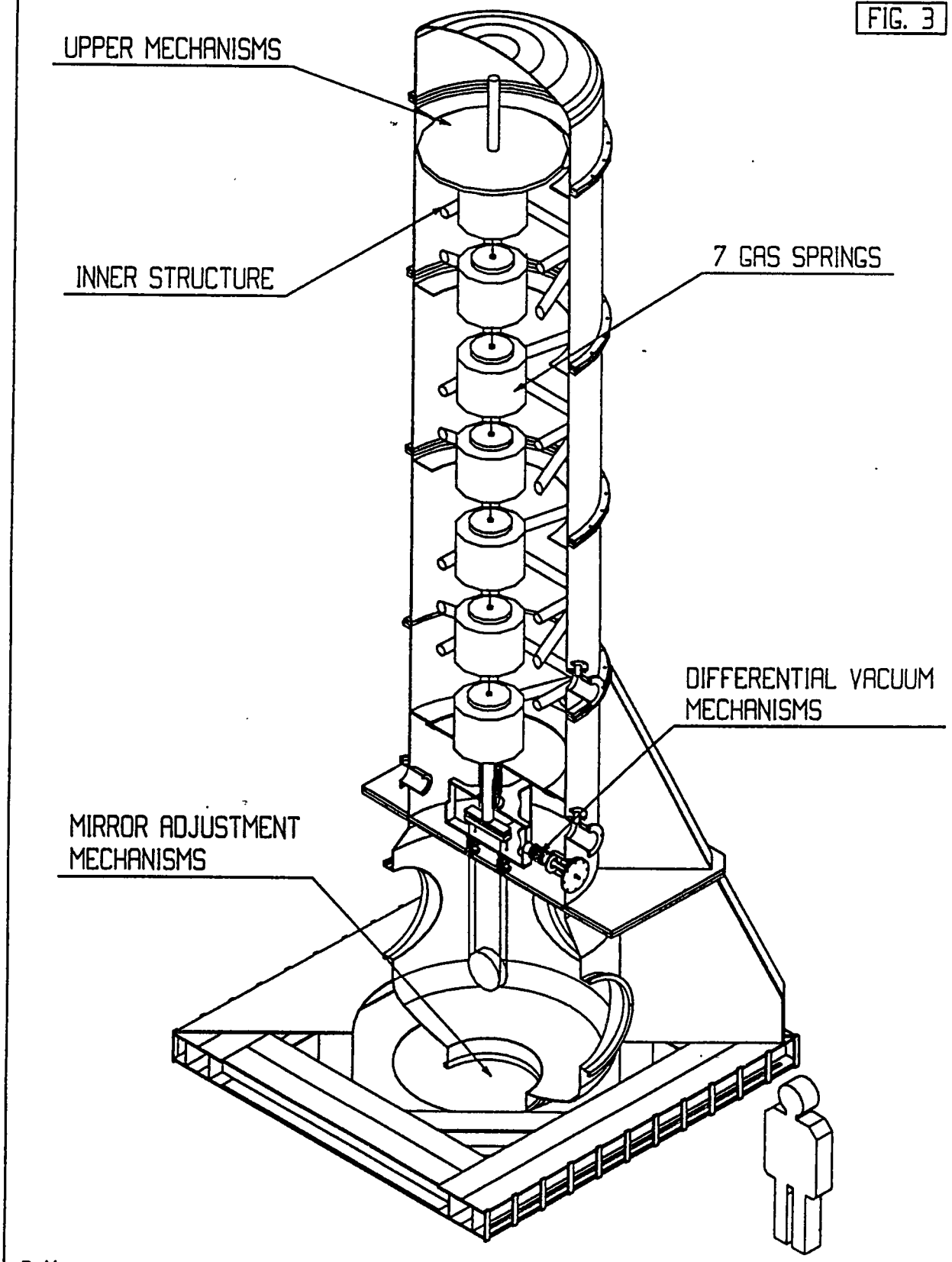

P. Mugnier
le 6-2-92

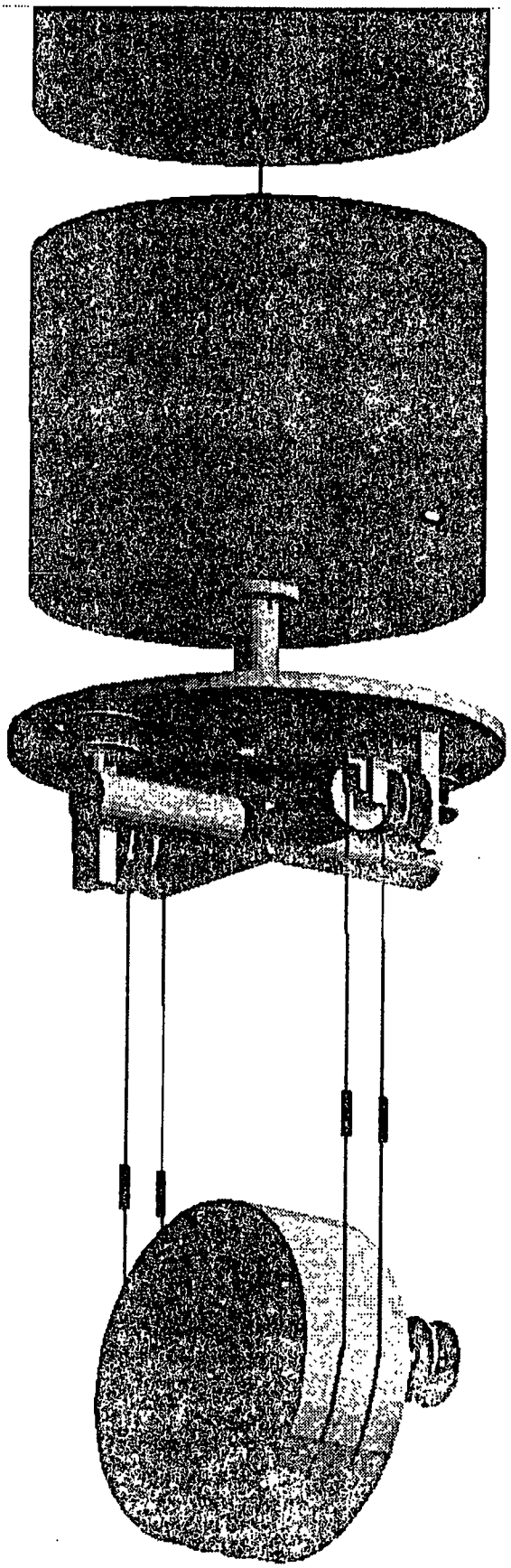

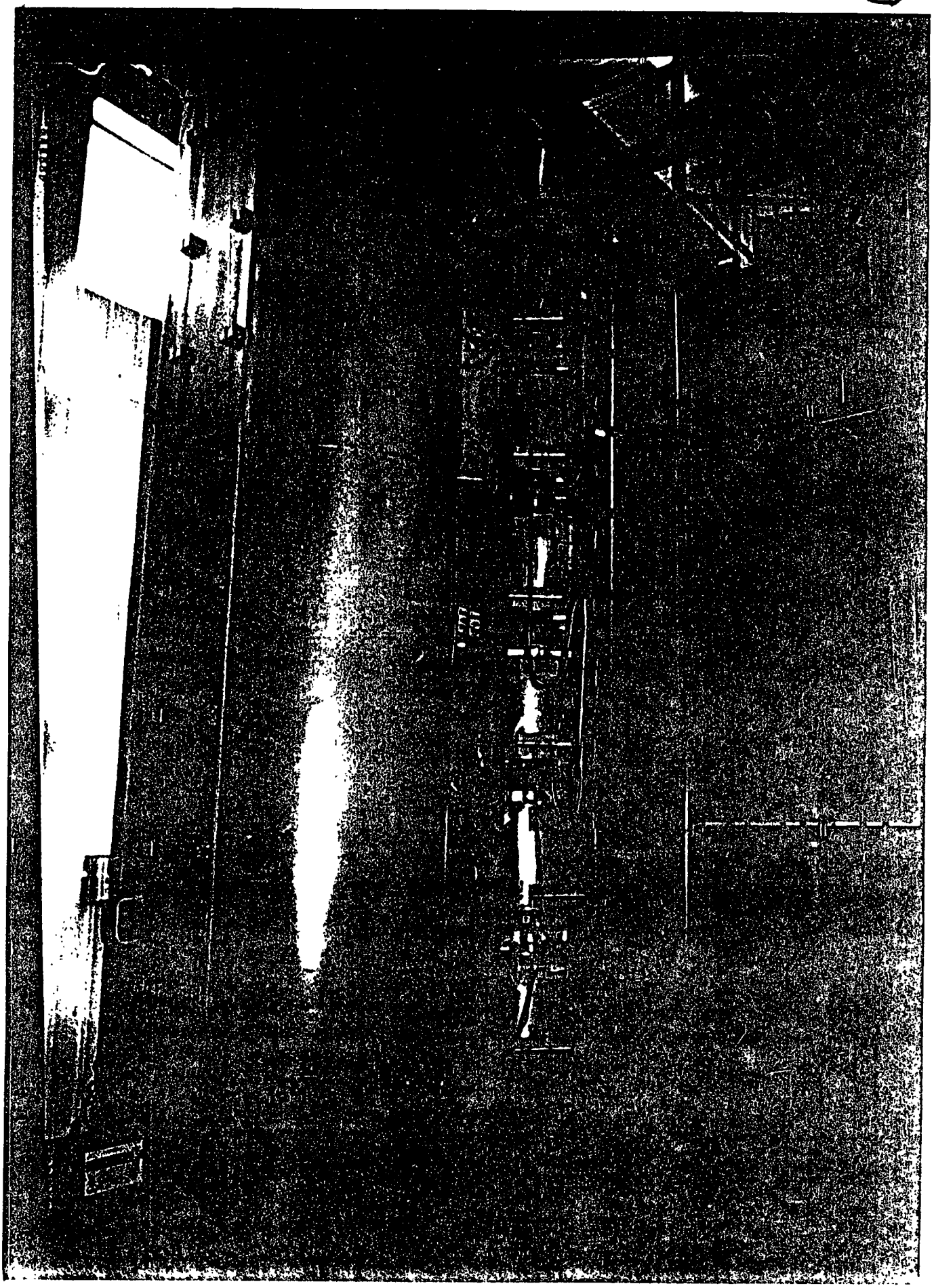

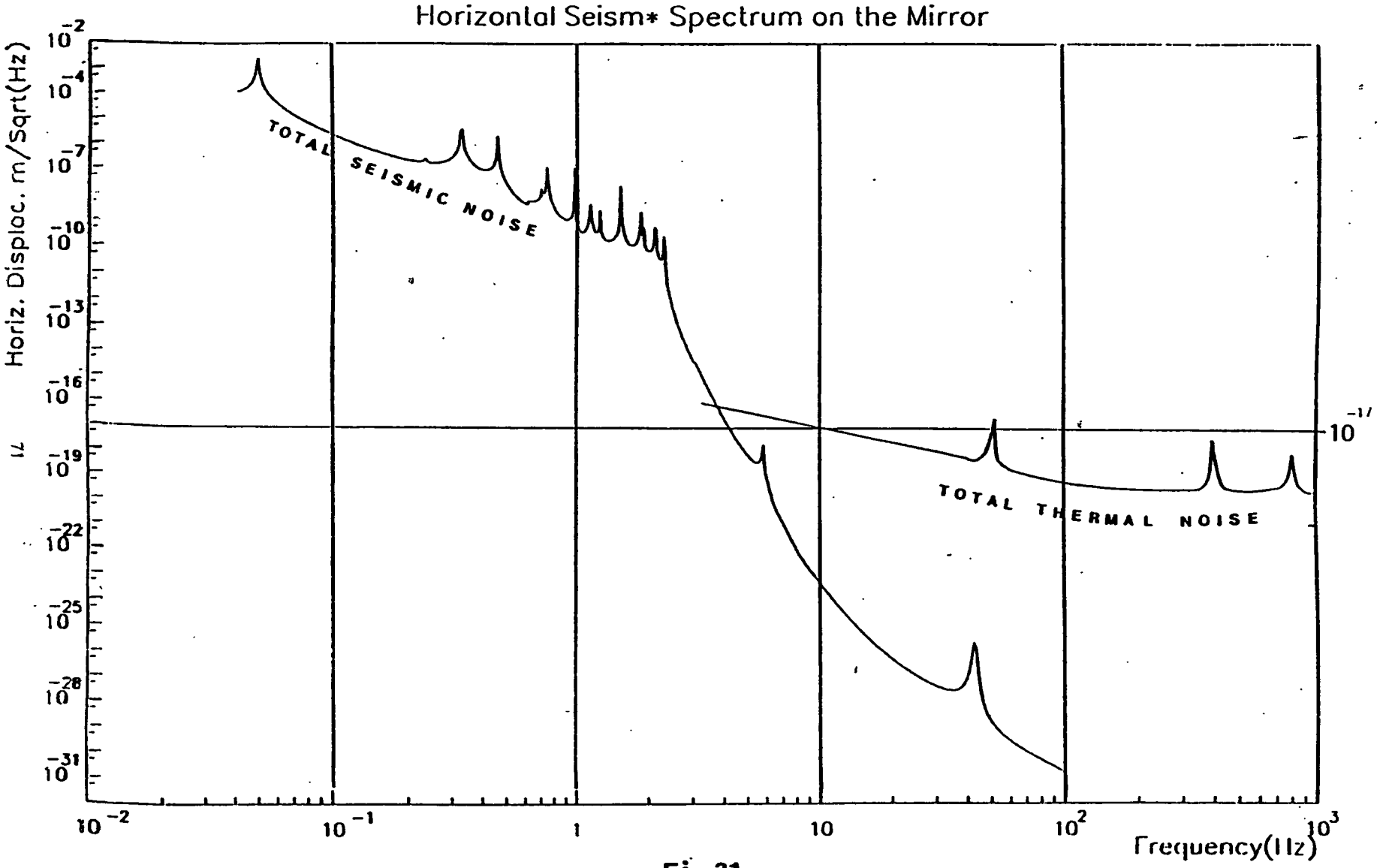
Horizontal Seism* Spectrum on the Mirror
Horiz. Displac. m/Sqrt(Hz)
TOTAL SEISMIC NOISE
TOTAL THERMAL NOISE
Frequency(Hz)

Fig.31

SYSTUS FRAMASOFT+CSI

VAX-2311 10-09-91

MIROIR 400/100

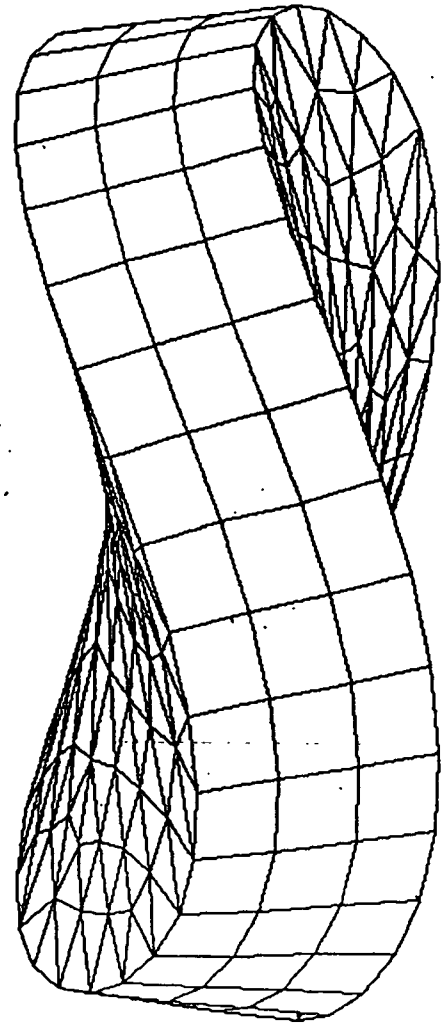

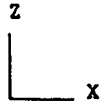

PROBLEMES MECANIQUES :

RESONANCES + AMORTISSEMENT

↓

BRUIT THERMIQUE

$$\tilde{h} \sim \frac{1}{L}\sqrt{\frac{4kT\omega_0}{MQ\omega^4}}$$

(modèle de bruit blanc)

↙

- OPTIMISATION de la GEOMETRIE ET DES MATERIAUX (MIROIRS, SUSPENSIONS)

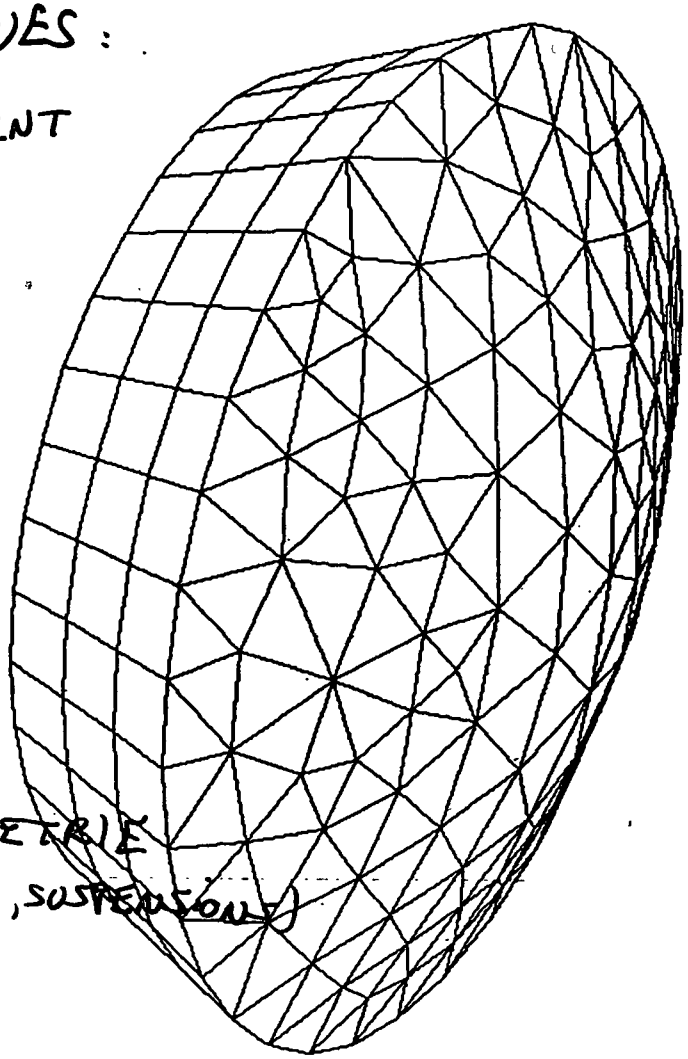

- RECHERCHE de MODELES REALISTES
  - de TECHNIQUES DE MESURE

FREQUENCE = 4741.7 Hz

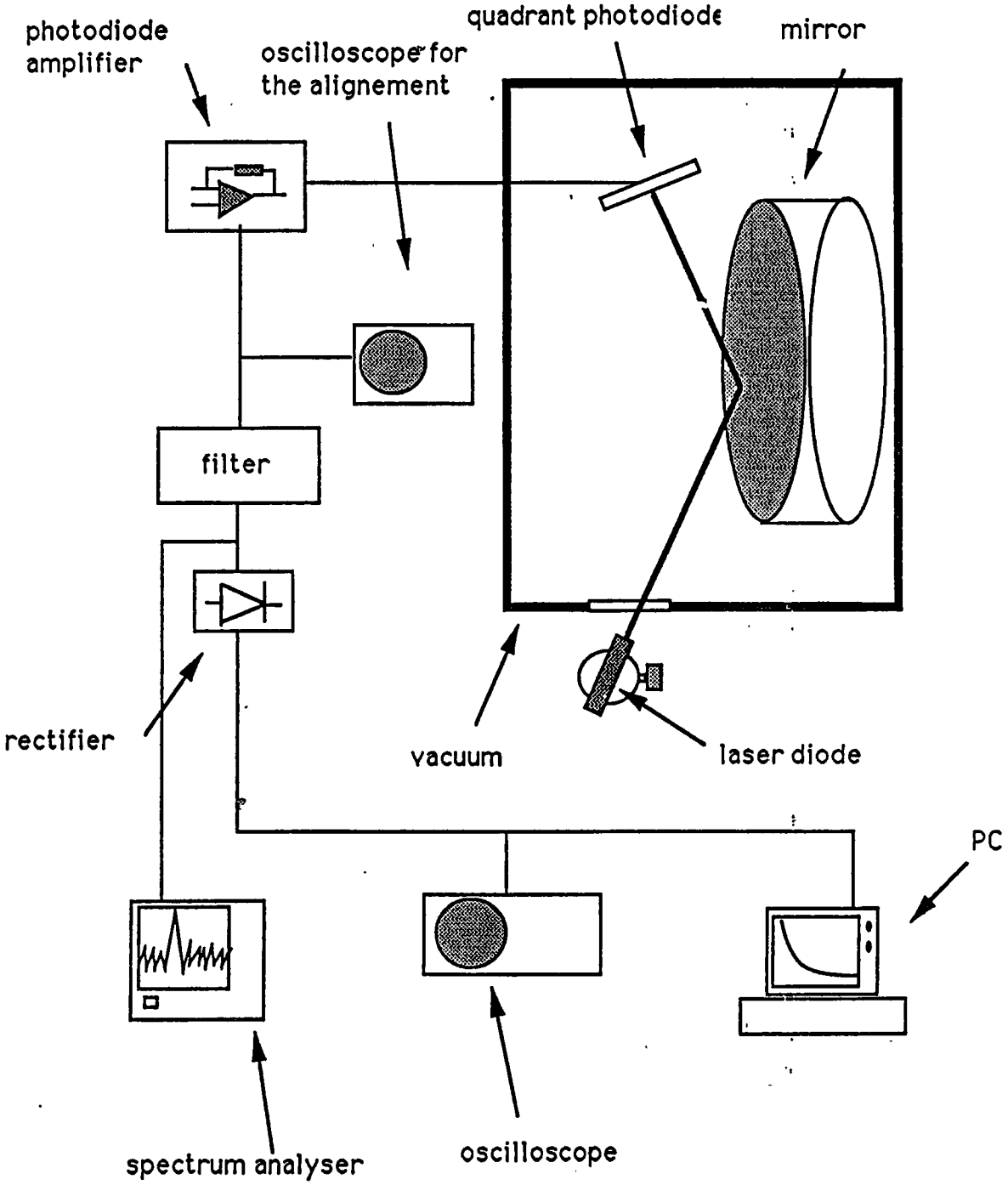
photodiode amplifier
oscilloscope for the alignement
quadrant photodiode
mirror
filter
rectifier
vacuum
laser diode
PC
spectrum analyser
oscilloscope

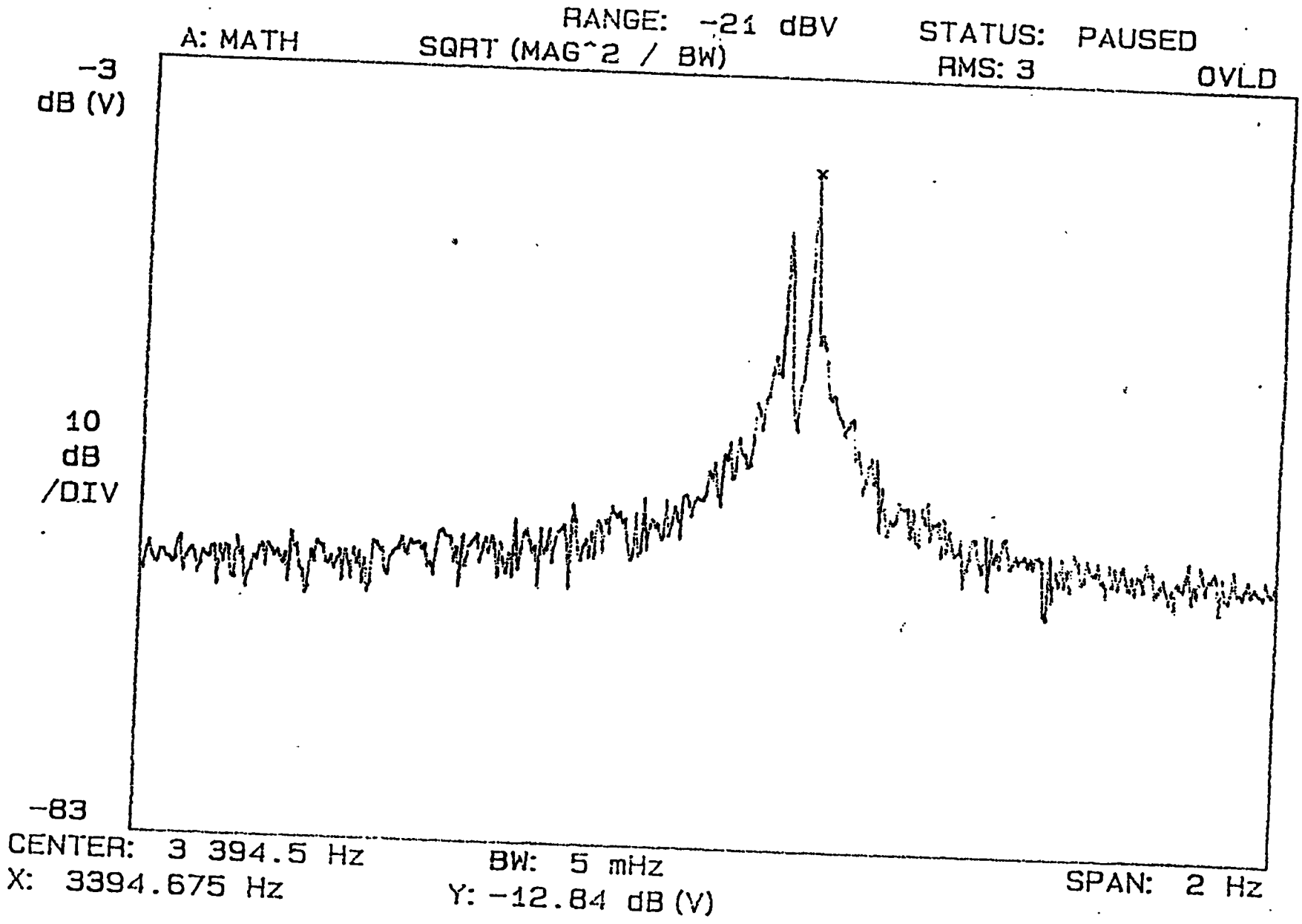
RANGE: -21 dBV
A: MATH
SQRT (MAG^2 / BW)
STATUS: PAUSED
RMS: 3
OVLD
-3
dB (V)
10
dB
/DIV
-83
CENTER: 3 394.5 Hz
BW: 5 mHz
SPAN: 2 Hz
X: 3394.675 Hz
Y: -12.84 dB (V)

$f = 3394\ Hz$ $\quad Q \# 1{,}1 \cdot 10^6$

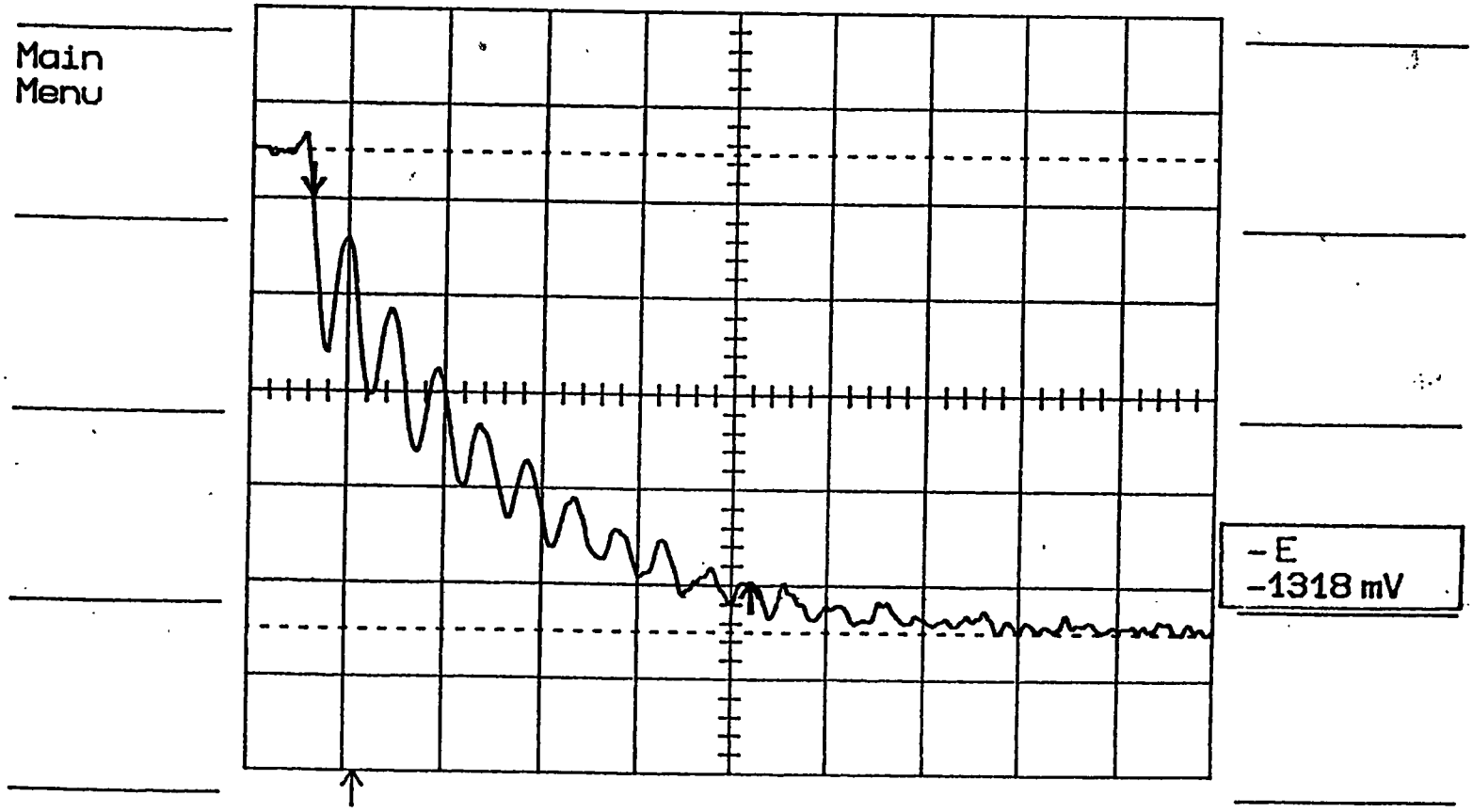

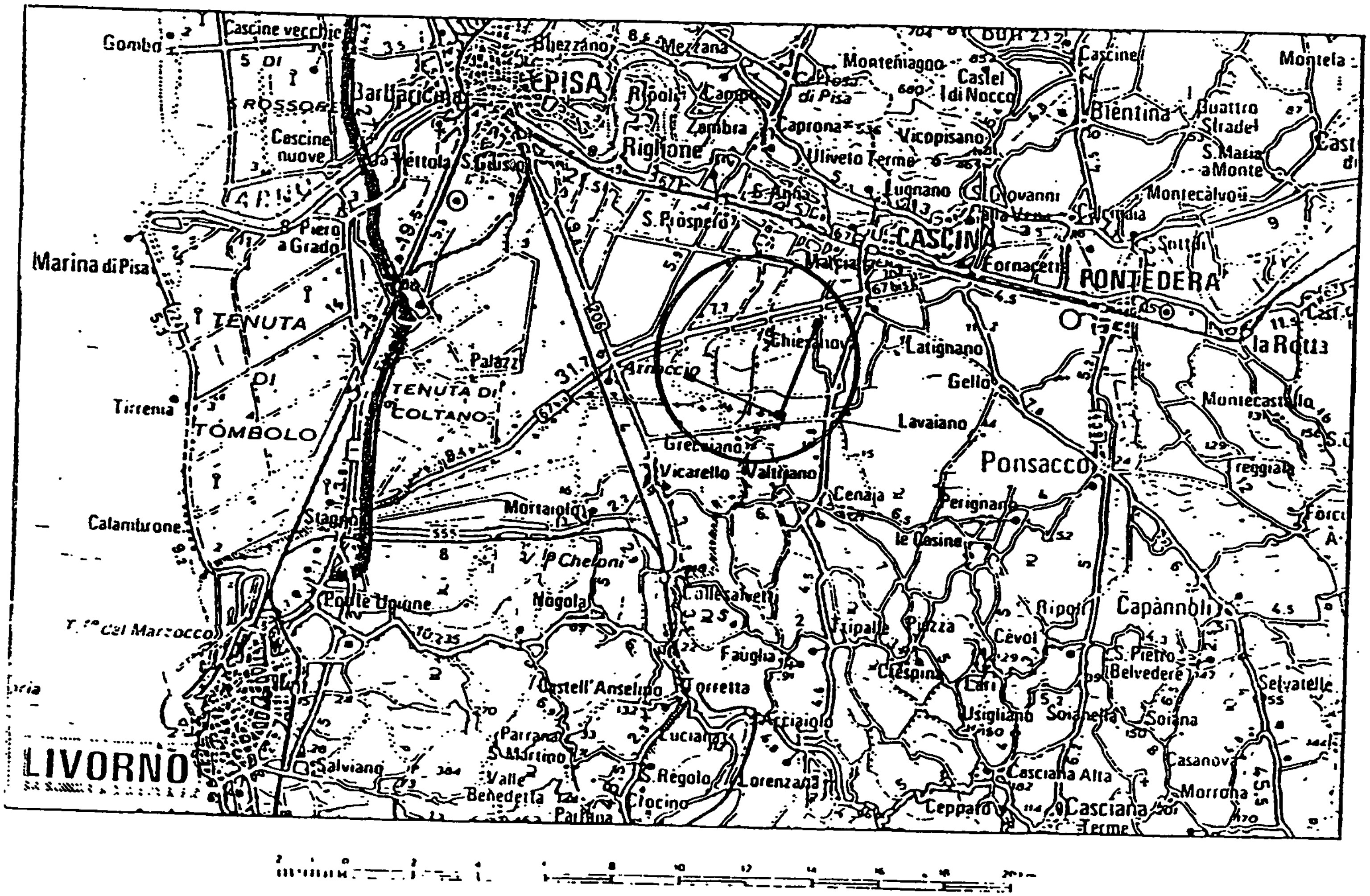

Gombo
Cascine vecchie
ROSSORE
Cascine nuove
Barbaricina
PISA
Bliezzano
Mezzana
Ripoli
Zambra
Riglione
S. Giusto
S. Piero a Grado
Marina di Pisa
TENUTA
DI
TOMBOLO
Tirrenia
Calambrone
Stagno
Palazzi
TENUTA DI COLTANO
S. Prospero
S. Anna
Montemagno
Castel di Nocco
Caprona
Vicopisano
Uliveto Terme
Lugnano
S. Giovanni alla Vena
Bientina
Quattro Strade
S. Maria a Monte
Montecalvoli
Calcinaia
CASCINA
Fornacette
PONTEDERA
la Rotta
Latignano
Gello
Lavaiano
Arnaccio
Grecciano
Vicarello
Valtriano
Mortaiolo
Cenaja
Perignano
le Casine
Ponsacco
Montecastello
Capannoli
Nugola
Collesalvetti
Fauglia
Crespina
Usigliano
Soianella
Soiana
Ripoli
Cevoli
S. Pietro Belvedere
Selvatelle
Casanova
Morrona
Casciana Alta
Casciana Terme
Ceppato
Lorenzana
Acciaiolo
Torretta
Luciana
S. Regolo
Crocino
Castell'Anselmo
Parrana S. Martino
Valle Benedetta
Salviano
LIVORNO

Fig. 1

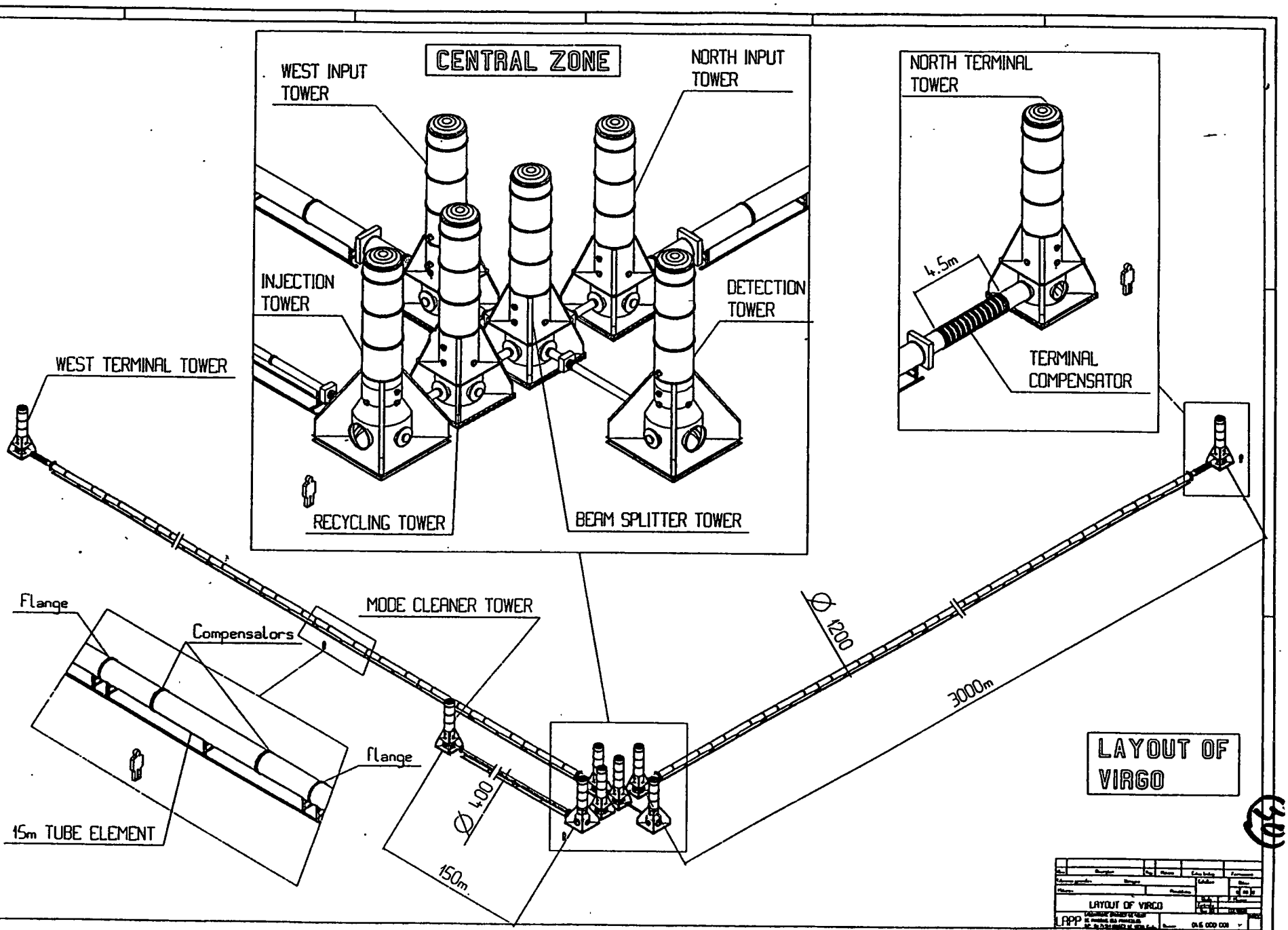
CENTRAL ZONE
WEST INPUT TOWER
NORTH INPUT TOWER
INJECTION TOWER
DETECTION TOWER
RECYCLING TOWER
BEAM SPLITTER TOWER
NORTH TERMINAL TOWER
4.5m
TERMINAL COMPENSATOR
WEST TERMINAL TOWER
MODE CLEANER TOWER
Flange
Compensators
flange
15m TUBE ELEMENT
Ø 400
150m
Ø 1200
3000m
LAYOUT OF VIRGO
LAYOUT OF VIRGO
LAPP

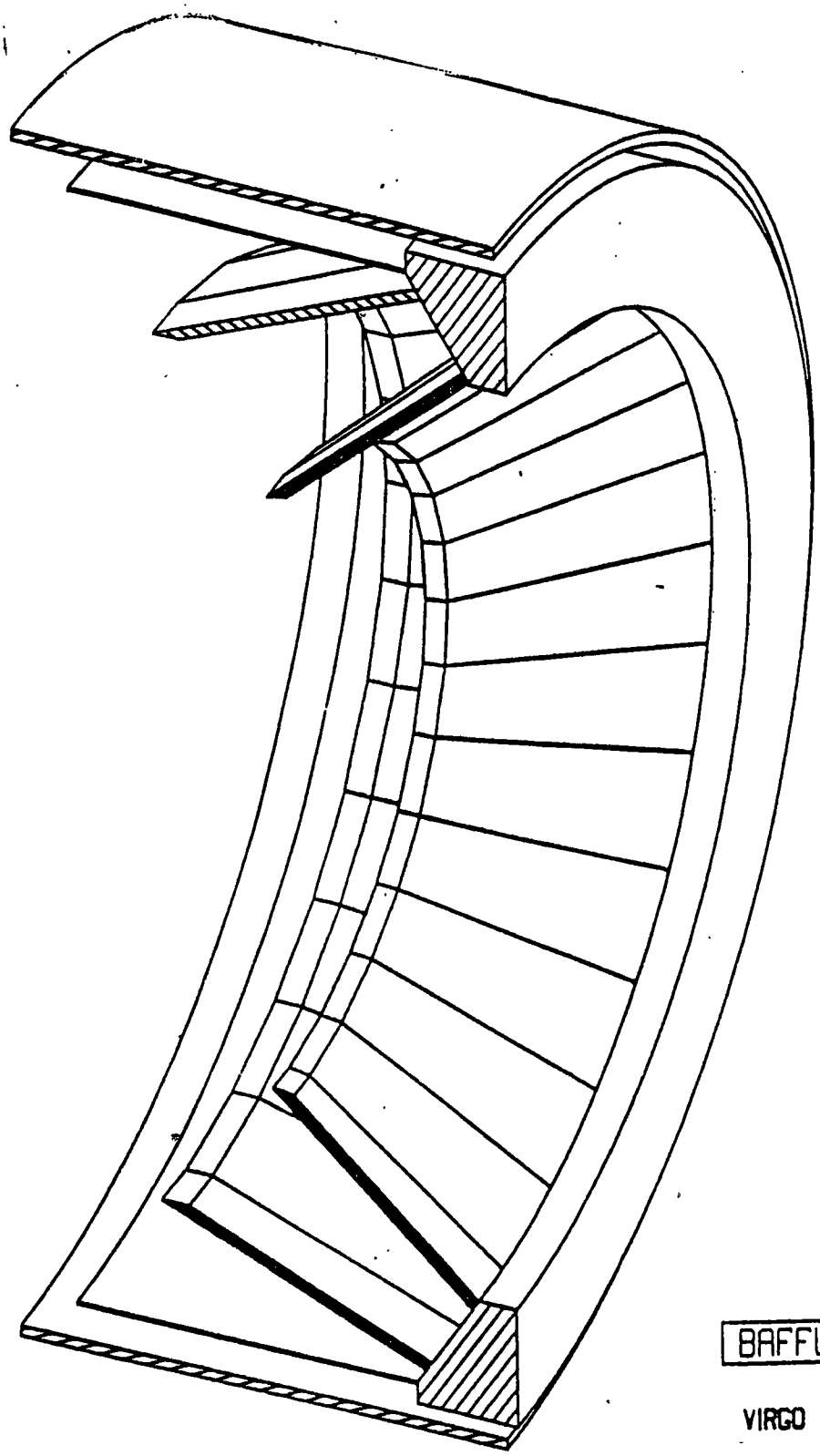

BAFFLE

VIRGO

11-04-1992 0.4 R2

IQOR302A

FIG.4

V.B R.R

requirement is to have a flexible system which allows us to record more informations for debugging purposes or to inject recorded data or simulated signal at various level in order to test and debug the system.

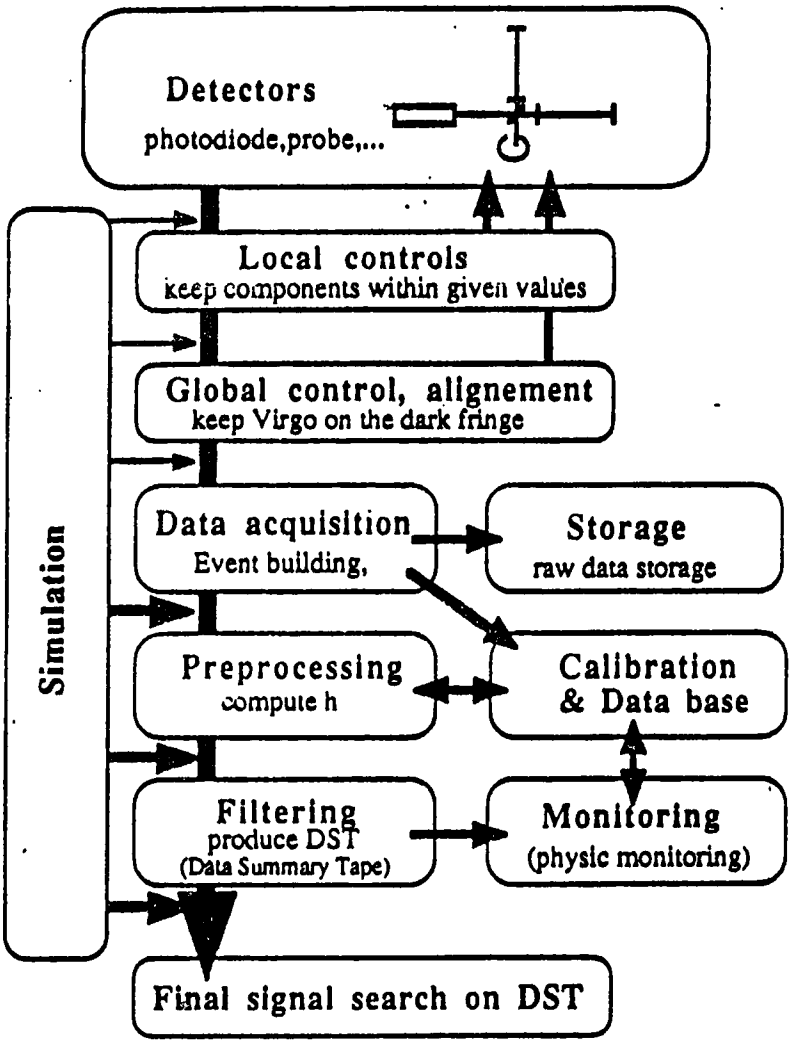

Figure 1. The Virgo data flow

3. Data flow implementation

MILESTONES

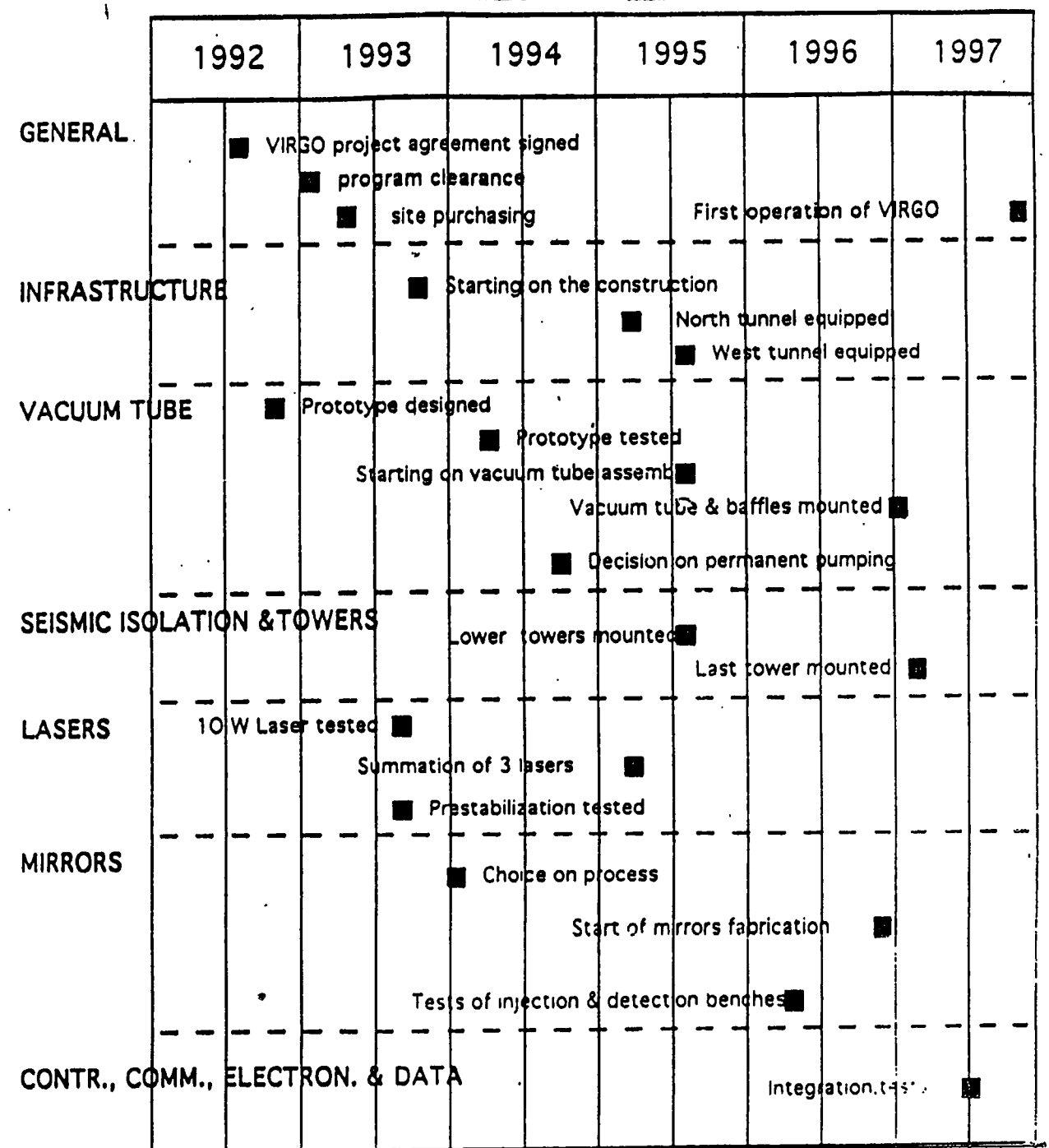

M. Ecus	0,5	1.5	2,42	5,02	10,32	29,02	2,35	1,07

62,19

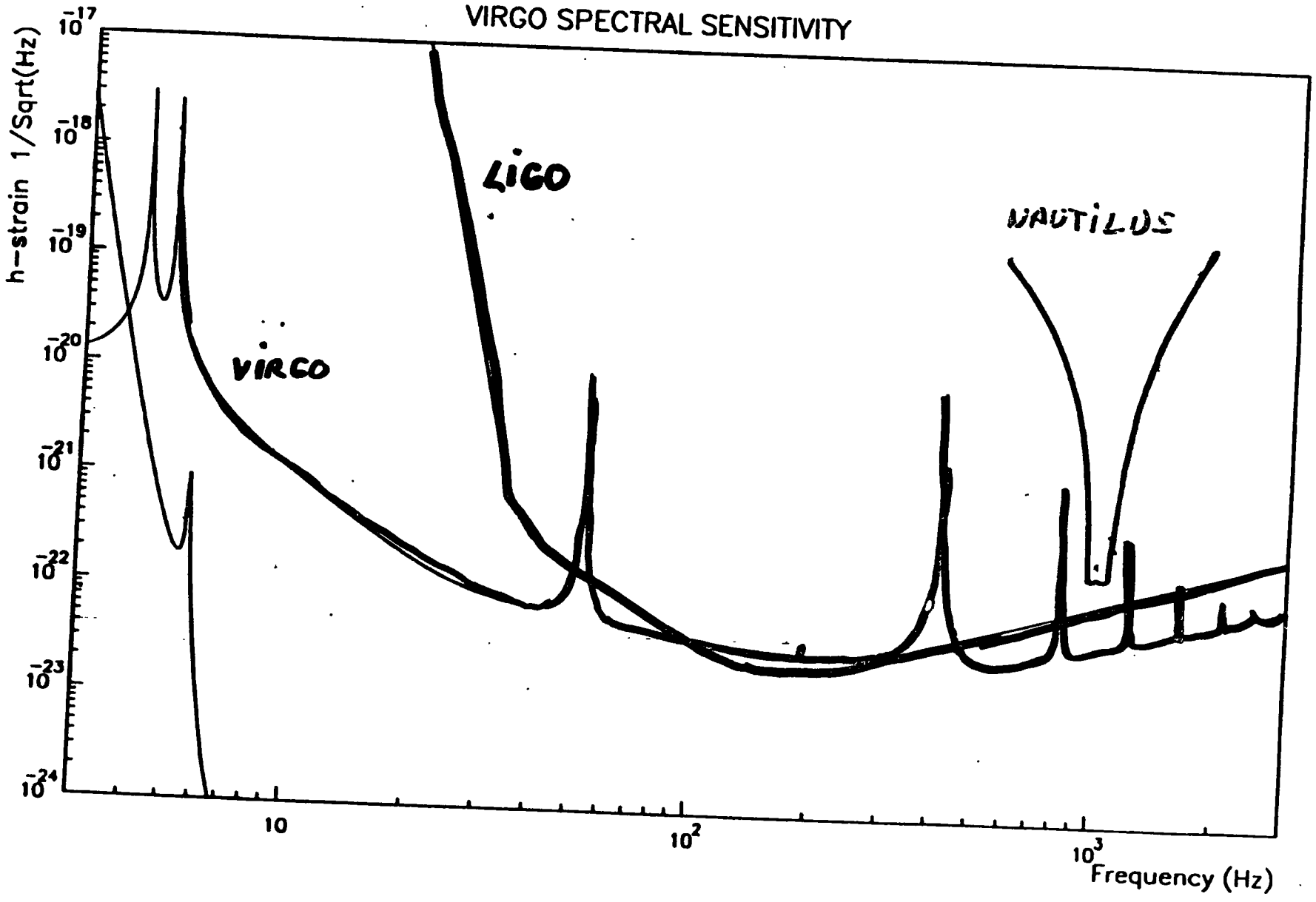
VIRGO SPECTRAL SENSITIVITY
h-strain 1/Sqrt(Hz)
10^{-17}
10^{-18}
10^{-19}
10^{-20}
10^{-21}
10^{-22}
10^{-23}
10^{-24}
LIGO
NAUTILUS
VIRGO
10
10^2
10^3
Frequency (Hz)

Viewgraphs presented at International Symposium on Neutrino Astrophysics, Takayama, Japan (October 1992)—sent to us by Seiji Kawamura.

Distributed by R. Vogt 11/12/92

PLEASE PASS ALONG PROMPTLY

A. Abramovici
J. Camp
A. Kuhnert
F. Raab
M. Regehr
R. Savage
L. Sievers
R. Spero
M. Zucker

Science Library -last

cc: W. Althouse
R. Vogt
S. Whitcomb
MIT Science Group
Project File
Science Library

European Projects

- VIRGO (cf Brillet) Pisa. 3 km. ≃ approved. Recycling Fabry-Perot design
- GEO. Germany-UK. Hannover. 8 km. Money frozen. Dual-recycling delay line design.

Delay-line: With Dual Recycling (Meers)

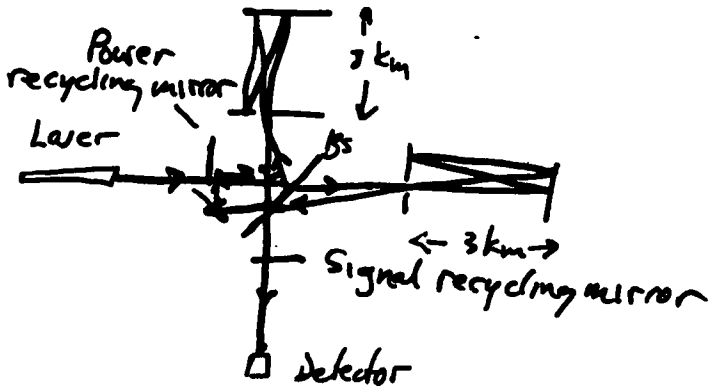

Groups presently operating prototypes of length 10 m and 30 m, sensitivity $\sim 10^{-16}$. Data run of 100 hrs set limit $\sim 10^{-17}$ on bursts. Further analysis going on. More runs possible.

Groups will collaborate with VIRGO.

Networks of GW detectors

- 2 detectors required for minimal confidence that an event is real
- 3 interferometers (6 bars) needed to reconstruct wave: direction, polarization, amplitude.
- 2 (nearby) detectors can search for cosmic background
- 1 interferometer can perform all-sky search for pulsars, with massive computing

Working with other instruments

- γ-ray burst detectors. 2 interferometers and BATSE (or equivalent) can reconstruct wave.
- ν burst detector. 2 interferometers and Superkam can reconstruct wave.

Such coincidences allow one to lower the threshold of gw detectors, increasing their range.

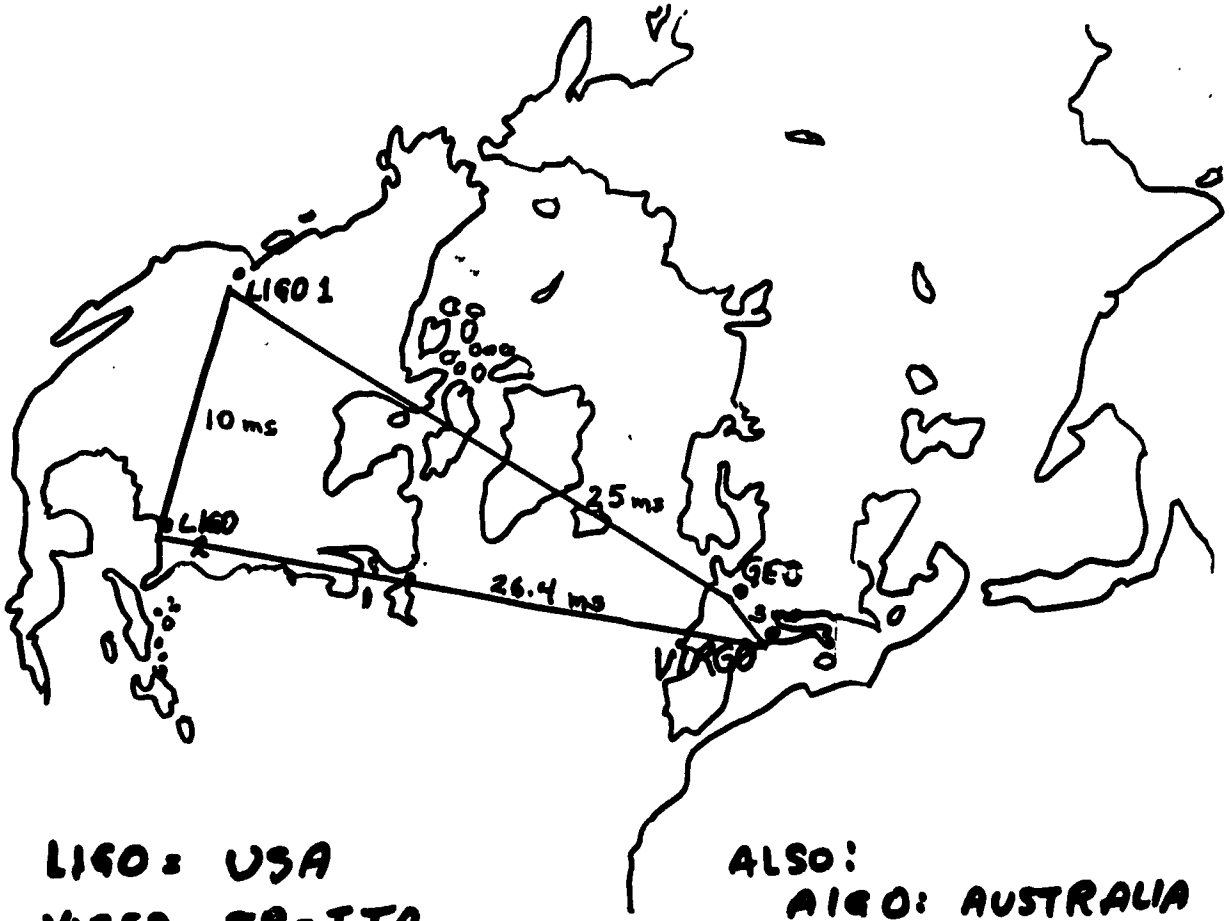

LIGO: USA
VIRGO: FR-ITA
GEO: GER-UK

ALSO:
AIGO: AUSTRALIA
TENKO: JAPAN

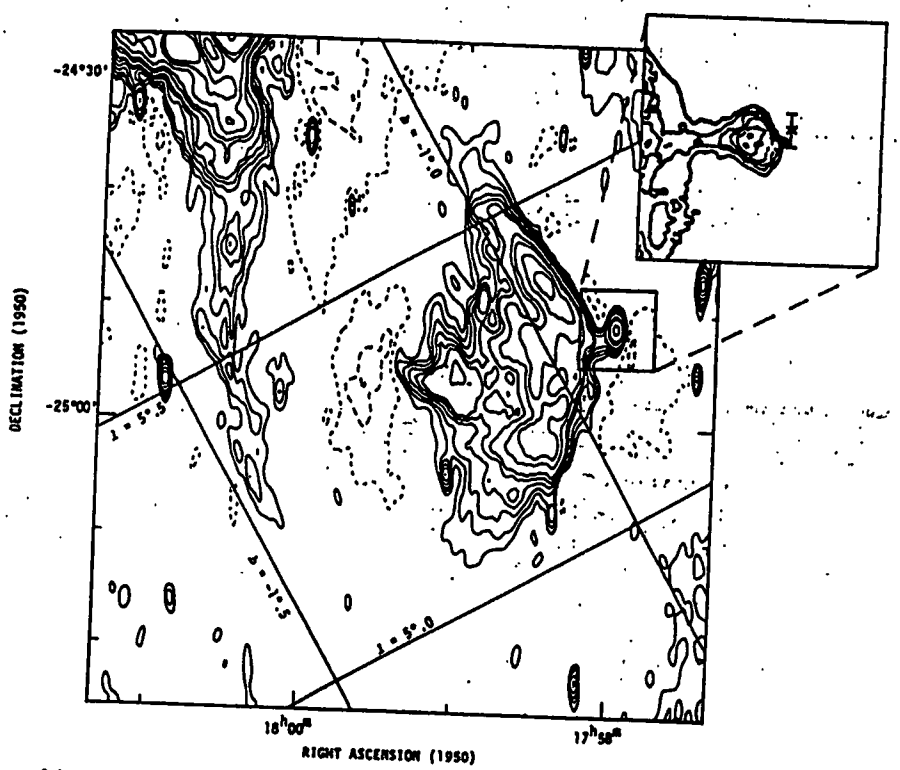

Figure 1. Radio image of the supernova remnant G5.4 − 1.2 (Caswell *et al.* 1987) with a VLA image of the compact component G5.27 − 0.90 (Becker & Helfand 1985) (inset). The timing position of the pulsar PSR 1758 − 24 is marked on the inset with a cross. Error bars in the declination direction are shown; in the right ascension direction the positional uncertainty is less than the width of the line.

the remnant as illustrated in Fig. 1 (inset). The position error in right ascension is smaller than the width of the line; the error in declination is larger because this pulsar lies close to the ecliptic plane. The pulsar is located at the extreme western edge of the compact nebula G5.27 − 0.90; the derived position is consistent with location within the small 'bump' on the Becker & Helfand (1985) image. Independent observations using the Very Large Array by Frail & Kulkarni (1991) confirm this location for the pulsar.

3 DISCUSSION

The location of the pulsar relative to G5.27 − 0.90 and G5.4 − 1.2 confirms the association with the supernova remnant and suggests that both the pulsar and the compact nebula are moving in a westerly direction at such a high velocity that they have overtaken the shell. Further evidence for the association is obtained from the agreement of the pulsar characteristic age with the estimated age for G5.4 − 1.2, about 14 000 yr (Caswell *et al.* 1987). Distance estimates for the pulsar and remnant are also in good agreement. Using the surface-brightness/diameter relationship of Caswell & Lerche (1979), Caswell *et al.* (1987) estimated the distance to G5.4 − 1.2 to be ~5 kpc which compares well with a distance to the pulsar of 4.4 kpc based on the dispersion measure (Table 1) and a new model for the galactic electron density distribution (Taylor, Lyne & Manchester, in preparation). Caswell *et al.* also suggested that G5.27 − 0.90 lies beyond ~5.9 kpc, based on the radial velocities of H_2CO absorption features. Given the small galactic longitude and the consequent uncertainties in the radial velocity–distance relation, this result is not inconsistent with associating G5.27 − 0.90 with the pulsar and with G5.4 − 1.2.

Table 1. Parameters for PSR 1758 − 24.

Right Ascension (J2000)	$18^h00^m59.^s87 \pm 0.^s03$
Declination (J2000)	$-24°50'57'' \pm 32''$
Right Ascension (B1950)	$17^h57^m55.^s14$
Declination (B1950)	$-24°50'35''$
Period	0.12487445209 ± 8 s
Period Derivative	$(127.898 \pm 0.010) \times 10^{-15}$
Second Period Derivative	$(-4.7 \pm 0.5) \times 10^{-24}$ s^{-1}
Period Epoch (Modified Julian Day)	47916.000
R.M.S. residual	930 μs
Dispersion Measure	289 ± 1 cm^{-3} pc
Mean Flux Density at 1520 MHz	0.7 mJy
Characteristic Age	15 500 years
Surface Magnetic Field Strength	4.0×10^{12} G

We conclude, therefore, that PSR 1758 − 24 is associated with both G5.4 − 1.2 and G5.27 − 0.90 and that, together, they form the eighth reasonably well-established pulsar–supernova remnant association after Vela (Large, Vaughan & Mills 1968), the Crab (Staelin & Reifenstein 1968),

ASTROPHYSICS FROM COALESCING BINARIES

- **Measure the masses of hundreds of neutron stars and dozens of black holes.** These masses are parameters that will be automatically measured as part of the detection of the binary.

- **Hubble's constant.** Easy if the event rate is a few per year from within 200 Mpc.

- **Cosmological mass distribution.** Length scales of 100–200 Mpc.

- **Observe black holes coalescing.** This provides a test of strong-field general relativity.

STOCHASTIC BACKGROUND

This could be left over from a number of processes inthe early universe, notably decaying cosmic strings. Two detectors situated within $\lambda/2\pi$ of each other (λ = gravitational wavelength) have optimum sensitivity:

$$\left(\frac{S}{N}\right)_{\text{stochastic}} = 3\left[\frac{f}{100\,\text{Hz}}\right]^{-5/2}\left[\frac{\sigma_{\text{bb}}}{10^{-22}}\right]^{-1} \times$$

$$\times\left[\frac{\Omega_{\text{gw}}}{10^{-8}}\right]^{1/2}\left[\frac{H_0}{100\,\text{km s}^{-1}\,\text{Mpc}^{-1}}\right],$$

where σ_{bb} is the broadband burst sensitivity of the detectors.

An experiment conducted at the lowest frequency gives the largest possible separation between detectors. Even at 100 Hz, however, the detectors need to be within 500 km of each other for optimum sensitivity.

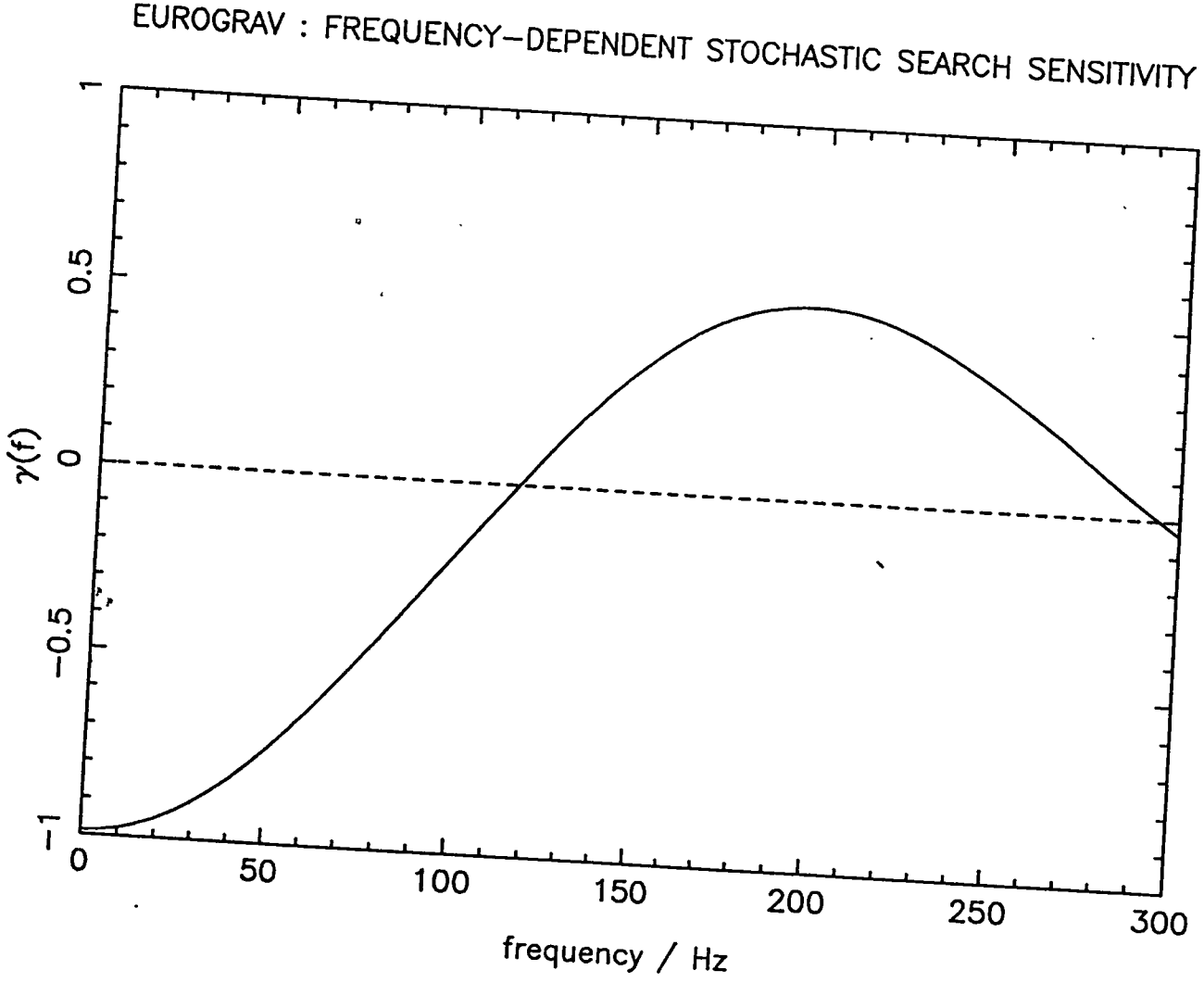

DXN 12–Jun–1992 20:50

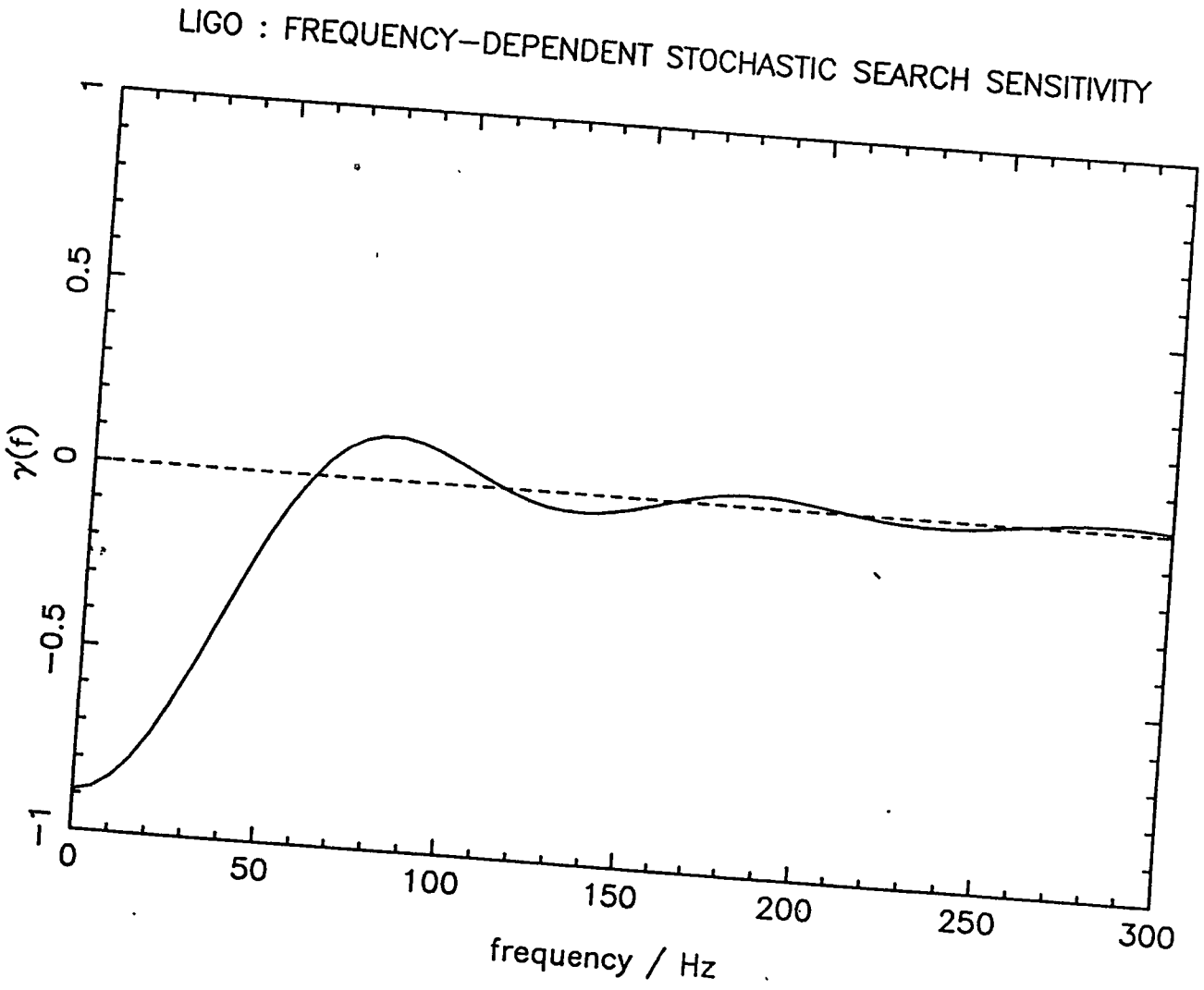
LIGO : FREQUENCY–DEPENDENT STOCHASTIC SEARCH SENSITIVITY
γ(f)
1
0.5
0
−0.5
−1
0
50
100
150
200
250
300
frequency / Hz

Projects of the laser interferometric gravitational wave detectors in Japan

K. Tsubono
Department of Physics, University of Tokyo
Bunkyo, Tokyo 113, Japan

I. Progress report in Japan

II. 3km×3km laser interferometer

III. 300m×300m laser interferometer

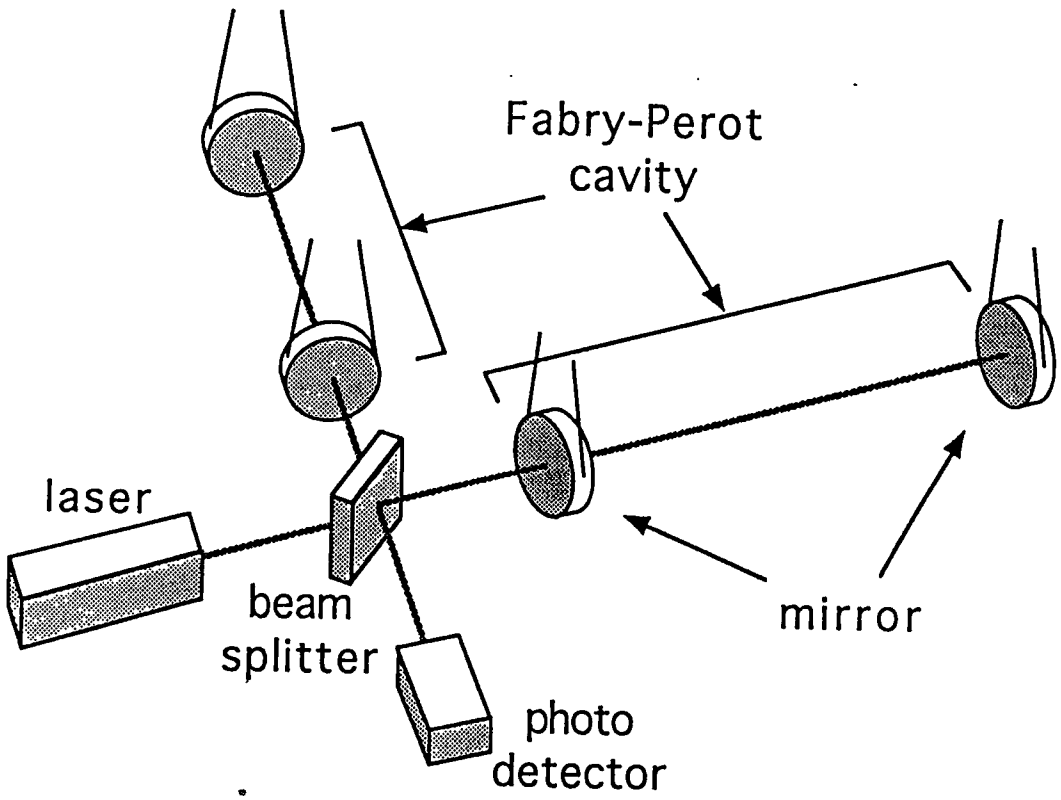

• Schematic view of the Fabry-Perot type laser interferometric gravitational wave detector

(3)

Progress report in Japan

R&D program (1991-1994, ~ $6M)

Institute of Space and Astronautical Science(ISAS)

100-m DL

National Astronomical Observatory(NAO)

20-m FP

The University of Electro-Communication

laser

Tokyo University

control & isolation

Kyoto University

GW theory

Insittute for Cosmic Ray Research(ICRR)

National Laboratory for High Energy Physics(KEK)

Tokyo Institute of Technology

ISAS 100-m DL

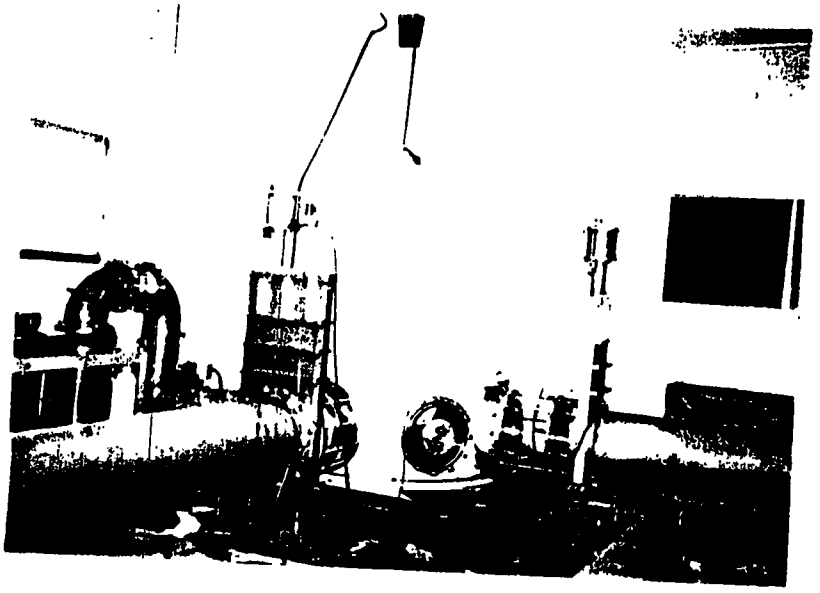

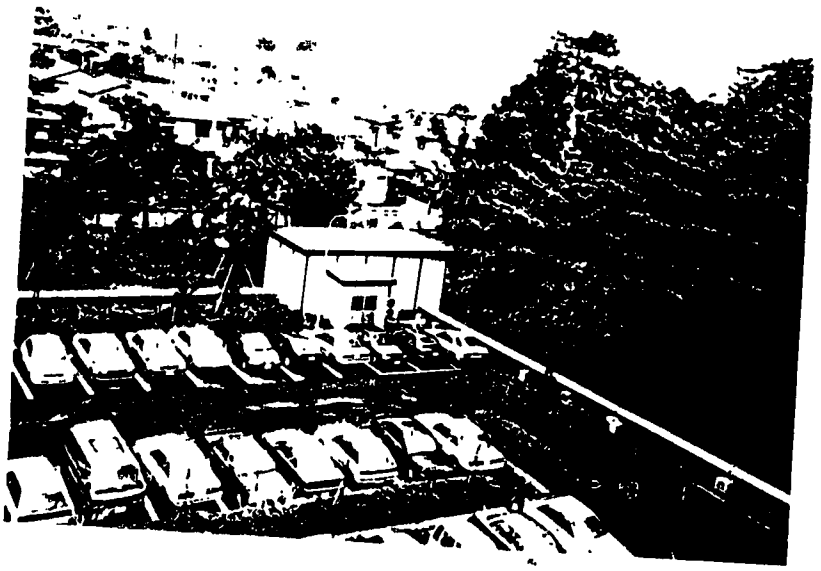

NAO 20-m FP

国立天文台　レーザー干渉計センタータンク
Fabry-Perot 型、基線長20m、アルミ合金製、内径1.4m、高さ2.1m

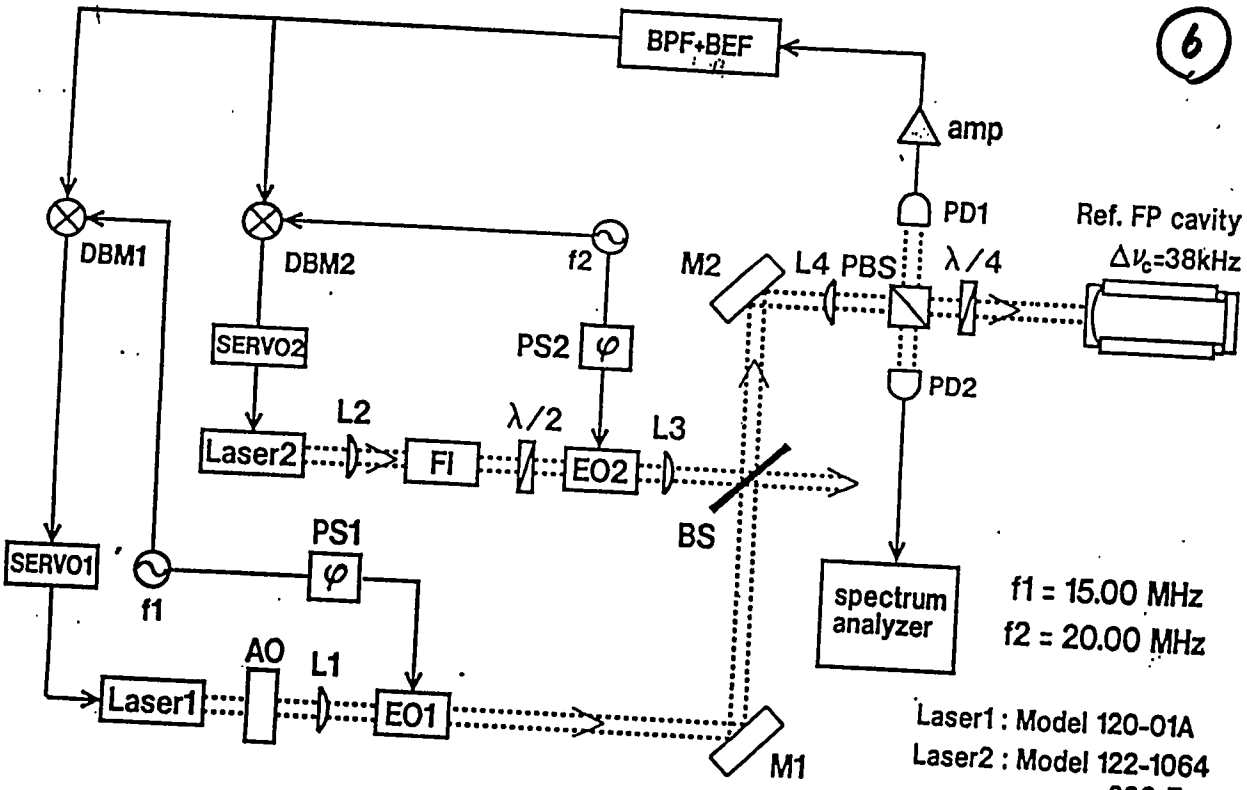

Univ. Electro-Communication

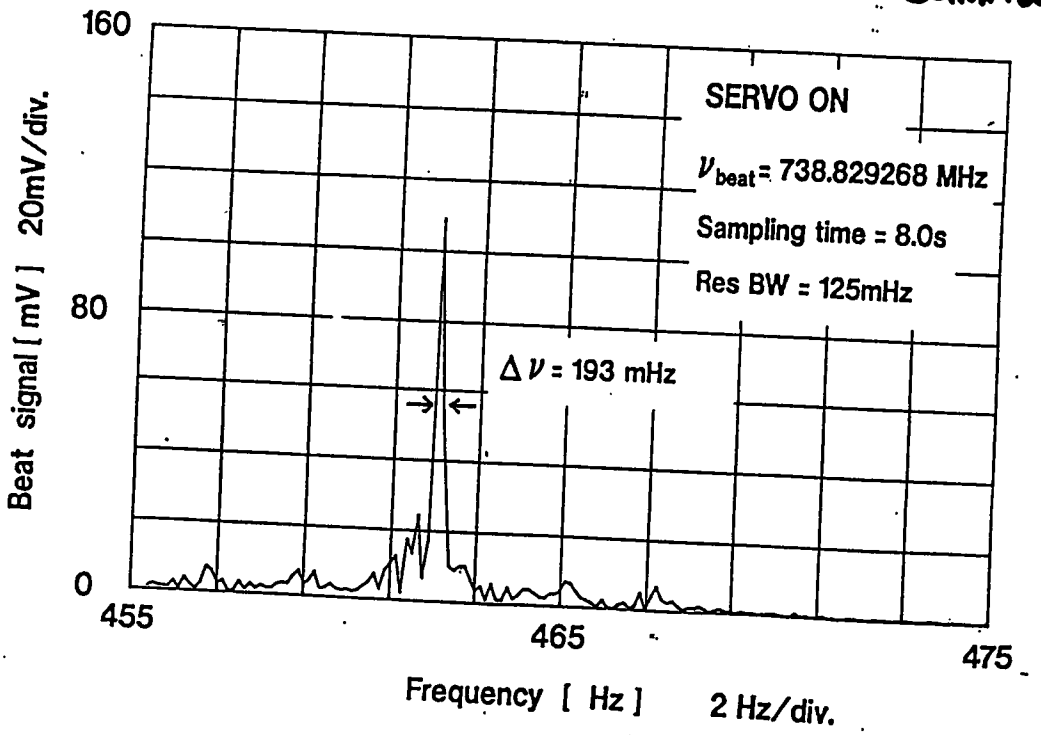

- Frequency satbilization of LD pumped Nd:YAG lasers

Univ. of Tokyo

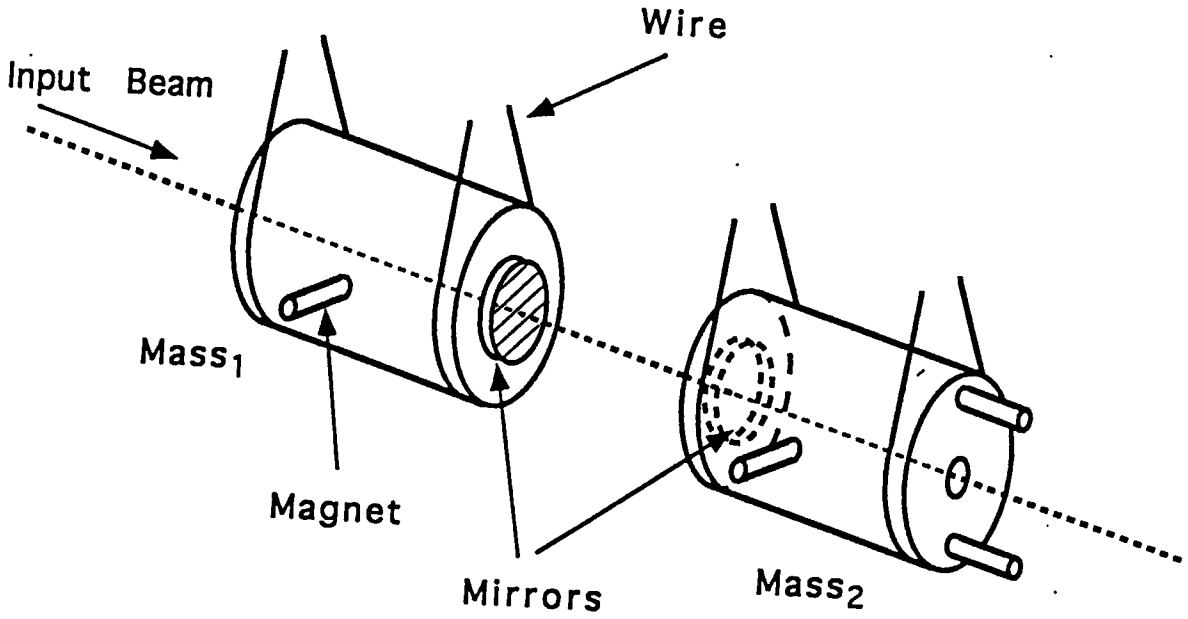

- Alignment control of the suspended Fabry-Perot cavity

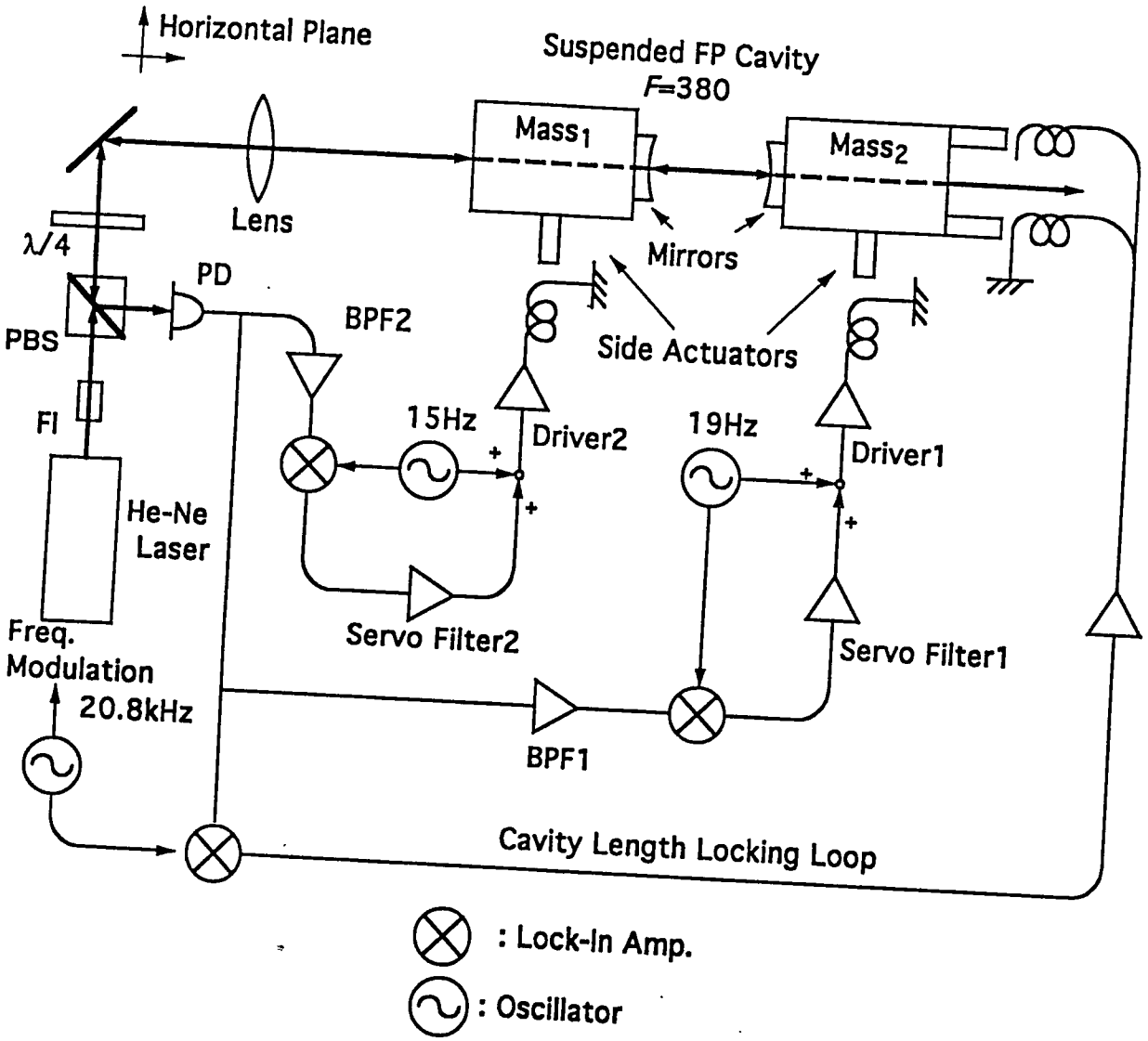

angle $< 4 \times 10^{-8}$ rad/$\sqrt{\text{Hz}}$

- Schematic diagram of the automatic alignment control of the suspended Fabry Perot cavity

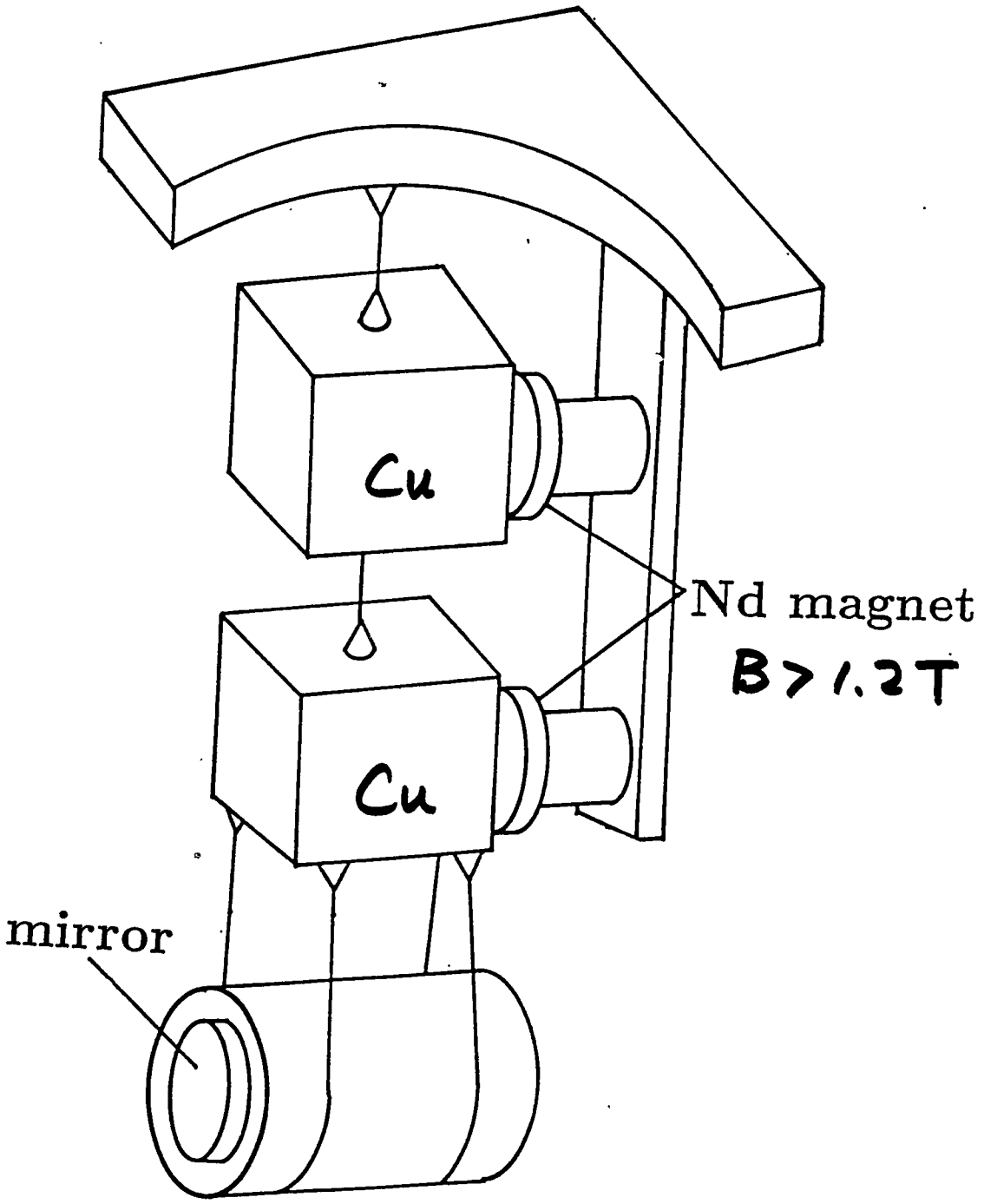

- Triple pendulum vibration isolation system for the suspended mirror

10

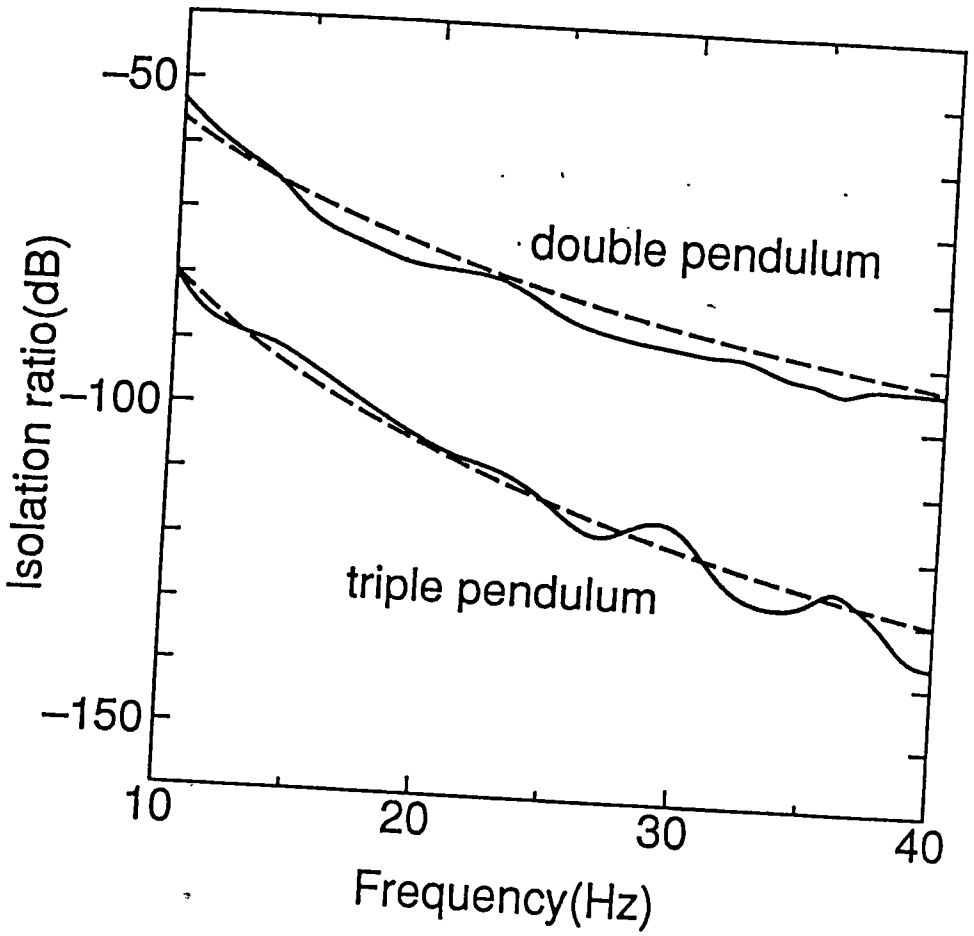

- **Measured and calculated vibration isolation ratio of the double and triple pendulums**

Univ. of Tokyo (12)

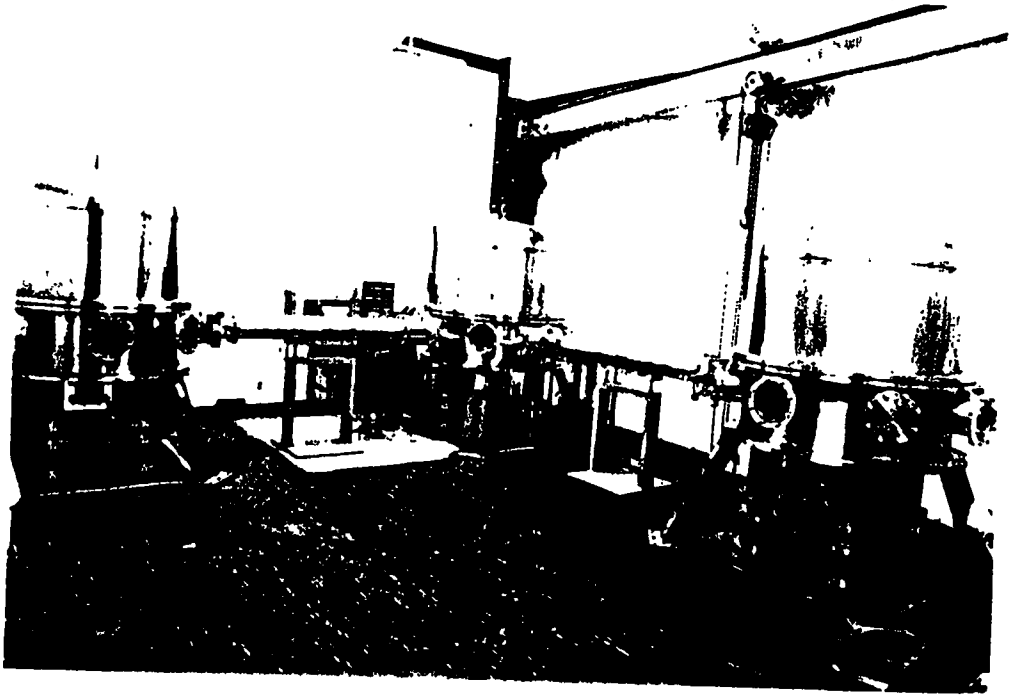

Operation of 3-m Fabry-Perot cavity with mirrors suspended by the double pendulum

- Cavity length L=3m
- Mirror reflectivity r^2=99%
- Mirror curvature R=5m
- Cavity finesse F~300
- Cavity FWHM $\delta\nu$ ~170kHz

ICRR & Univ. of Tokyo

see Kuroda's poster

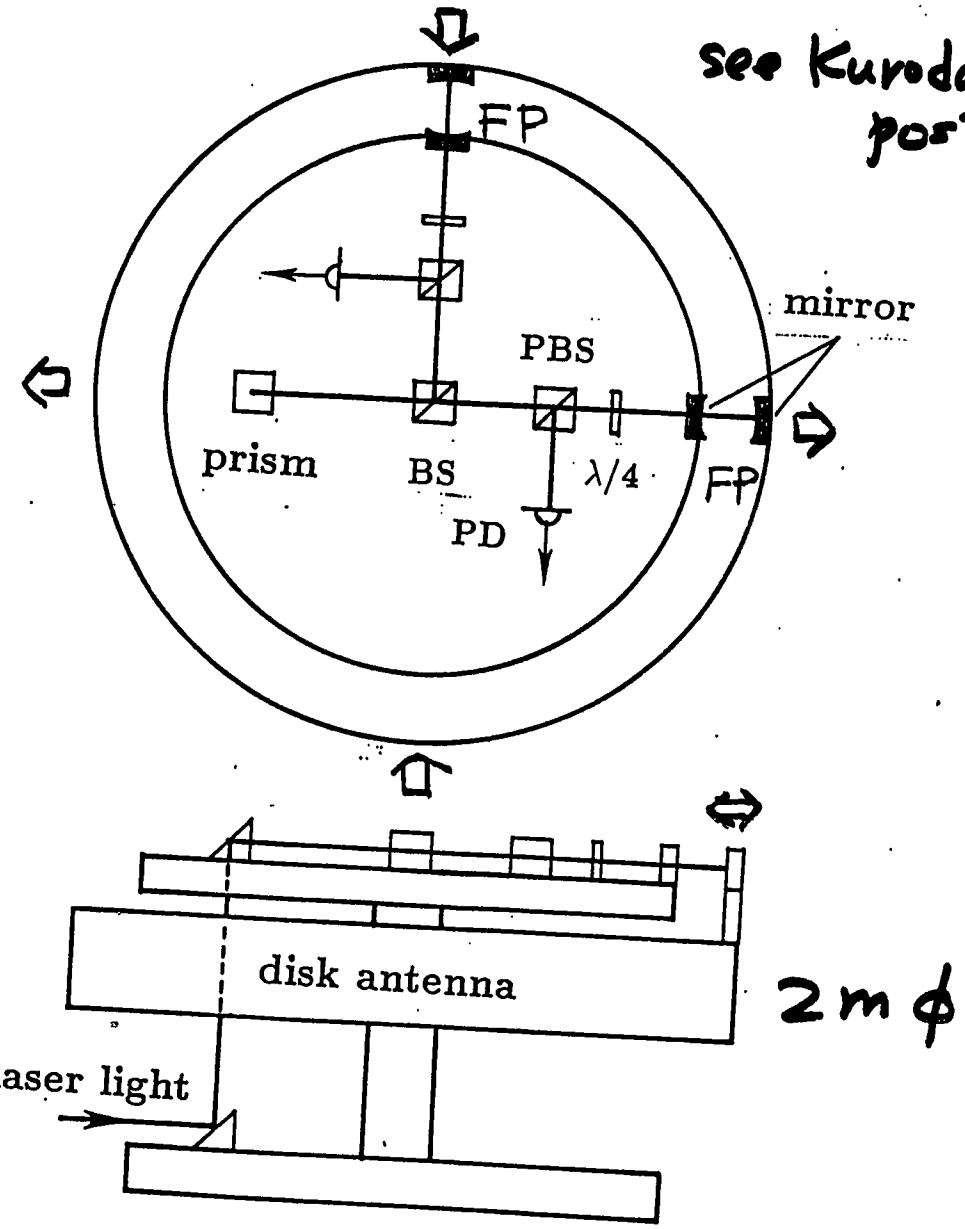

disk antenna

+ laser interferometer

Schematic View of Laser Transducer System

see Mio's poster

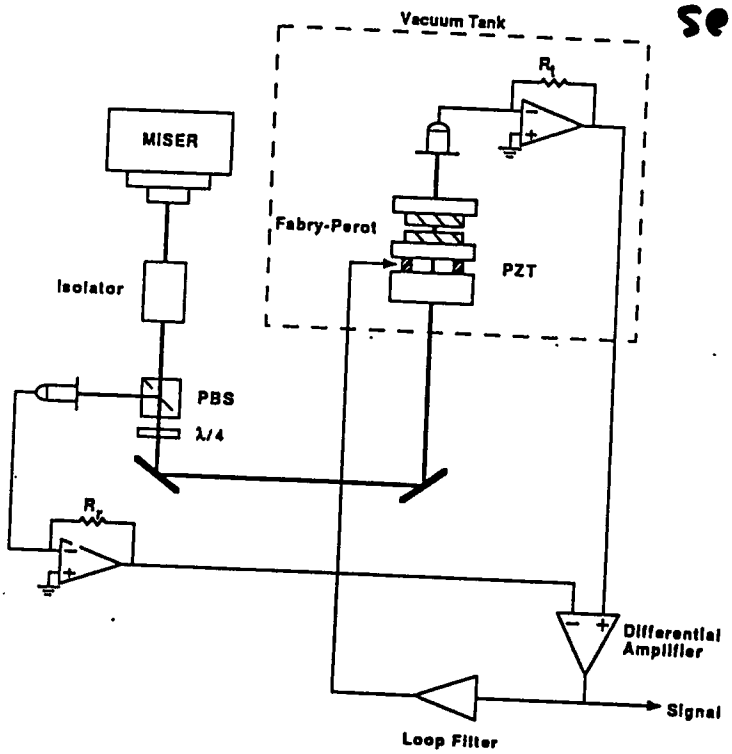

Noise Spectrum of Laser Transducer

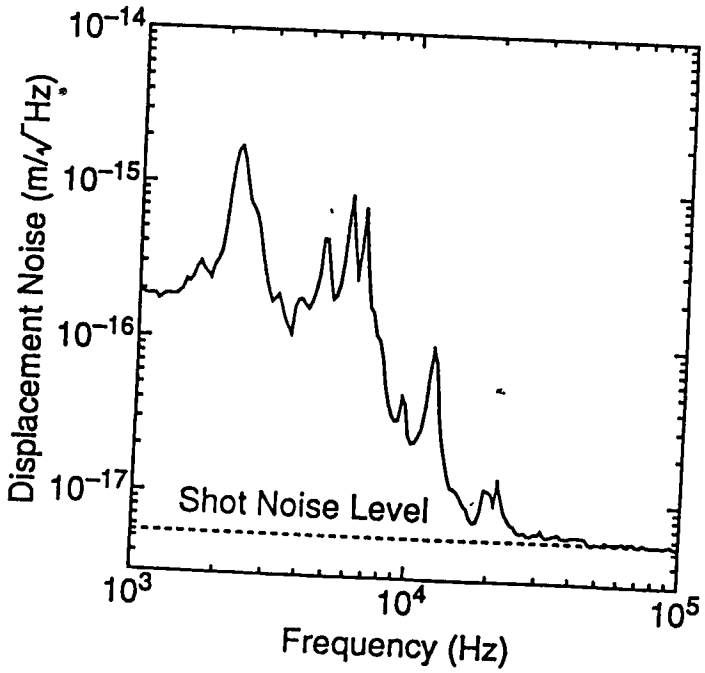

See Ogawa's poster

Seismic noise

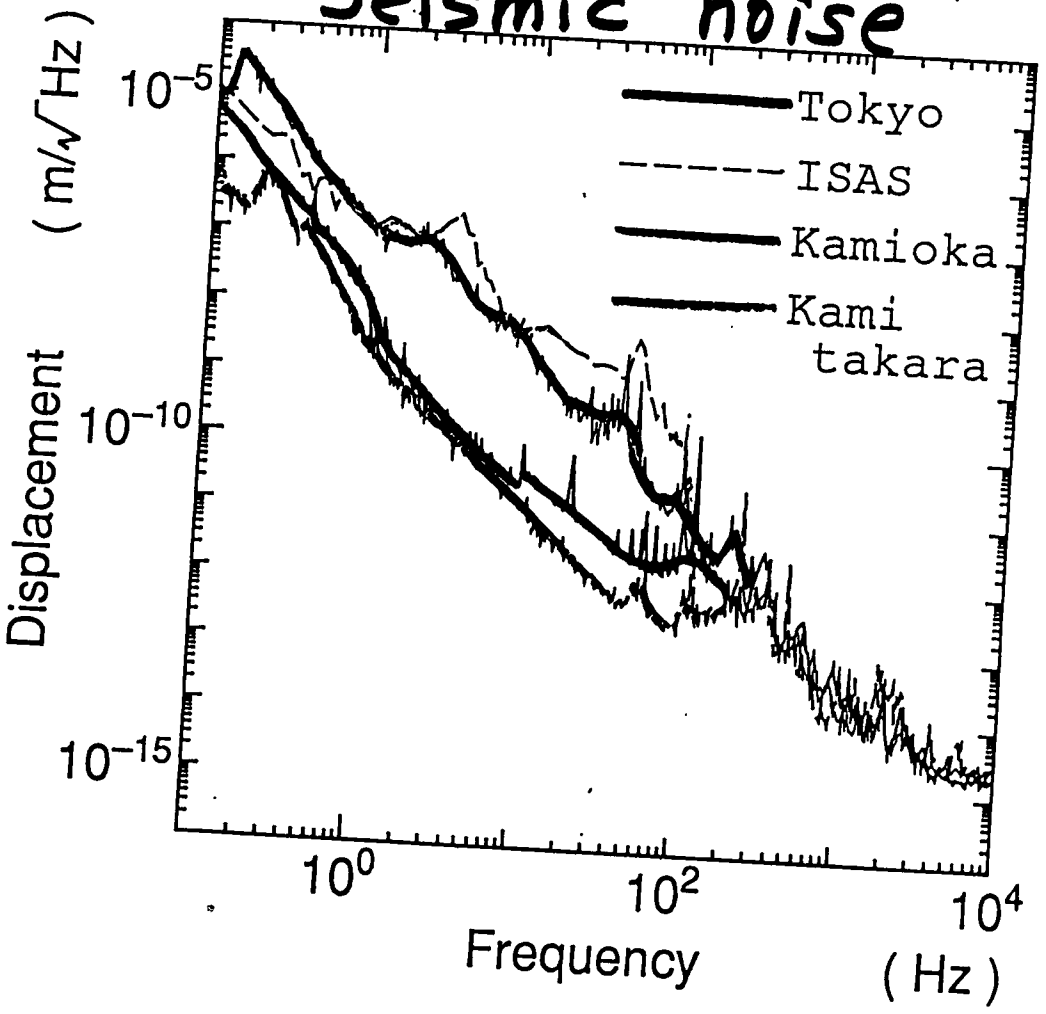

noisy $1 \times 10^{-7}\ m/\sqrt{Hz}$ @ 1 Hz

quiet $\sim 3 \times 10^{-9}\ m/\sqrt{Hz}$ @ 1 Hz

3km×3km Fabry-Perot cavity type laser interferometer

Conceptual design(1990)

- Sensitivity: $h_{\rm rms} = 10^{-21}$ at 1kHz
- Laser: Nd:YAG laser
  - P=1kW
  - Frequency noise $\delta\nu/\nu \sim 10^{-21}/\sqrt{\rm Hz}$
  - Intensity noise $\delta P/P \sim 10^{-9}/\sqrt{\rm Hz}$
- FP Cavity: finesse=80

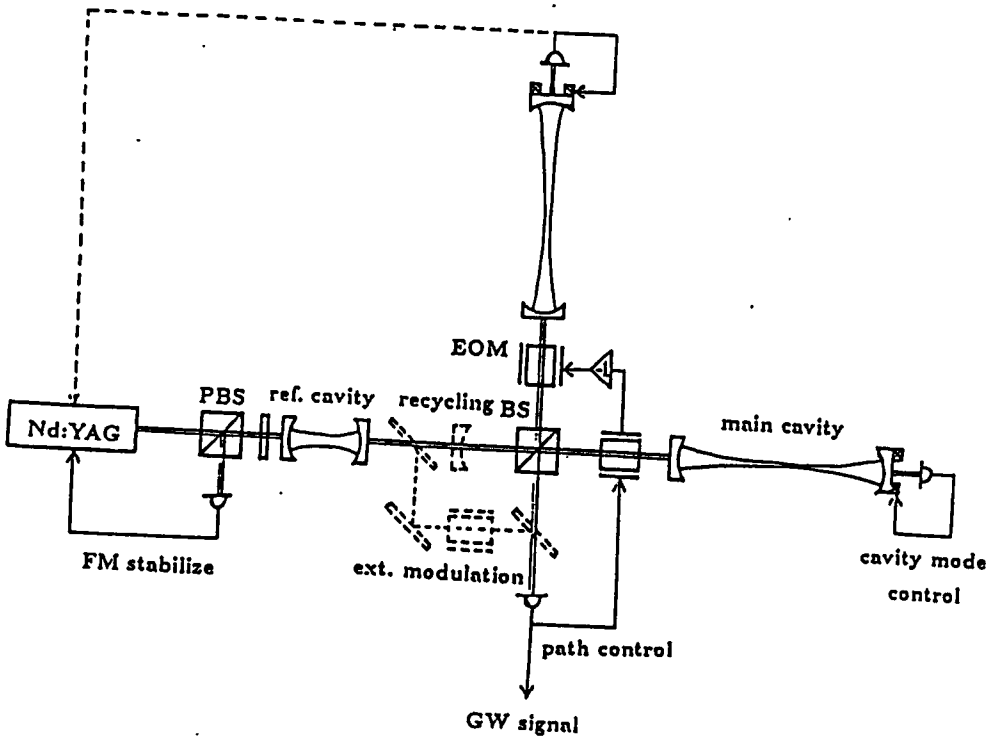

- Conceptual design of a 3km×3km Fabry-Perot type laser interferometer

300m×300m Fabry-Perot cavity type laser interferometer

- 300m×300m Fabry-Perot cavity type
  - quite feasible with the present technology
- $h_{\min} = 10^{-20}$
  - covers GW sources within the distance of Andromeda galaxy (700kpc)

Problems:

- GW sources?
  - two orders improvement over the present detector
- Too late?
  - three years construction
- Sufficient sensitivity?
  - main obstacles: thermal noise and seismic noise
    ⇒future technology will achieve $h_{\min} \sim 10^{-21}$

300m×300m Fabry-Perot cavity type laser interferometer

Design parameters

- Sensitivity: $h_{\rm rms} = 10^{-20}$ at 1kHz with 1kHz bandwidth
- Frequency range: 100Hz-5kHz
- Laser:
  - LD pumped Nd:YAG laser
  - Power=1W, Recycling gain=33
- FP cavity mirror:
  - 70mm(ϕ)× 100mm(ℓ), (m $\sim$ 1kg, Q $\sim 10^5$)
  - Near mirror R=97.5%, loss$\leq$ 100ppm
  - End mirror R=99.99%, loss$\leq$ 100ppm

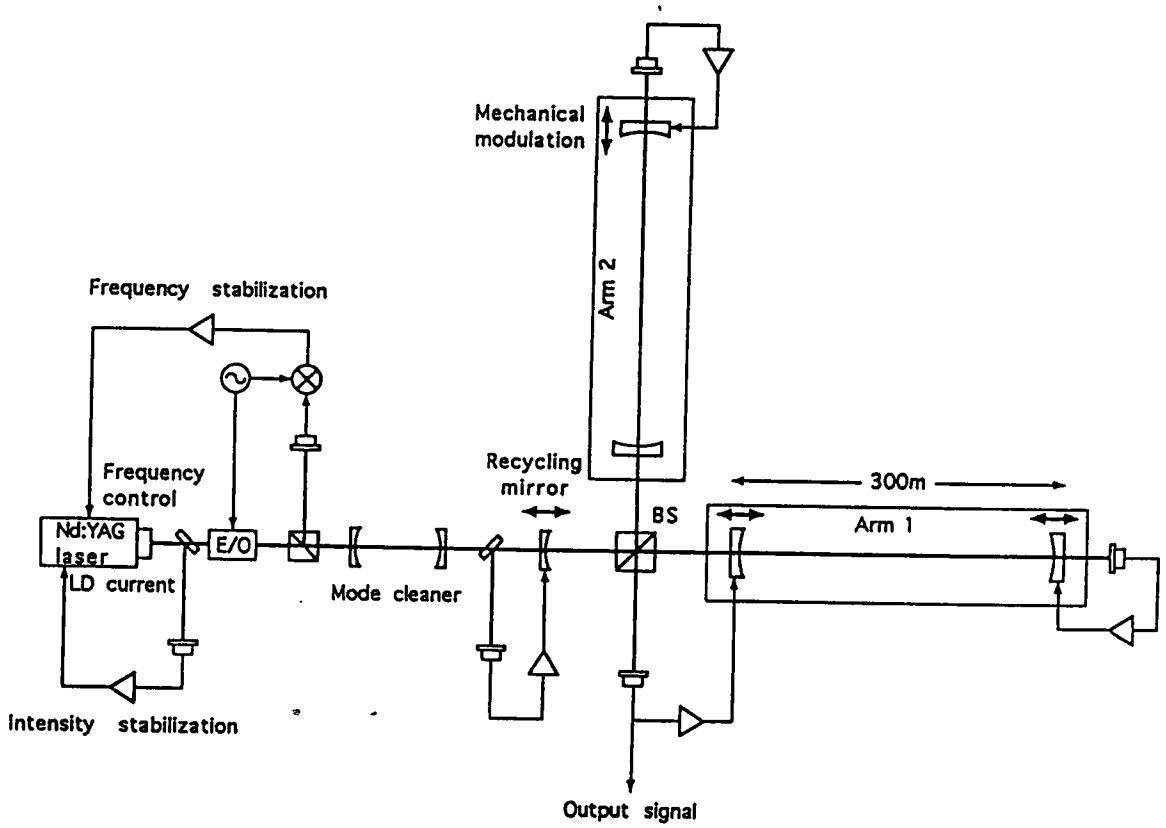

$h_{min} \sim 10^{-20}$

➡ $h_{min} \sim 10^{-21}$

- Conceptual design of a 300m×300m Fabry-Perot type laser interferometer

VIRGO

- PRESENTATION
- CRITICAL TECHNOLOGIES
- CONSTRUCTION DETAILS

ALAIN BRILLET
FOR
THE VIRGO COLLABORATION

VIRGO

FRENCH - ITALIAN INTERFEROMETER FOR G.W. DETECTION

1982 FIRST STUDIES

1986 COLLABORATION ORSAY - PISA

1989 PROPOSAL

1992 - "FINAL DESIGN"

- APPROVAL BY { CNRS in FRANCE / GOVT.
- APPROVAL BY INFN in ITALY

1993 - APPROVAL BY GOVT. in ITALY (?)

- START CONSTRUCTION

1997 - 1998

- END OF CONSTRUCTION
- DETECTIONS (?)

Scientific objectives

First detection of gravitational radiation
coïncidence detection with more than two antennas
or observation of a periodic source (Virgo)

Tests of the polarization properties
coïncidences between antennas with different orientations

Propagation velocity of gravitational waves
timing of events, with more than 3 antennas

Tests of gravity theories in strong field
coalescence of a binary black hole

Morphology of a supernova core
mass, angular momentum, ...

Neutron star equation of state
comparison with numerical models for supernovae or coalescences

Hubble's constant
observation of a coalescing binary associated with a visible galaxy (expected precision @ 1%)

Homogeneity and isotropy of the Universe
through statistics on coalescences up to 500 Mpc

The early universe
stochastic background : cosmic strings, phase transitions, generation of supermassive objects

RECYCLING INTERFEROMETER

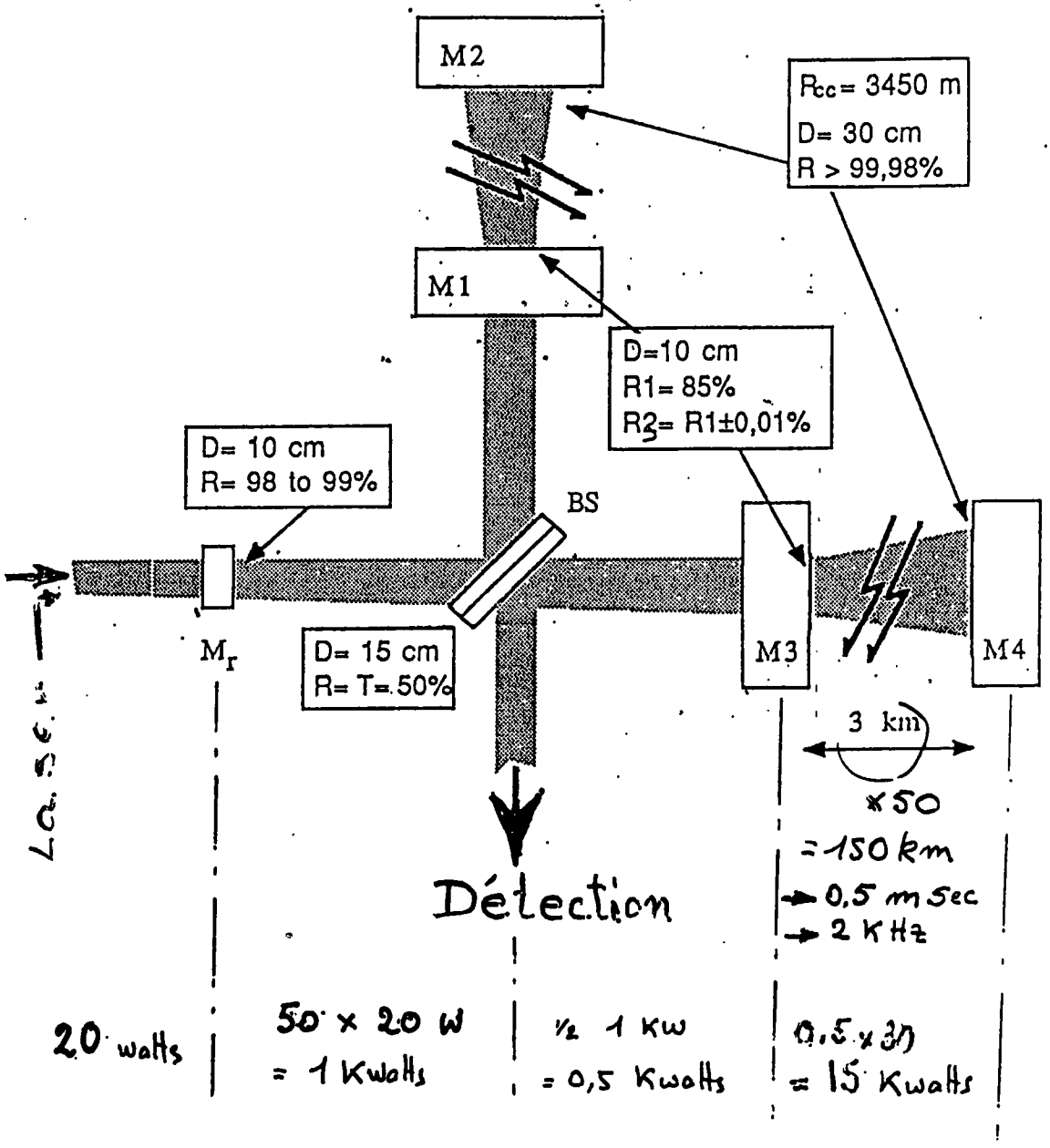

Ref. "Optimisation of long-baseline optical interferometers for Gravitational wave detection" Phys. Rev. D (1988) J.Y. Vinet, B. Meers, C.N. Man et A. Brillet.

Ground-based optical interferometers (VIRGO, LIGO, ... projects)

The main limitations

1) Low frequencies (below 10 Hz) --> Seismic noise

Typical ground motion : $\Delta x = \frac{4\,10^{-6}}{\omega^2}\ \mathrm{m.Hz^{-1/2}}$, or $\Delta h = \frac{\Delta x}{L} = \frac{3\,10^{-11}}{f^2}\ \mathrm{Hz^{-1/2}}$

An attenuation of 10^{10} is then needed @ 10 Hz

2) Intermediate frequencies (10 to 200 Hz) --> Thermal noise

$$\Delta h = \frac{1}{L}\sqrt{\frac{4\,kT\,\omega_o}{MQ\,\omega^4}}\ , \text{typically } \Delta h = 1\,0^{-22}\ \mathrm{Hz^{-1/2}} @ 1\,0\,0\ \mathrm{Hz}$$

for M=100 kg, $Q = 10^6$, and L = 3 km

3) High frequency (above 200 Hz) --> Shot noise

$$\Delta h = \frac{\lambda}{2\pi L_{eq}}\sqrt{\frac{h\nu}{\eta P}} = 2\,1\,0^{-23}\sqrt{\frac{1\ \mathrm{kW}}{\eta P}}\ \mathrm{Hz^{-1/2}}$$

for $\lambda = 1\mu m$, and Leq = 100 km

Solutions to the shot-noise problem :

- high power Nd:YAG lasers
- coherent addition of lasers
- recycling
- Squeezing ??

CRITICAL TECHNOLOGIES

VACUUM
- LOW H_2 OUTGASSING RATE
- PRESSURE STABILITY, CLEANLINESS

SEISMIC ISOLATION
$> 10^{10}$ @ $10 H_z$

MATERIALS
- HIGH MECHANICAL Q
  - WIRES
  - SILICA
  - DESIGN
- ULTRA LOW ABSORPTION
- HIGH HOMOGENEITY

} OPTICAL MATERIAL

MIRRORS
- VERY LOW LOSSES $< 10^{-5}$
- HIGH UNIFORMITY $< \lambda/100$
- LARGE SIZE > 30 cm

LASER
RELIABILITY, HIGH POWER ($\gg 10$W CW)

STABILITY
- FREQUENCY $< 10^{-20}/\sqrt{Hz}$
- AMPLITUDE $< 10^{-8}/\sqrt{Hz}$

OPTRONICS
SHOT-NOISE LIMITED OPERATION

LASER STABILITY REQUIREMENTS

[DUE TO INTERFEROMETER ASYMETRIES(1) AND TO USE OF RESONANT CAVITIES (2)]

FREQUENCY (length asymetry and scattered light)

1 $$\frac{\delta\nu}{\nu} < \tilde{h}\left(\frac{\delta F}{F} + \frac{\delta L}{L}\right)^{-1}$$

$$< 10^{-23} \times 10^{+4} = 10^{-19}\ H_z^{-1/2}$$

$$\rightarrow \delta\tilde{\nu} < 10^{-5}\ H_z/\sqrt{H_z}$$

2 $\Delta\nu \ll \Delta\nu_c$ $\quad \Delta\nu \ll 50 H_z$ $(\leq 0.005 H_z)$

POWER (mirors recoil, inperfect contrast)

$$\frac{\delta\tilde{P}}{P} < 10^{-8}/\sqrt{H_z}$$

GEOMETRY

- SINGLE TRANSVERSE MODE
- BEAM POINTING STABILITY $\delta\tilde{\theta} < 10^{-10}\ rd/\sqrt{H_z}$

$\Rightarrow$ ACTIVE STABILIZATION AND PASSIVE FILTERING of the LASER BEAM

Laser stabilizations

ORSAY + PISA

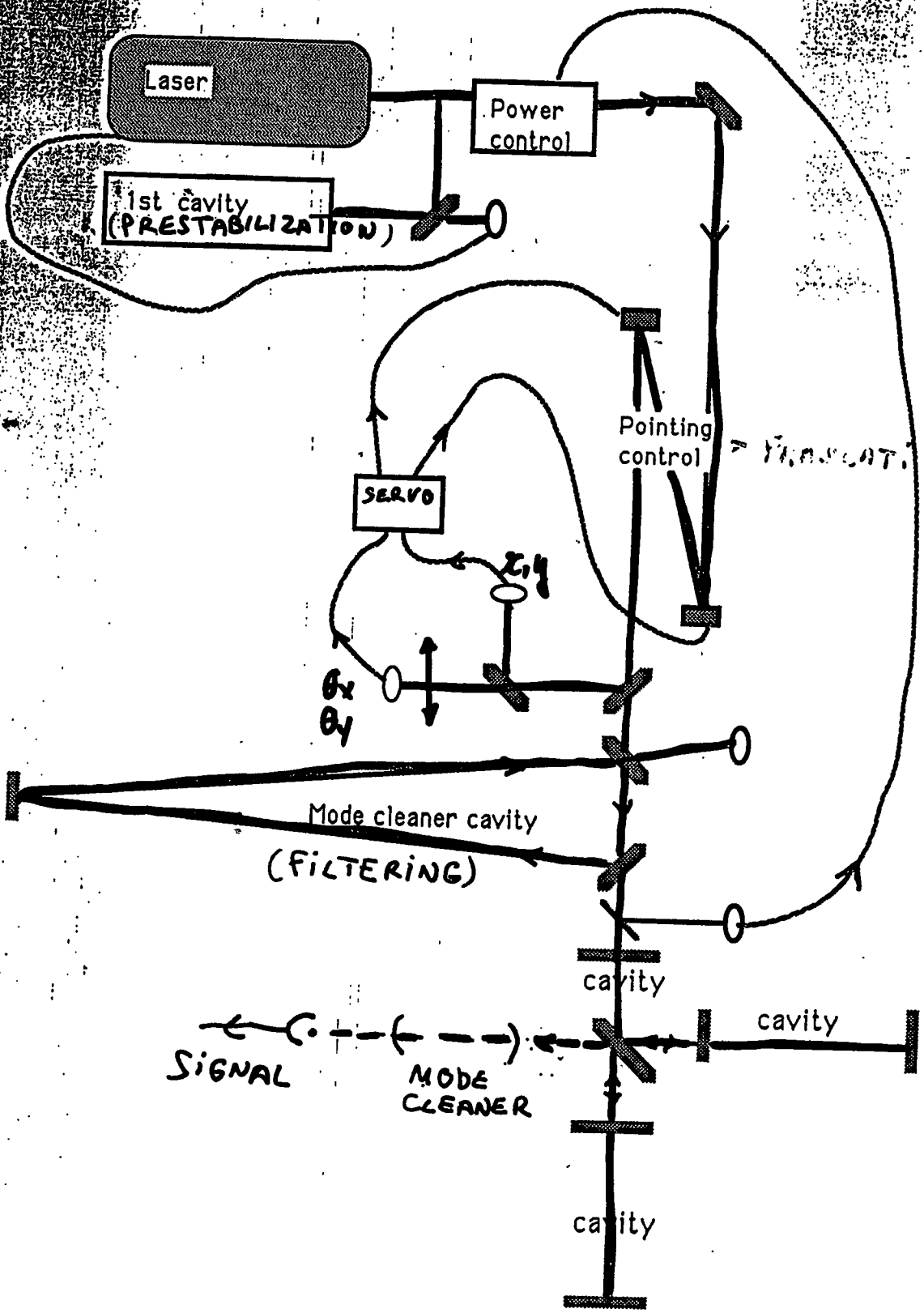

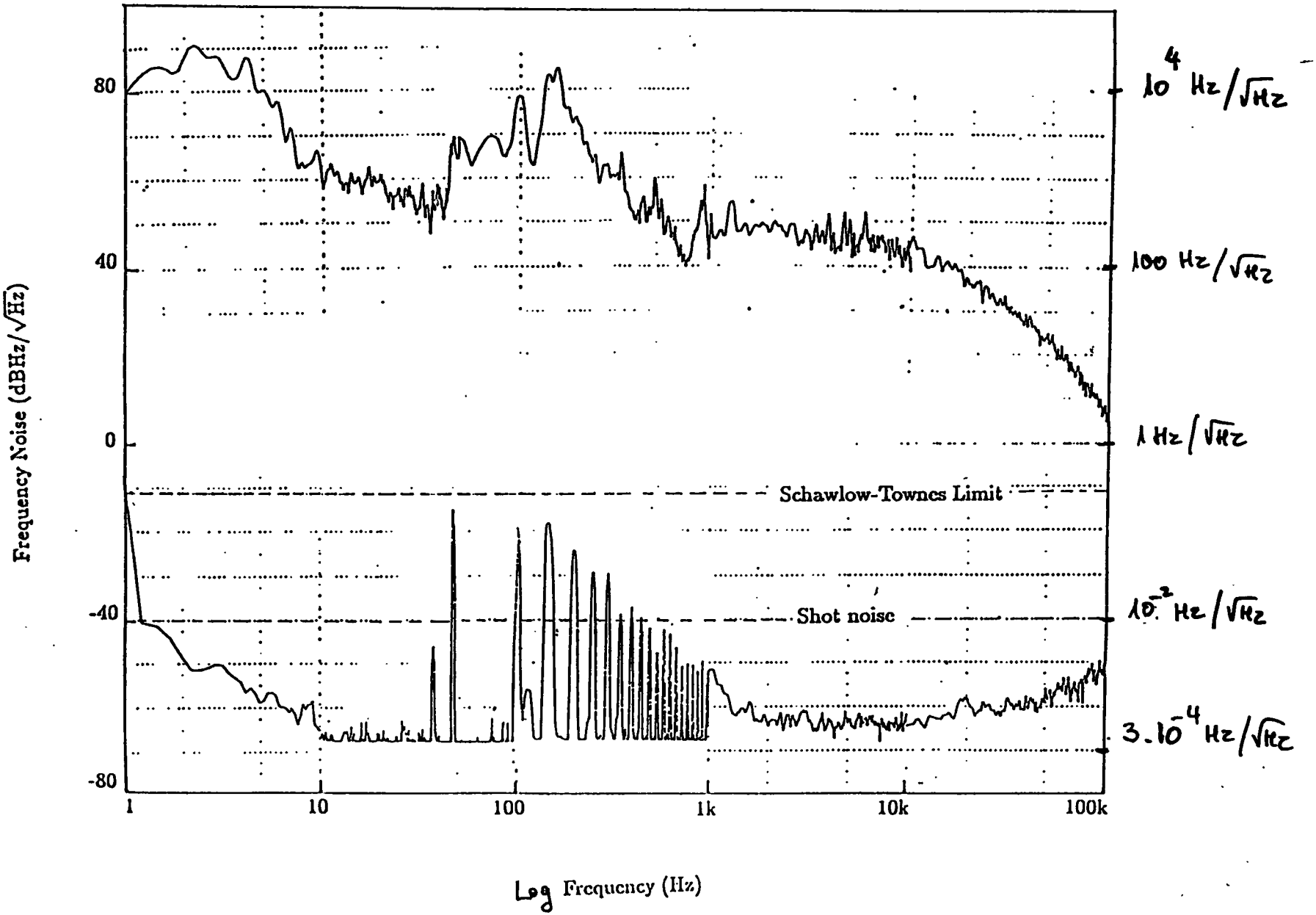
80
40
0
-40
-80
1
10
100
1k
10k
100k
Frequency Noise (dBHz/√Hz)
Log Frequency (Hz)
Schawlow-Townes Limit
Shot noise
10^4 Hz/√Hz
100 Hz/√Hz
1 Hz/√Hz
10^-2 Hz/√Hz
3.10^-4 Hz/√Hz

STABILISATION DE FREQUENCE

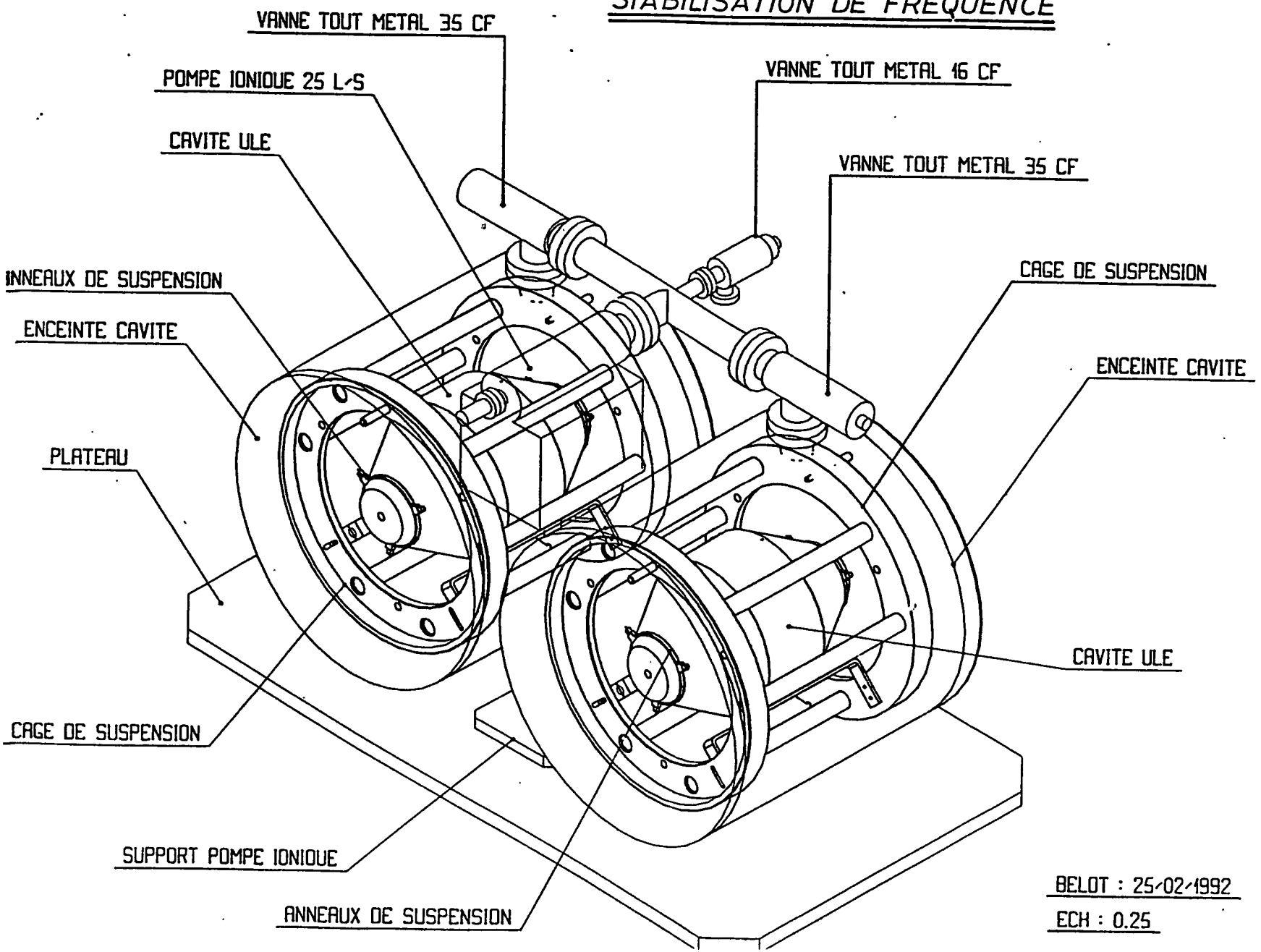

BELOT : 25/02/1992

ECH : 0.25

Suppression des oscillations de relaxation du laser YAG

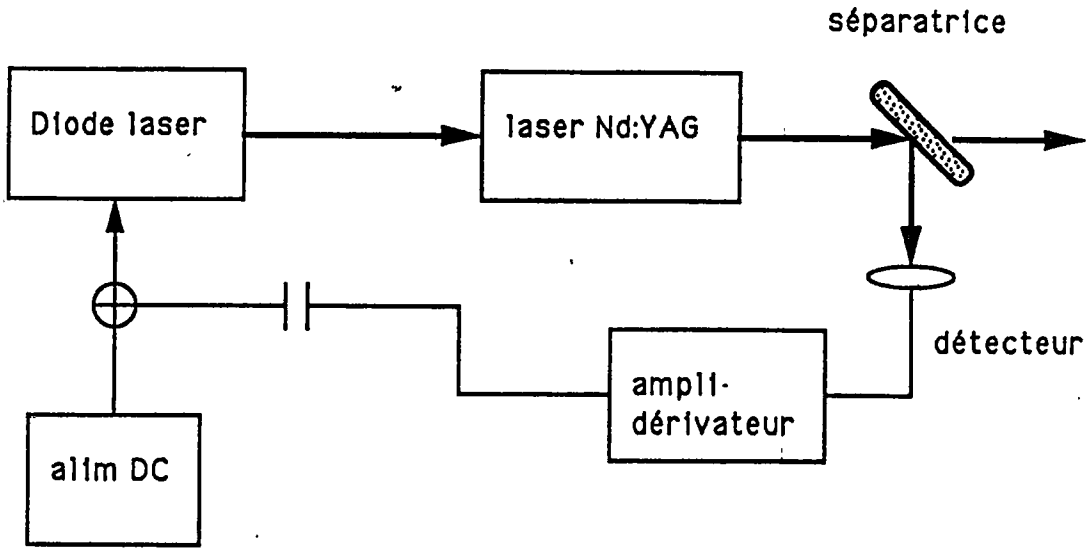

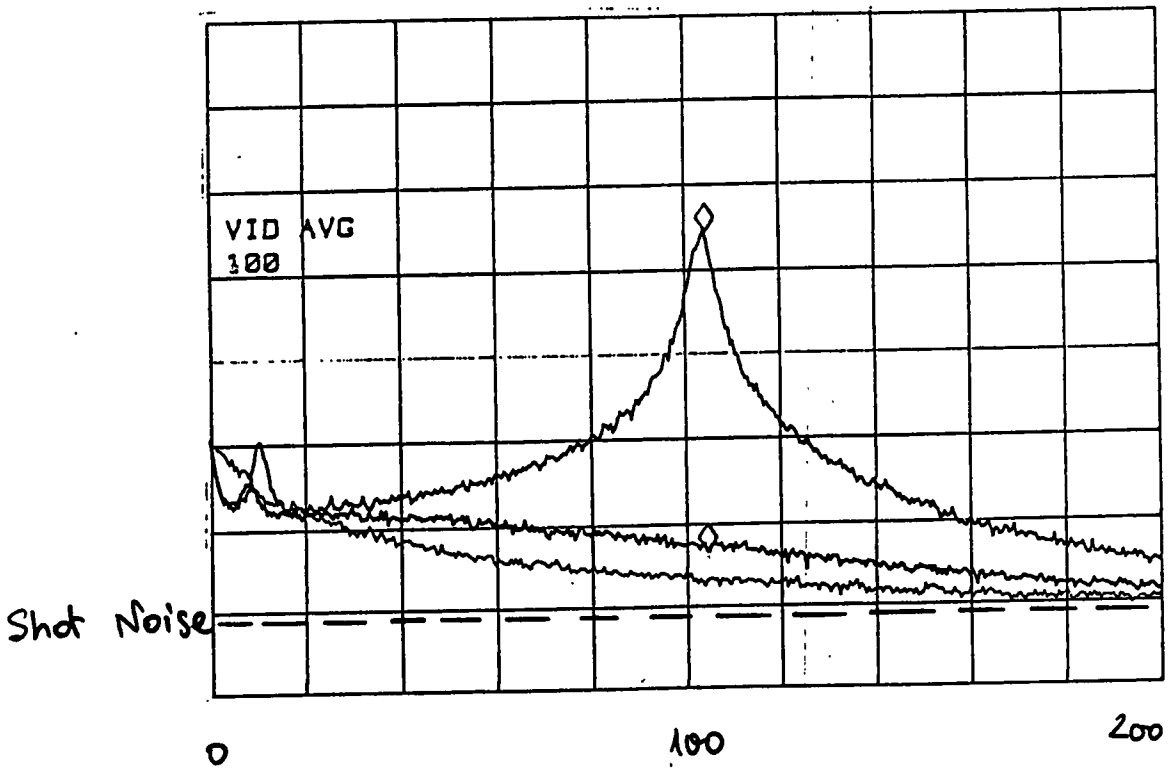

beam, and to use low thermal impedance submounts to extract the waste heat with minimum temperature rise. The pump array consist of an array of 10 diodes mounted on individual water cooled submounts, placed themselves on an insulating mounting, serving to hold the set of diodes.

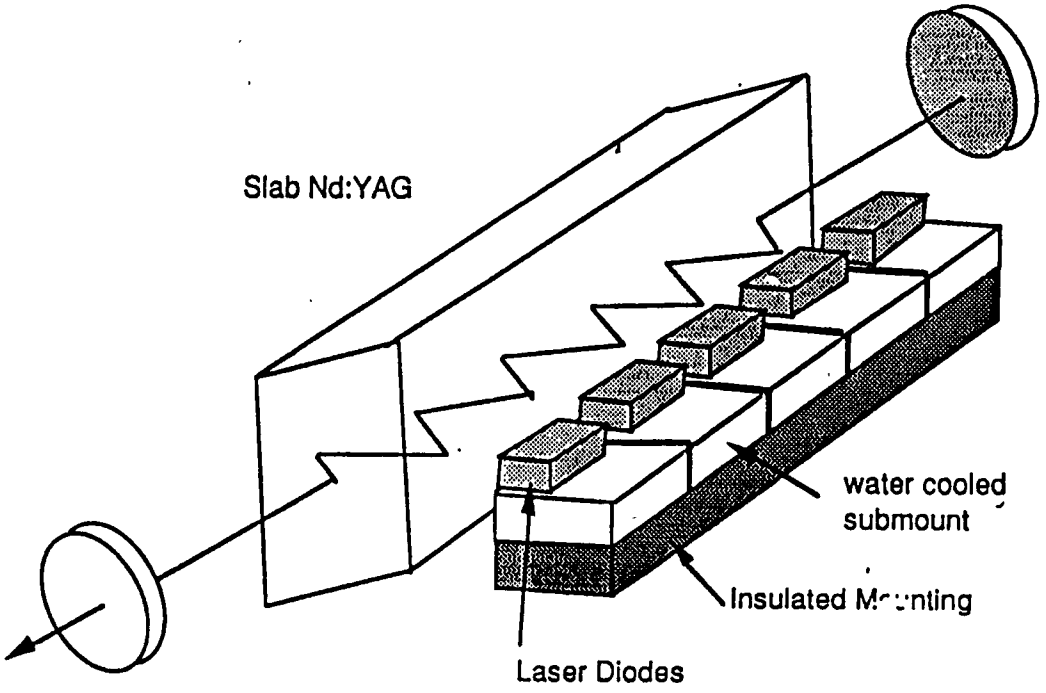

1.2 Performance of the Prototype

The output power will depend on many parameters: the pumping efficiency, the extraction efficiency, the cavity losses, the gain per pass in the medium, and the optimum output coupler. To choose the resonator parameters, one must consider two factors which play important roles: the filling factor and the aperture losses. A large beam radius fills well the volume of the slab but may be severely clipped by the slab edges and losses are the major obstacle to the laser performance. Therefore we choose a beam radius which is a good compromise between the two conditions. The other factor that counts in the design of the cavity is the ease of monomode operation. The first two conditions are quite contradictory with the third one, but we can find a way to fulfill all the conditions if we add a diaphragm into the cavity to select spatially only the TEM_{00} mode.

To avoid spatial hole burning in the laser and appearance of parasitic oscillations, we will use a ring cavity in a x configuration, formed by four mirrors. It is easy to find the equivalent linear cavity and to apply the usual stability conditions. If we take a cavity length of about 50 cm and a curved mirror of 1m radius of curvature, the TEM_{00} mode

le 8 Octobre 1992

R_c R 50 = 0,5 mm

R R 50 2P %

L = 25 cm

L = 25 cm.

2w horizontal = 760 µm

2w vertical = 970 µm

P = 2,30 W

16,0°C

105, 2-3

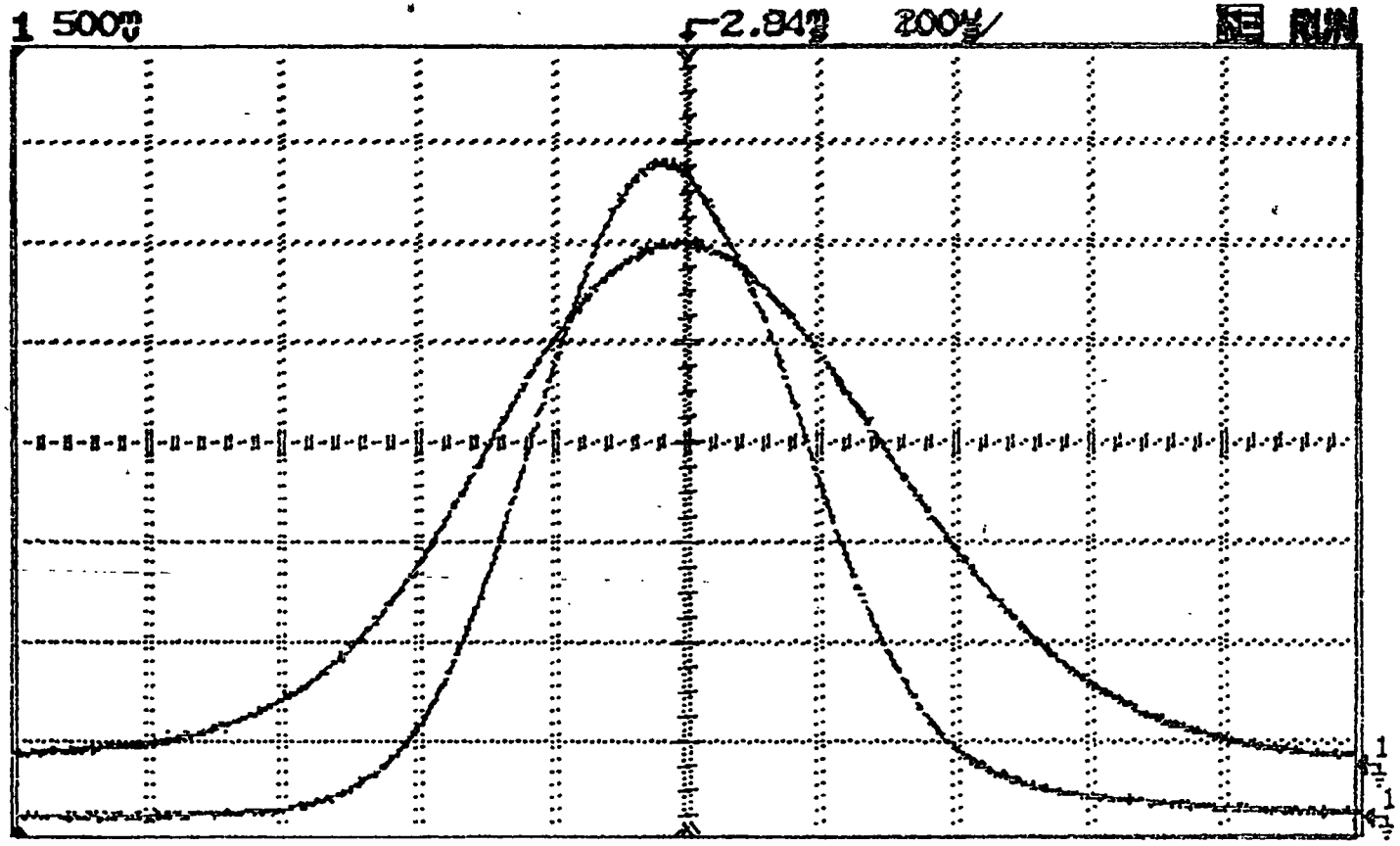

(16)

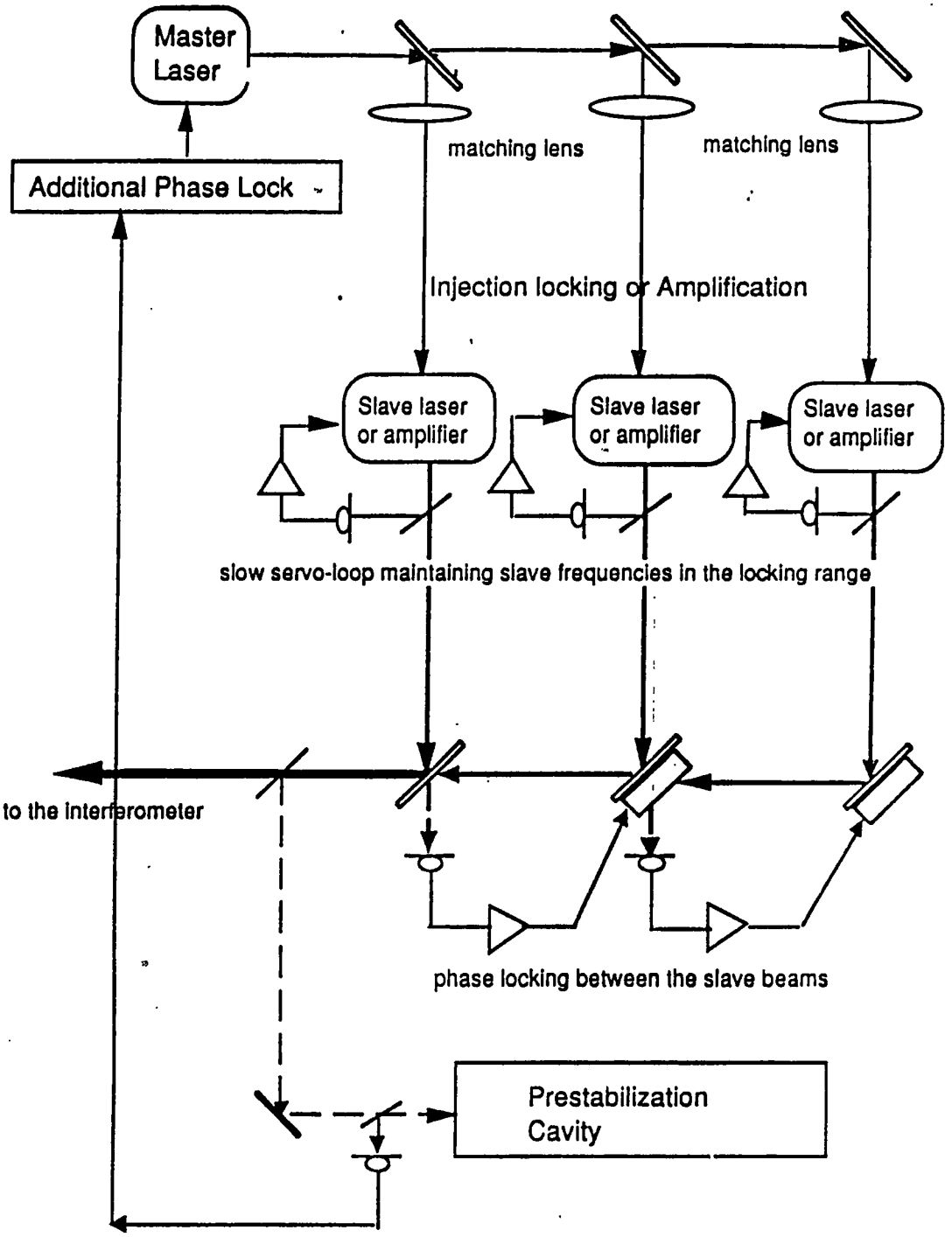

Figure 1 : Virgo Laser System and the Phase-Locking loops

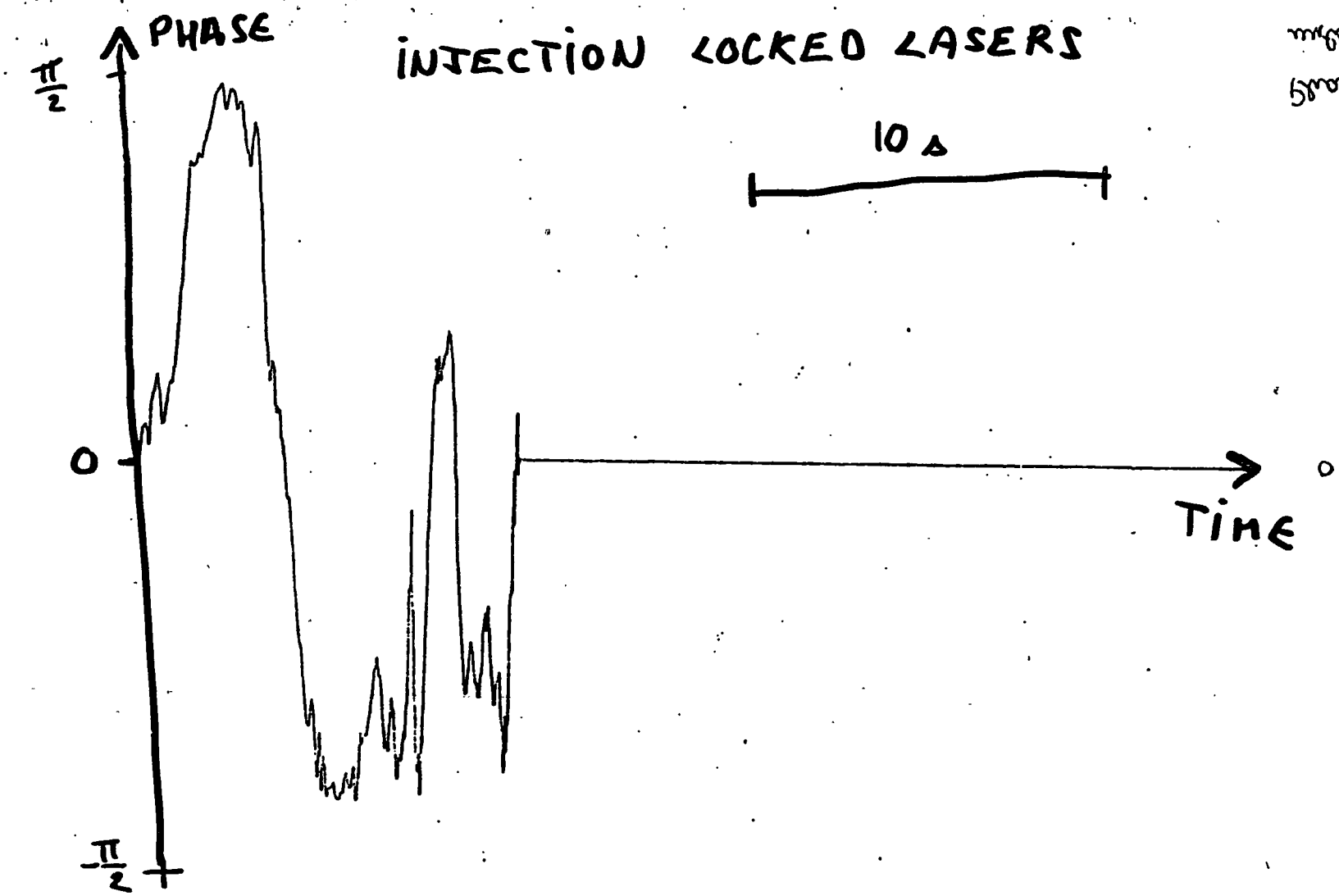
INJECTION LOCKED LASERS
PHASE
$\frac{\pi}{2}$
0
$-\frac{\pi}{2}$
10 s
Time

Pour une direction transverse

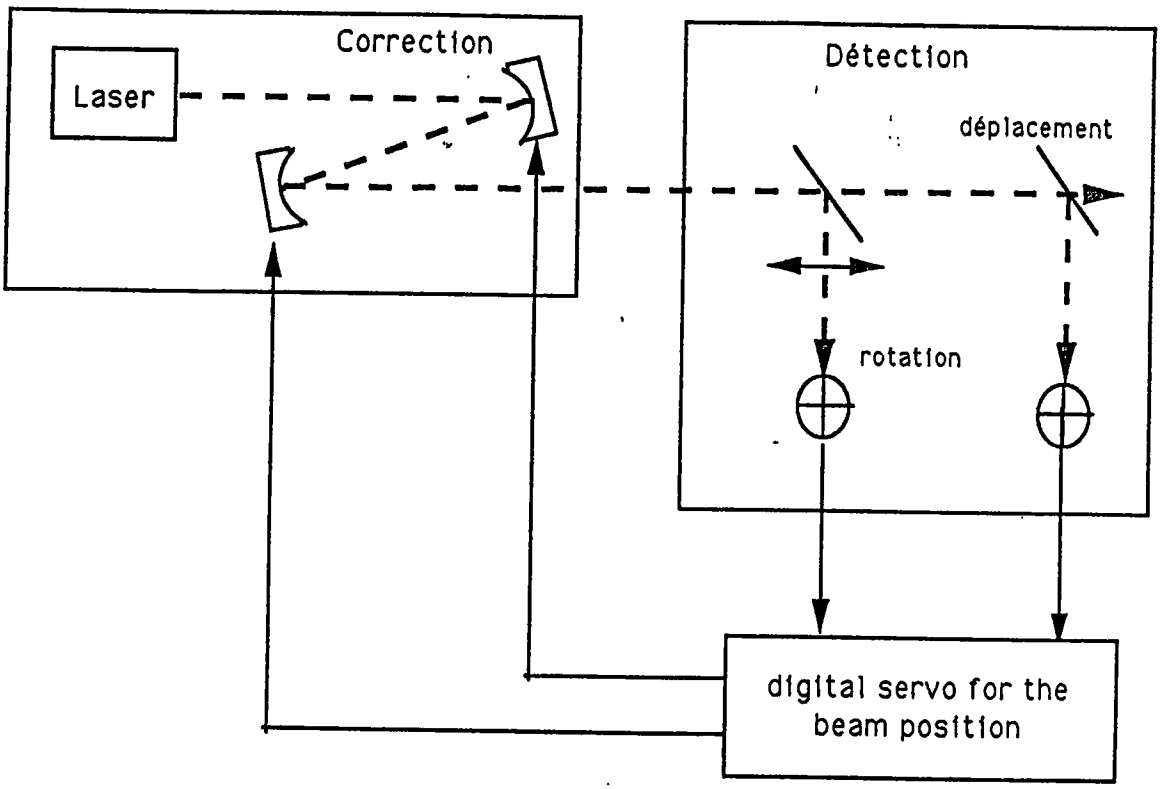

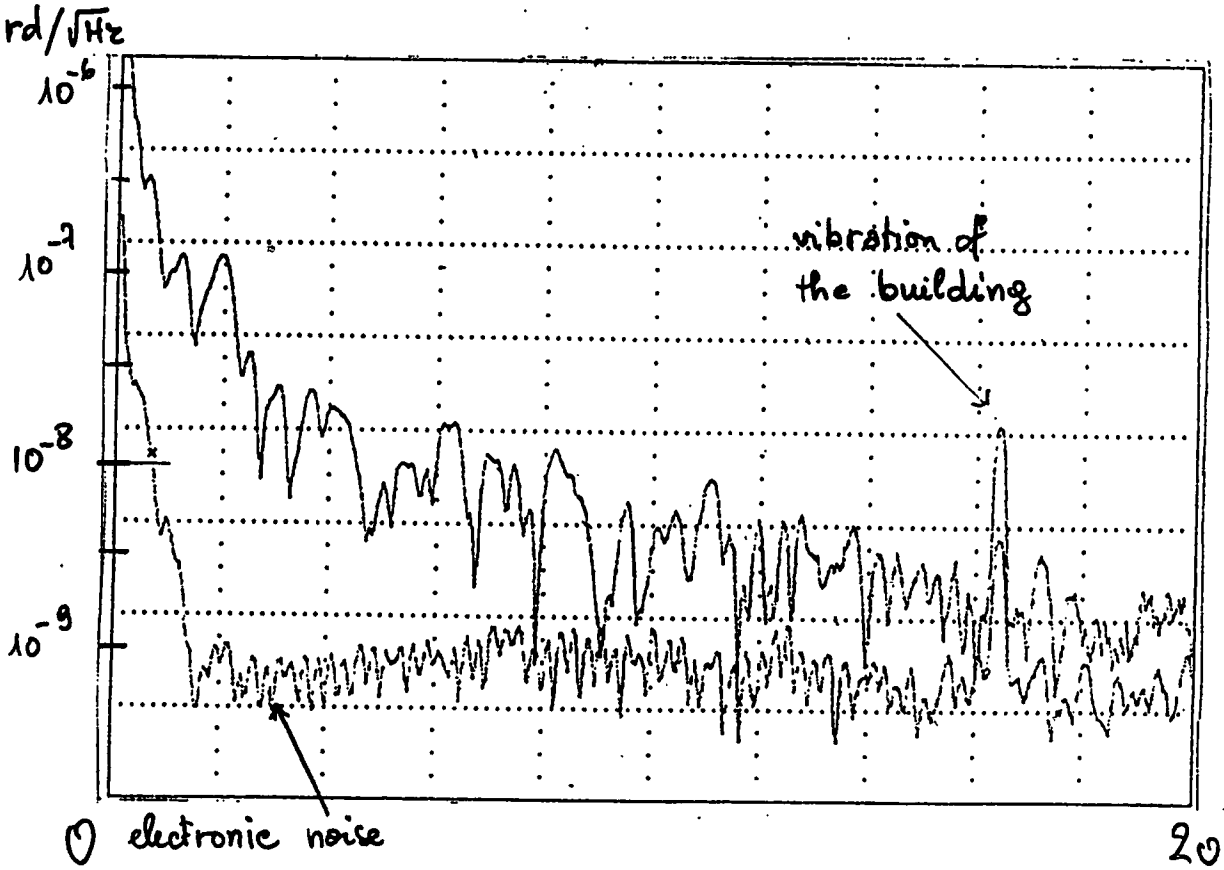

Measurement of absolute beam displacement.

FIG. 3

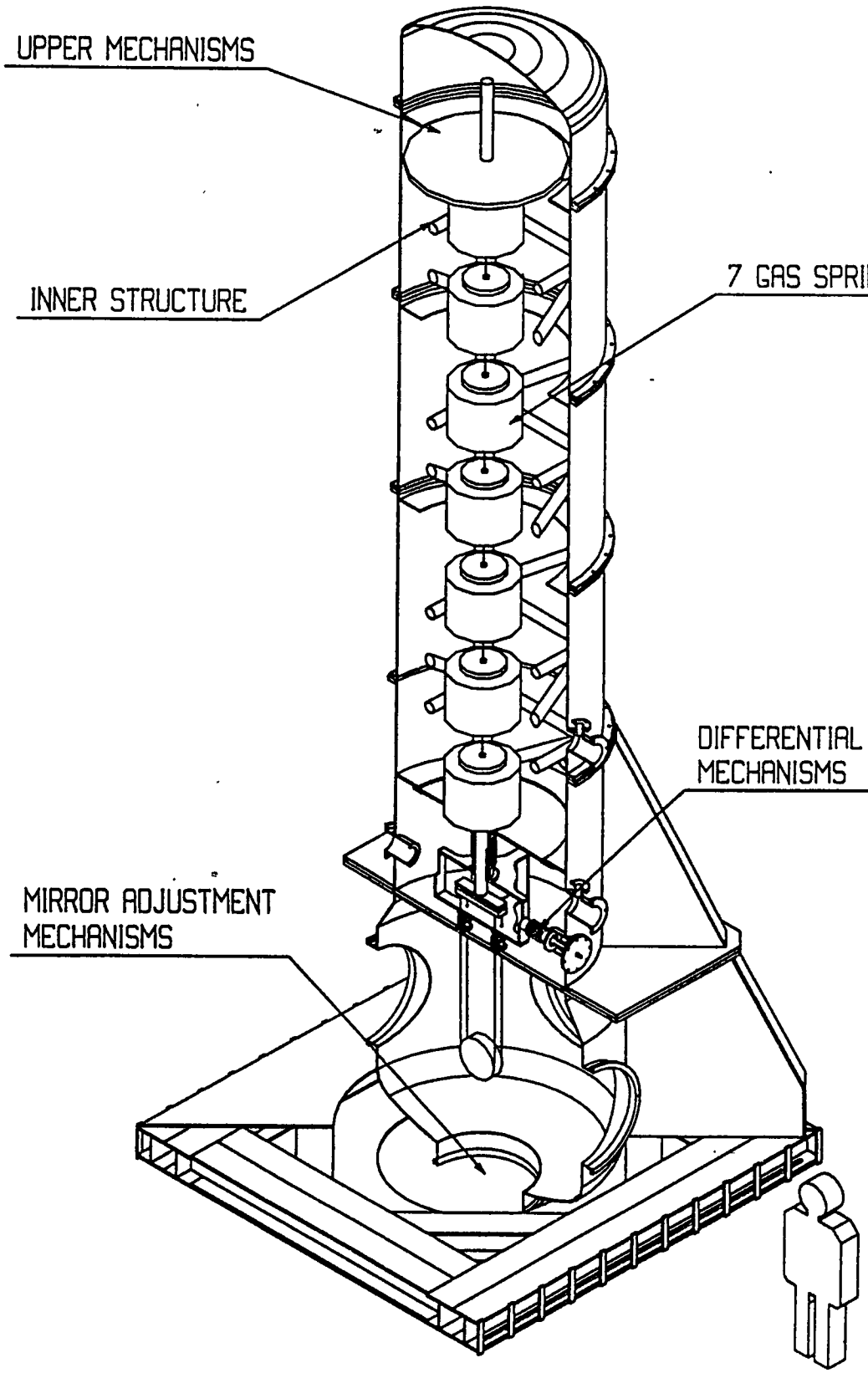

P. Mugnier
le 6-2-92

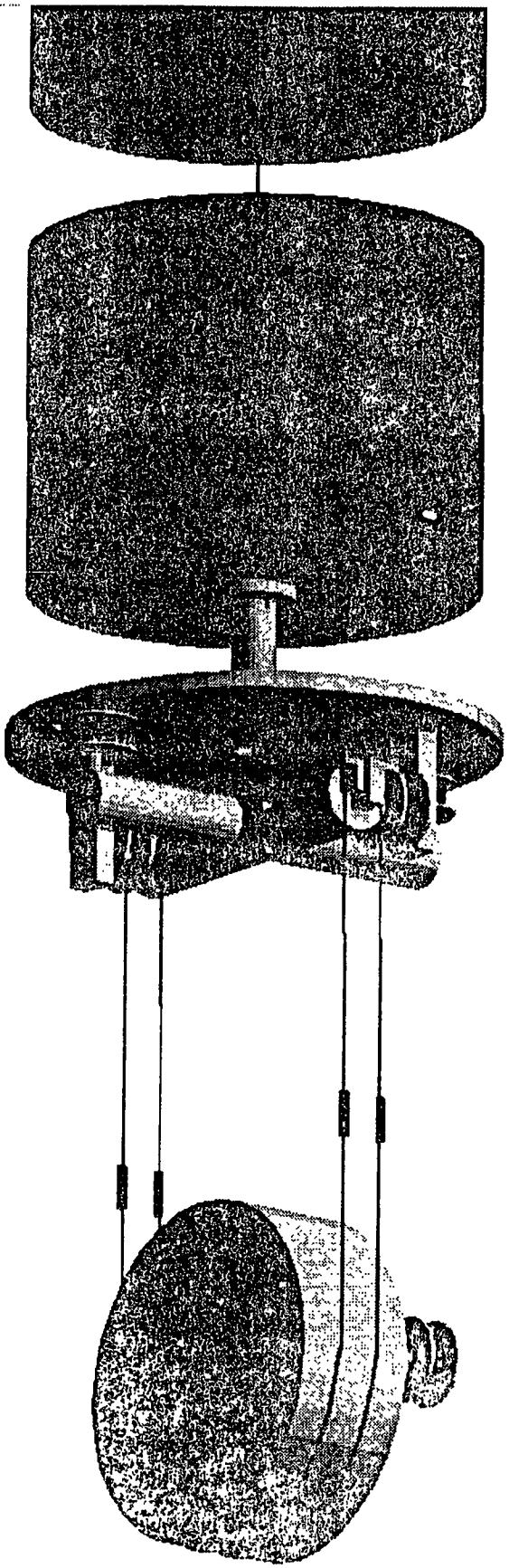

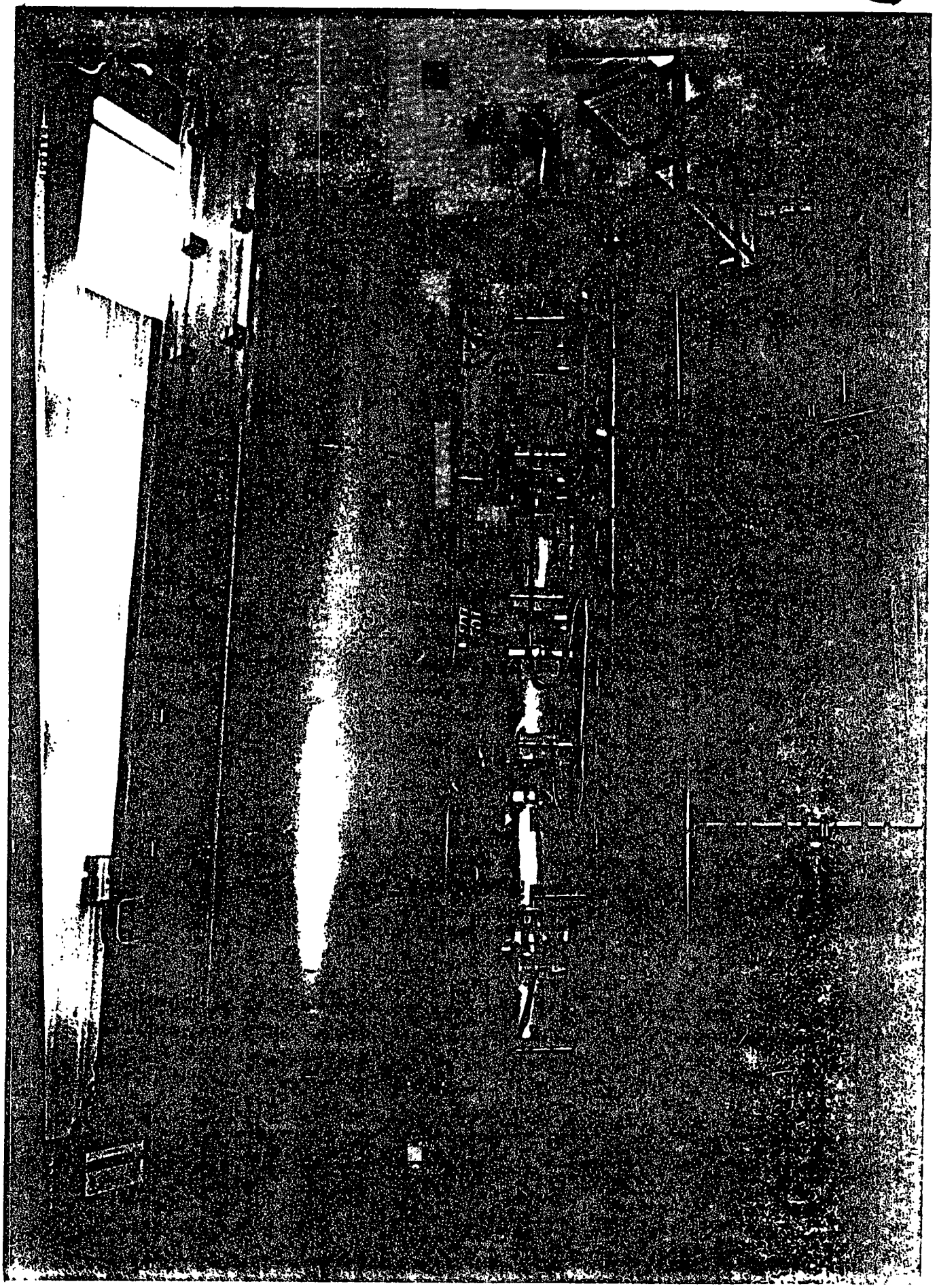

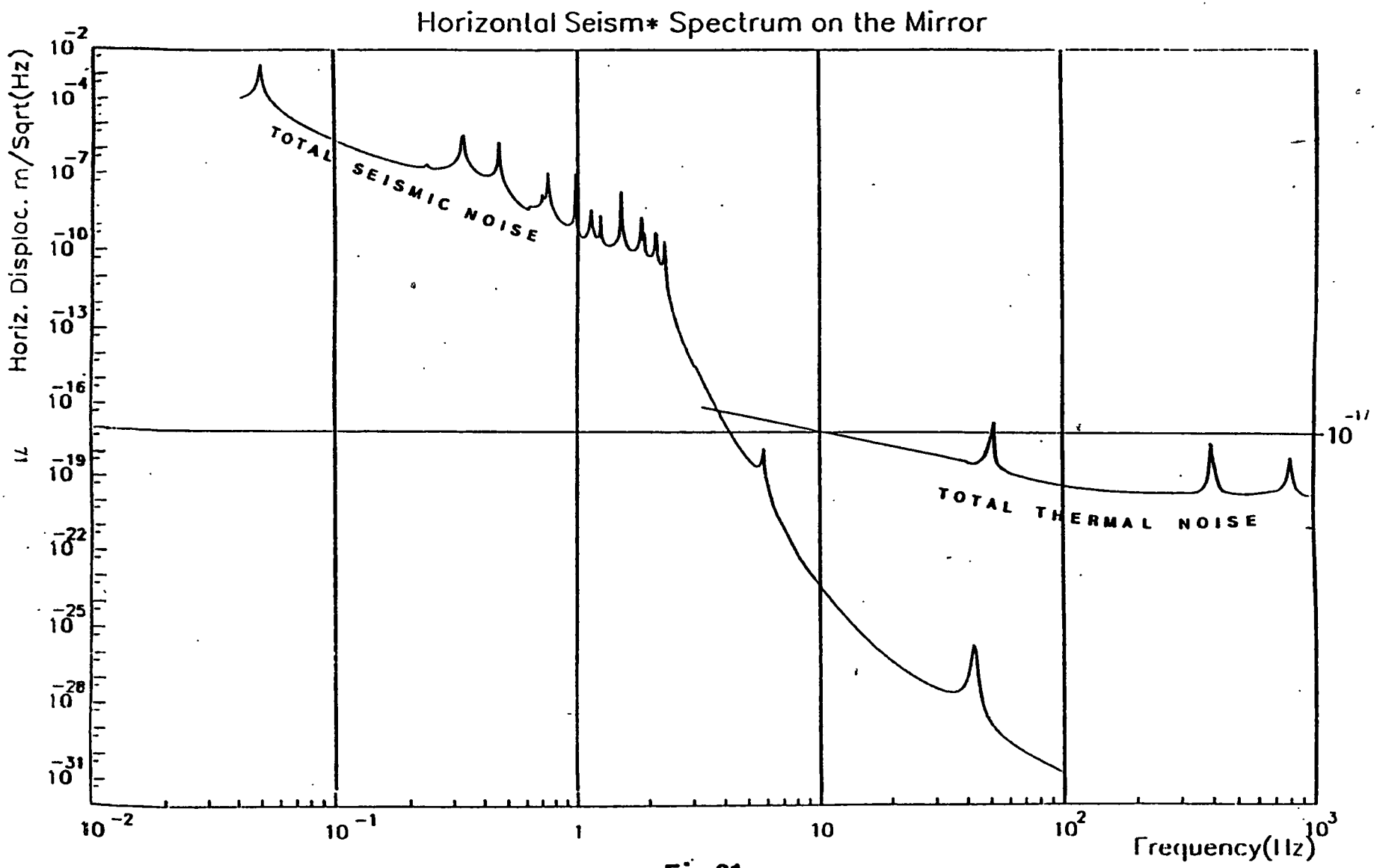
Horizontal Seism* Spectrum on the Mirror
Horiz. Displac. m/Sqrt(Hz)
TOTAL SEISMIC NOISE
TOTAL THERMAL NOISE
Frequency(Hz)

Fig.31

SYSTUS FRAMASOFT+CSI

VAX-2311 10-09-91

MIROIR 400/100

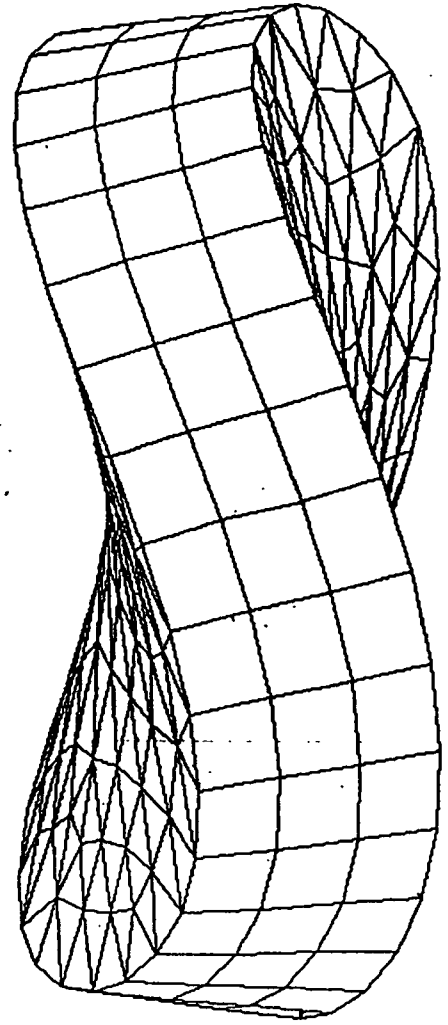

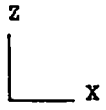

PROBLEMES MECANIQUES :

RESONANCES + AMORTISSEMENT

⇓

BRUIT THERMIQUE

$$\tilde{h} \sim \frac{1}{L}\sqrt{\frac{4kT\omega_0}{MQ\omega^4}}$$

(modèle de bruit blanc)

↙

- OPTIMISATION de la GEOMETRIE ET DES MATERIAUX (MIROIRS, SUSPENSIONS)

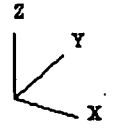

- RECHERCHE de MODELES REALISTES
  - de TECHNIQUES DE MESURE

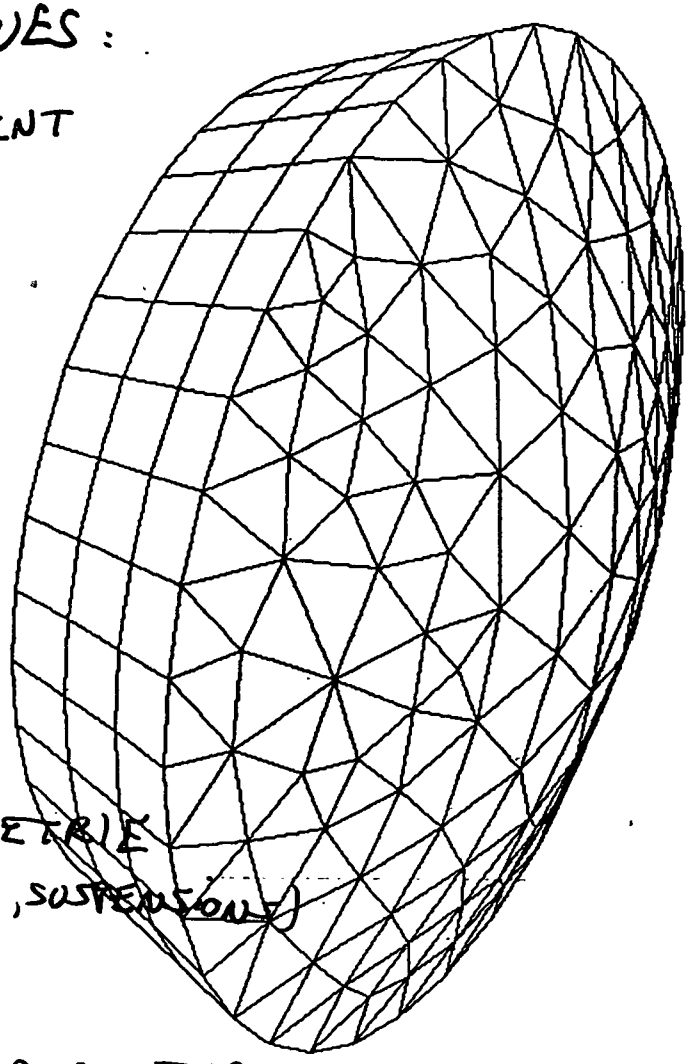

FREQUENCE = 4741.7 Hz

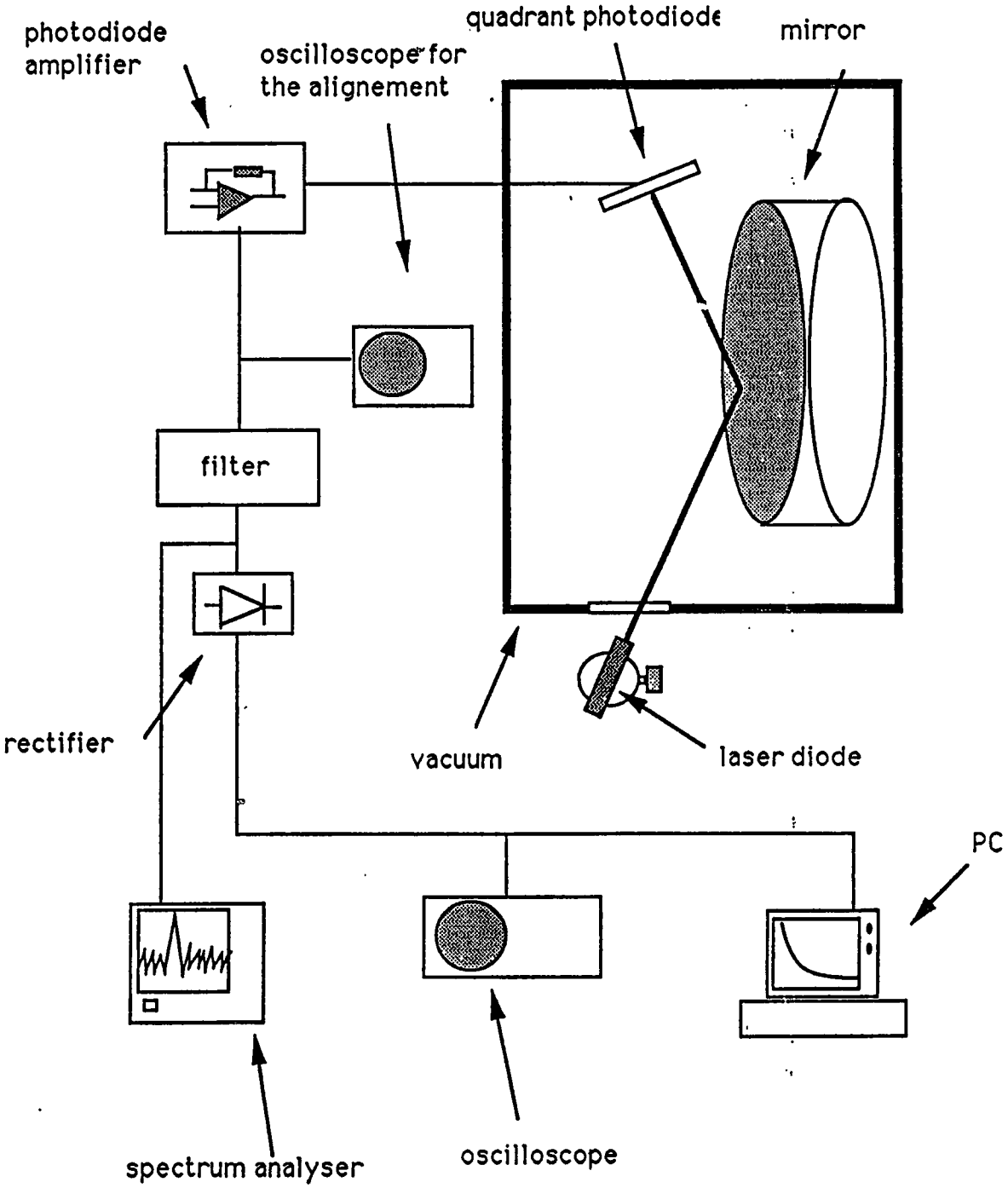
photodiode amplifier
oscilloscope for the alignement
quadrant photodiode
mirror
filter
rectifier
vacuum
laser diode
PC
spectrum analyser
oscilloscope

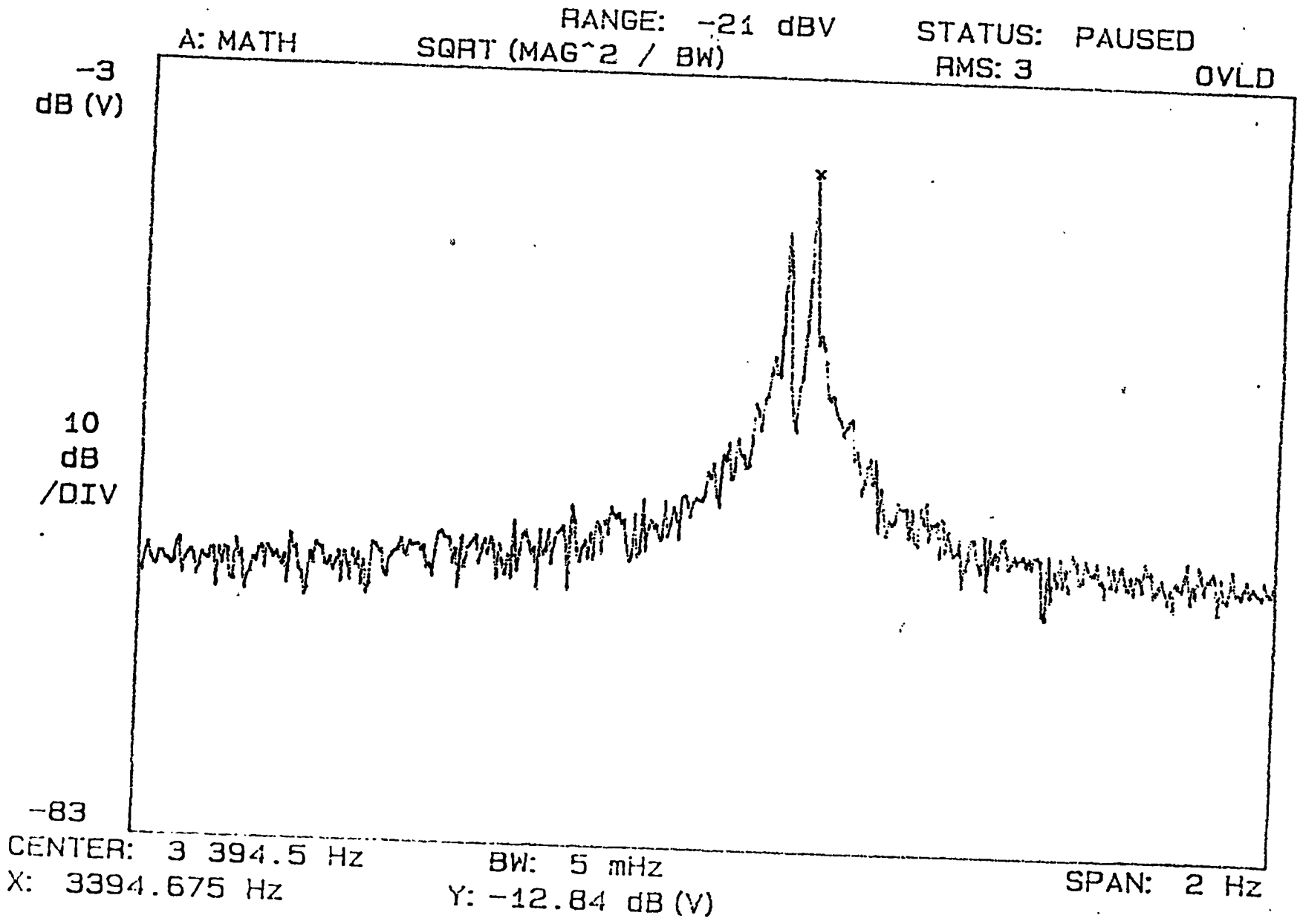
RANGE: -21 dBV
A: MATH
SQRT (MAG^2 / BW)
STATUS: PAUSED
RMS: 3
OVLD
-3
dB (V)
10
dB
/DIV
-83
CENTER: 3 394.5 Hz
BW: 5 mHz
SPAN: 2 Hz
X: 3394.675 Hz
Y: -12.84 dB (V)

$f = 3394\ Hz$ $\quad Q \# 1{,}1 \cdot 10^6$

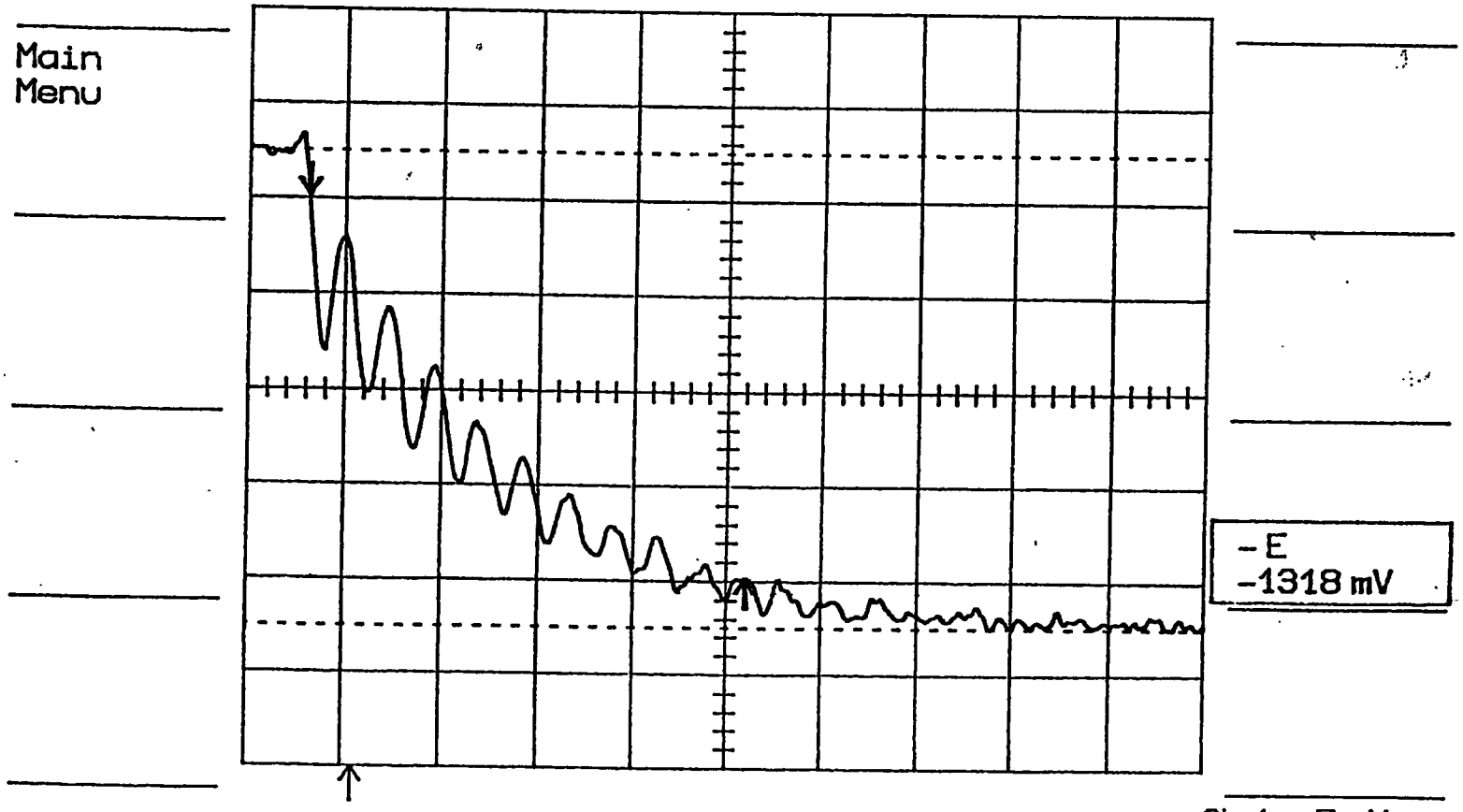

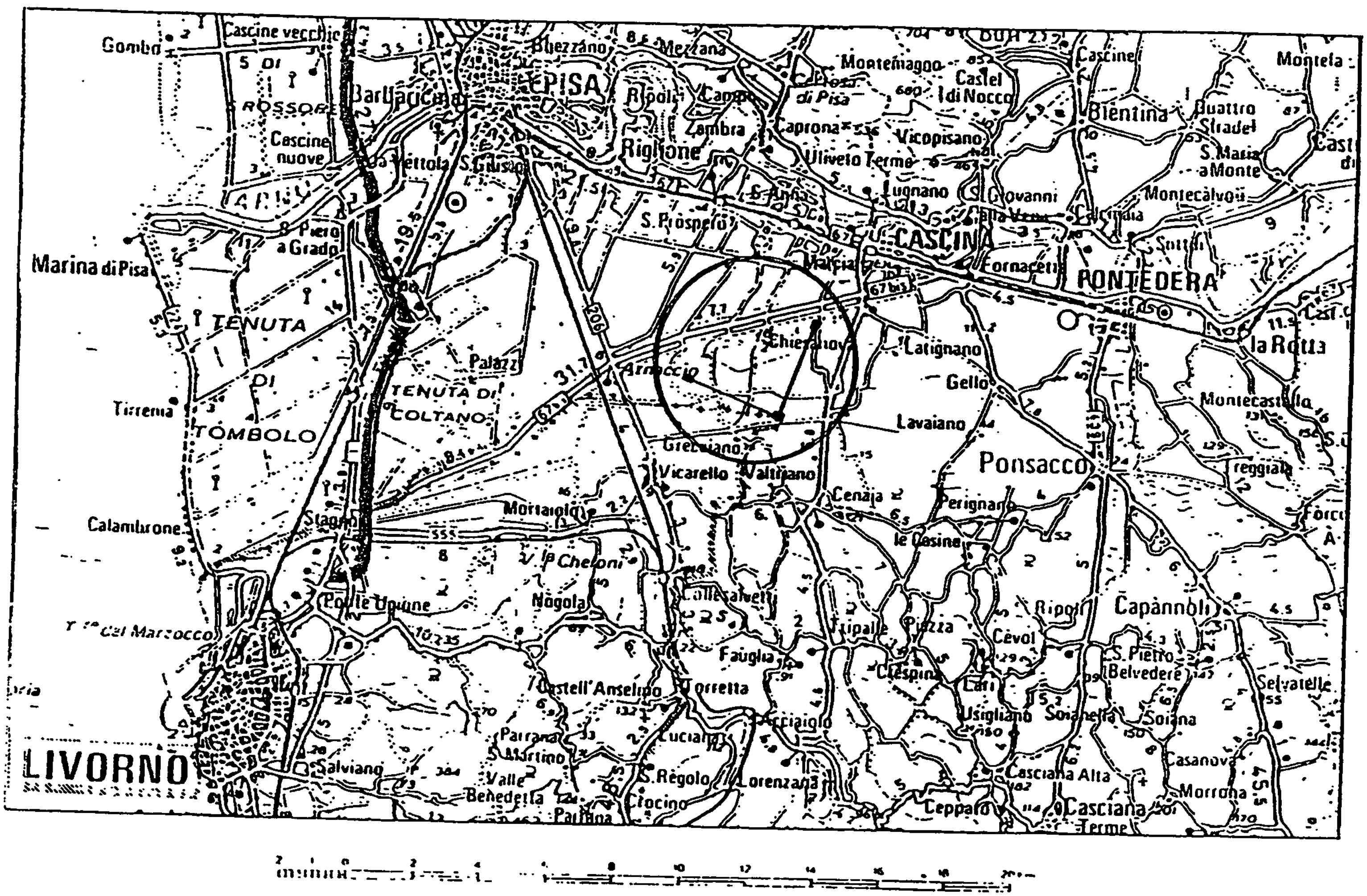
PISA
Barbaricina
Gombo
Cascine vecchie
ROSSORE
Cascine nuove
Marina di Pisa
Piero a Grado
TENUTA
DI
TOMBOLO
Tirrenia
Calambrone
LIVORNO
Mezzana
Montemagno
Castel di Nocco
Caprona
Vicopisano
Uliveto Terme
Lugnano
Zambra
Riglione
S. Prospero
CASCINA
Fornacette
PONTEDERA
Bientina
Quattro Strade
S. Maria a Monte
Montecalvoli
Calcinaia
Latignano
Gello
Lavaiano
Ponsacco
la Rotta
Montecastello
Treggiaia
Arnaccio
Grecciano
Vicarello
Valtriano
Cenaia
Perignano
le Casine
TENUTA DI COLTANO
Palazzi
Mortaiolo
Stagno
Ponte Ugione
Nugola
Collesalvetti
Fauglia
Crespina
Torretta
Castell'Anselmo
Parrana
S. Martino
Valle Benedetta
Salviano
S. Regolo
Lorenzana
Acciaiolo
Luciana
Usigliano
Lari
Cevoli
Capannoli
Ripoli
Soianella
Soiana
S. Pietro Belvedere
Selvatelle
Casanova
Morrona
Casciana Alta
Casciana Terme
Ceppato
Montefoscoli
Cascine

Fig. 1

29

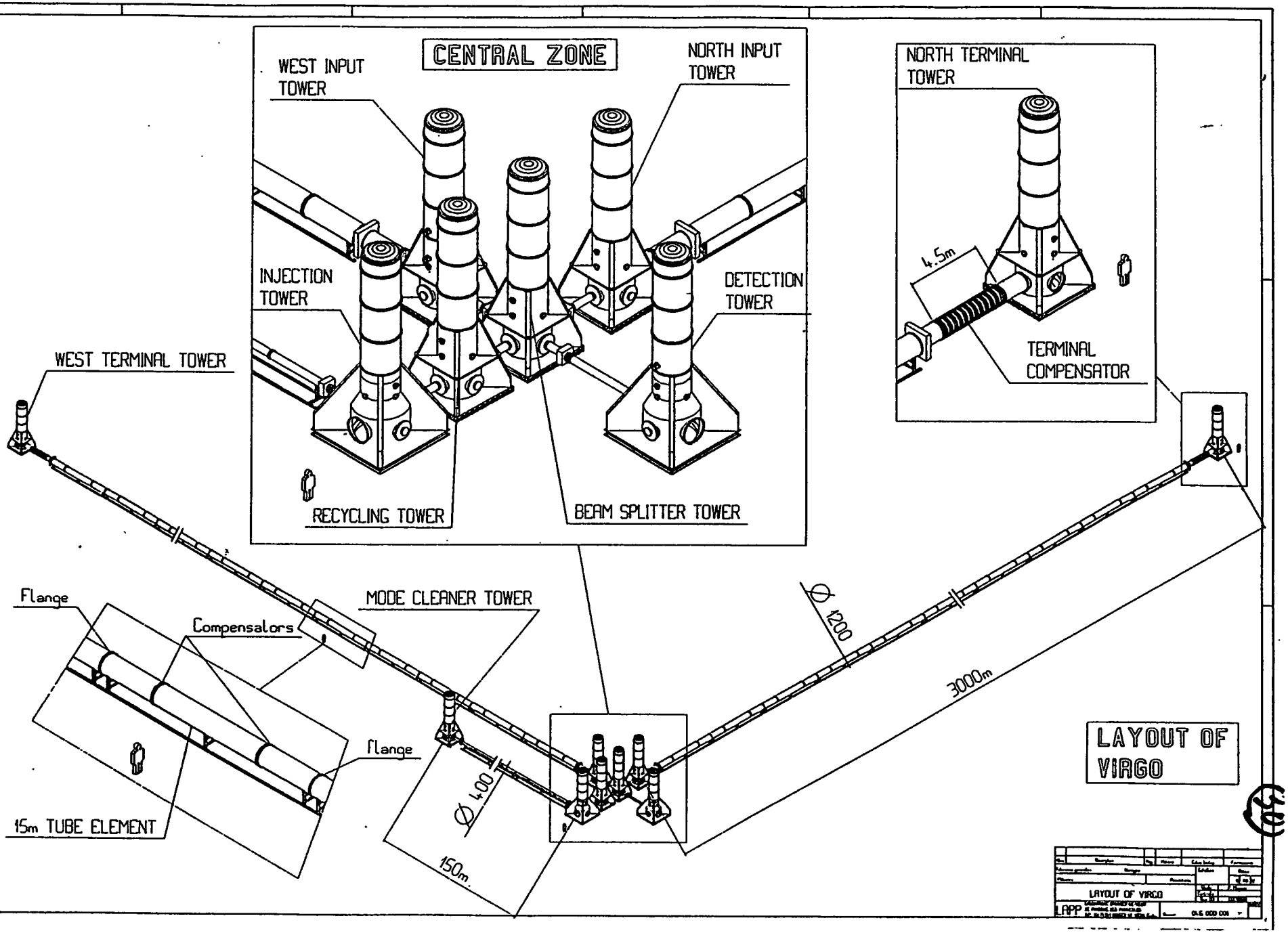
CENTRAL ZONE
WEST INPUT TOWER
NORTH INPUT TOWER
INJECTION TOWER
DETECTION TOWER
RECYCLING TOWER
BEAM SPLITTER TOWER
NORTH TERMINAL TOWER
4.5m
TERMINAL COMPENSATOR
WEST TERMINAL TOWER
MODE CLEANER TOWER
Flange
Compensators
Flange
15m TUBE ELEMENT
Ø 400
150m
Ø 1200
3000m
LAYOUT OF VIRGO
LAYOUT OF VIRGO
LAPP

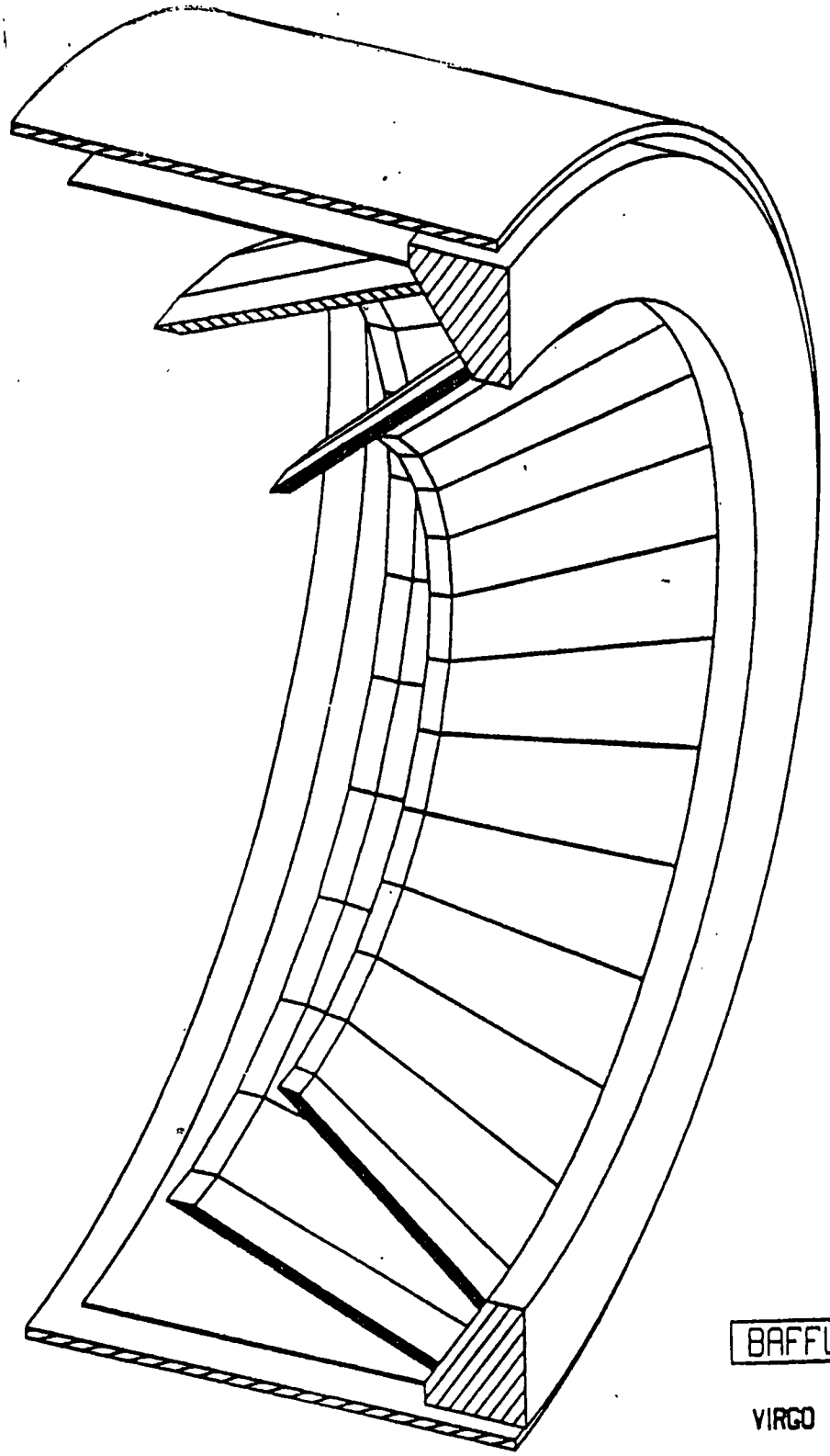

BAFFLE

VIRGO

11-04-1992 0.4 R2

12 OR 302A

FIG.4

V.B R.R

requirement is to have a flexible system which allows us to record more informations for debugging purposes or to inject recorded data or simulated signal at various level in order to test and debug the system.

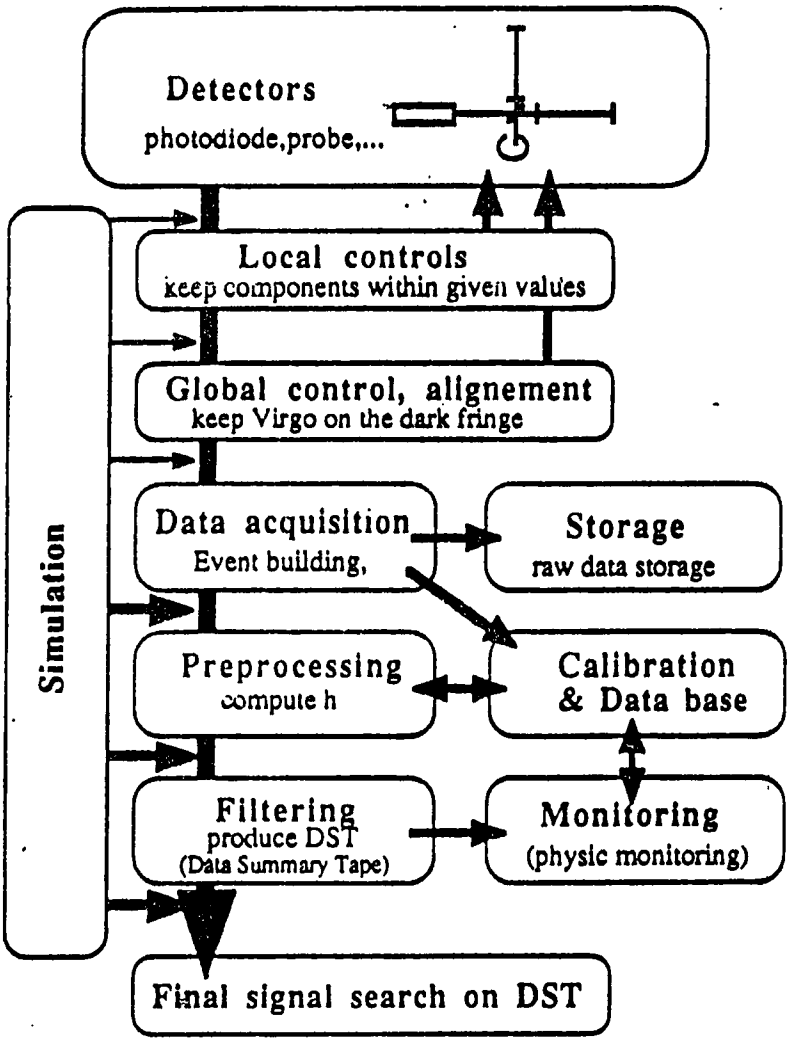

Figure 1. The Virgo data flow

3. Data flow implementation

MILESTONES

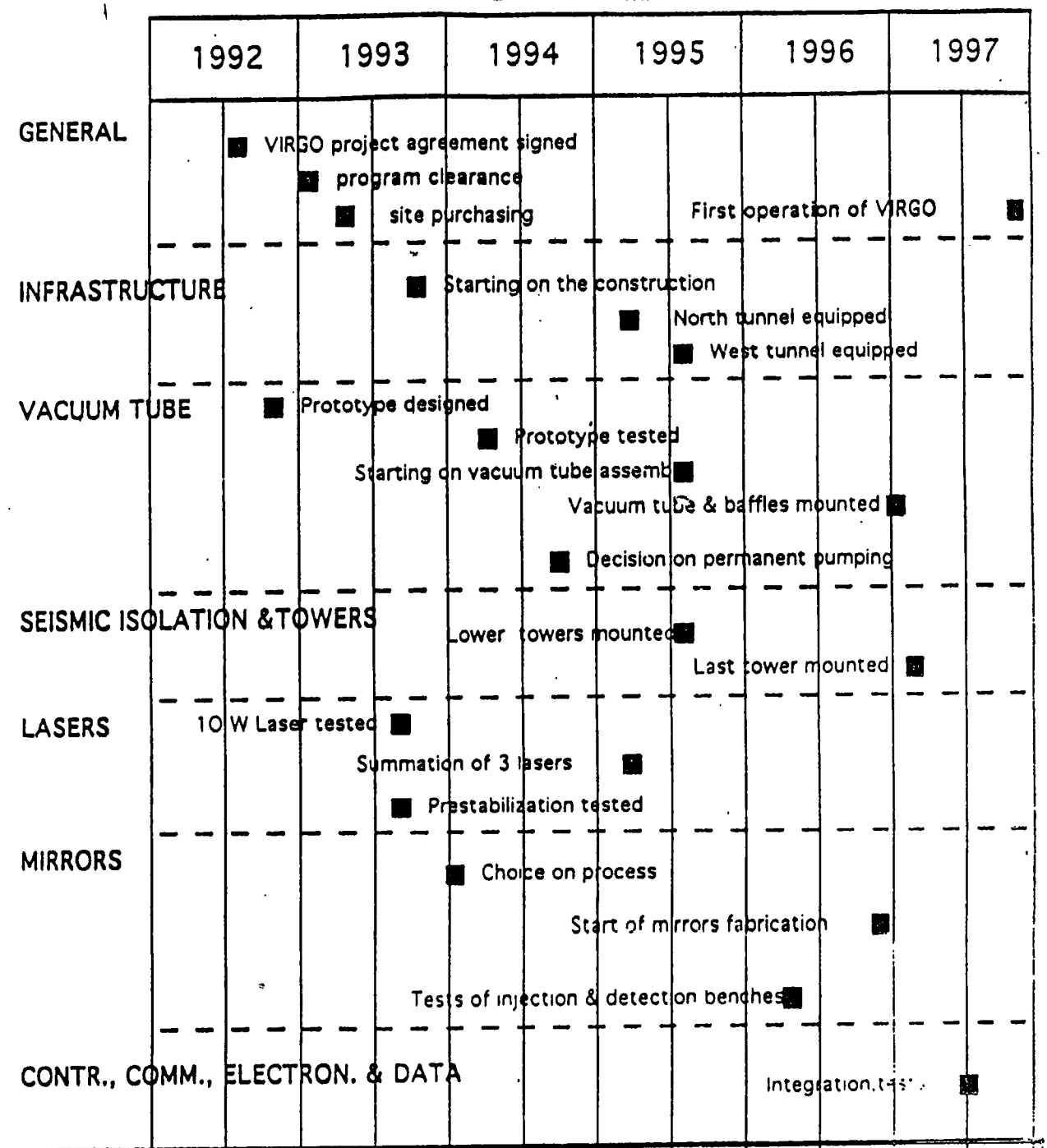

M. Ecus	0,5	1.7	2,42	15,02	10,32	29,02	2,35	1,07
62,19								

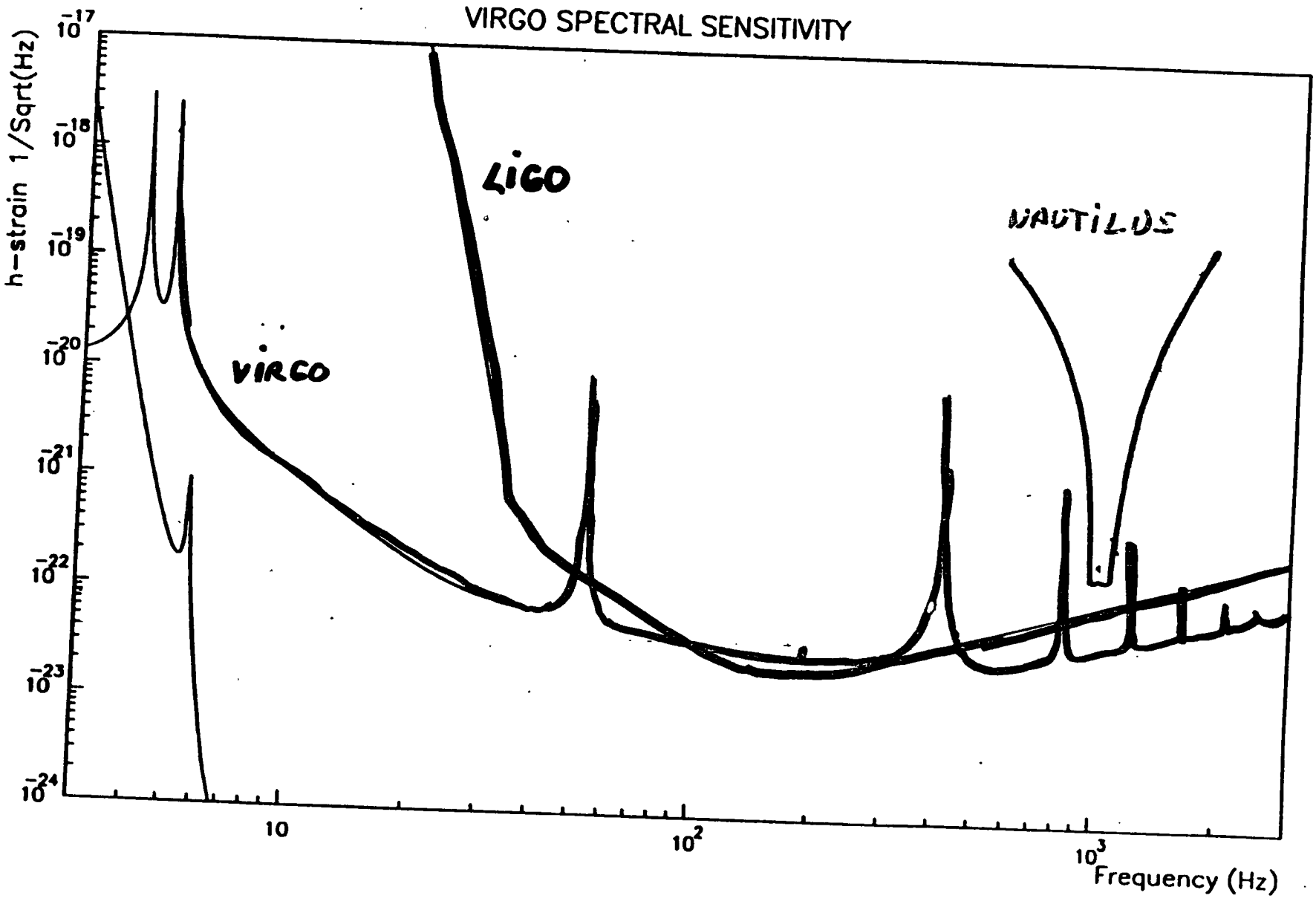
VIRGO SPECTRAL SENSITIVITY
h-strain 1/Sqrt(Hz)
10^{-17}
10^{-18}
10^{-19}
10^{-20}
10^{-21}
10^{-22}
10^{-23}
10^{-24}
LIGO
VIRGO
NAUTILUS
10
10^2
10^3
Frequency (Hz)